Multisensory integration and decision-making in *Drosophila* larvae

Andreas Braun

TESI DOCTORAL UPF / 2015

Thesis Supervisor

Dr. Matthieu Louis

SENSORY SYSTEMS AND BEHAVIOUR
EMBL/CRG SYSTEMS BIOLOGY RESEARCH UNIT
CENTRE FOR GENOMIC REGULACION (CRG)

The logic of science is the logic about business and of life.

(John Stuart Mill)

Uncertainty is an uncomfortable position. But certainty is an absurd one.

(Voltaire)

One may even say strictly speaking, that almost all our knowledge is only probable; and in the small number of things that we are able to know with certainty, the principle means of arriving at the truth - induction and analogy - are based on probabilities.

(Pierre Simon Laplace)

Acknowledgements

I would like to thank Matthieu, for his supervision, and for sharing the successes and disappointments along the way. Without his constant support and unwavering commitment, I would not have been able to finish this study. This project has been a fruitful and close collaboration with Rubén Moreno Bote and Alexandre Pouget. Rubén developed the theoretical framework in this thesis and was always available for questions and discussions. Alex, although quite busy, was always willing to give feedback and took charge of the modeling at a later stage of the project. I want to thank Ximena for reliable help to finish the experimental work during the last year of my PhD. I want to extend my gratitude to Justin, Octavi and Mariana who were also willing to perform behavioral experiments for me. Thanks to Elena, Ibrahim, Elie and David for proofreading and commenting on the manuscript of this thesis. Special thanks to Julia, Aljo, Mariana, Samson, Tommaso, Natalia, Ibro, Elena, Eliem, and "AJ"-Ajinkya for personal support during this thesis, great conversations and for sharing huge amounts of coffee and tea. Further thanks to Alex, Daeyeon, Moraea, Vani, Avinash, Nicole, David and Bala for being very engaging, ready to extend a helping hand when needed and sharing the days and nights in the lab. I want to thank the members of my thesis committee Johannes Jäger, Fyodor Kondrashov, Albert Compte and extended collaborator Zach Mainen for feedback and advise. Likewise, I thank the member of my PhD panel James Sharpe, Barbara Webb, Gonzalo de Polavieja, Jérôme Solon and Rubén Moreno Bote for critical reading of this thesis. I am grateful to the LaCaixa foundation for

granting me PhD scholarship. Big thanks to the CRG community, which made the CRG a special place to work.

I want to thank Majo for her understanding and keeping me from going crazy during the last months of my thesis. Thanks to all off my friends, for the fun together, good memories and counsel I've received. Last but not least, I am grateful to my family for their unconditional support that enables me to follow my ideals.

Abstract

Numerous studies have shown that a wide range of behaviors from sensory processing to motor control involve near-optimal probabilistic inference. Most of these studies have focused on vertebrates, suggesting that the ability to perform probabilistic inference requires large nervous systems. Yet, neural theories of probabilistic inference can be implemented with the most basic neural networks. To explore the possibility that organisms with small nervous systems perform near-optimal probabilistic inference, I tested the ability of *Drosophila* larvae to integrate information from unisensory and multisensory cues.

Larvae were placed in a circular behavioral arena, where their positions were monitored during exposure to single or combined sensory gradients. Combined gradients consisted either of two odor gradients or a thermosensory and an odor gradient, to test within and cross-modal integration respectively. In collaboration with theorists, I predicted the optimal behavior for the combined gradients given the behavior in the single sensory conditions, with a Bayesian model. The behavior of the larvae matched the predictions of the Bayesian model closely for both, the within and cross-modal, scenarios of integration. Another suboptimal model with fixed weights failed to predict the combined behavior. This work sets the stage for a systematic analysis of the neural computations underlying probabilistic inference in an insect brain amenable to genetic manipulations and physiological inspections.

Resumen

Numerosos estudios han demostrado que una amplia gama de comportamientos, desde el procesamiento sensorial al control motor, intervienen en la inferencia probabilística casi-óptima. La mayoría de estos estudios se centran en vertebrados, surigiéndo que se requiere de un sistema nervioso complejo para desarrollar dicha inferencia probabilística. Sin embargo, las teorías neutrales de inferencia probabilística pueden ser implementadas con redes neuronales mas básicas. Para investigar si organismos que poseen un reducido sistema nervioso son capaces de desarrollar inferencia probabilística casi-óptima, he examinado la habilidad que posee la larva de *Drosophila* para integrar información proveniente de señales uni y multisensoriales.

Las larvas se colocaron en una area circular, donde se examinaron sus posiciones en función del gradiente único o combinado al que fueron expuestas. Los gradientes combinados consisten en dos gradientes de olor o bien en uno de olor y el otro termo sensorial, para así examinar la integración intramodal o intermodal respectivamente. En colaboración con teóricos y aplicando el modelo Bayesian, predije el comportamiento óptimo para gradientes combinados partiendo del comportamiento observado en condiciones de gradiente único. El comportamiento de la larva se ajustó a las predicciones del modelo Bayesian para ambos escenarios de integración, el intra e intermodal. Sin embargo, el modelo sub-óptimo con pesos fijos falló en la predicción del comportamiento combinado. Este trabajo sienta las bases para un análisis sistemático de los cómputos neuronales corroborando la inferencia

probabilística en cerebros de insectos susceptibles a manipulaciones genéticas e inspecciones fisiológicas.

Preface

Karl Popper compared science to a building on piles, erected over a swamp. In his analogy the piles have to be driven only as deep as to support the weight of the building and not until they reach firm ground (Popper 1963). In a similar fashion, our thinking about decision-making was guided by the notion of unbounded rationality[1] for a long time. We were supposed to be consistently rational decision-makers (Smith 1776), driven to maximize our utility[2] (Bentham 1780). In short, humans have been regarded as *homo economicus*[3]. Even Adam Smith, the originator of this view, conceded that economic principles were not the only guides of our behavior (The Theory of Moral Sentiments, (Smith 2010)). However, for a long time most experts disregarded this view.

In recent decades the efforts of a few researchers drove Popper's piles deeper into the mud. Unbounded rationality was replaced by bounded rationality, thus acknowledging constraints in time and information (Gigerenzer and Todd 1999). By now it is clear that we deviate from rational decision-making in many high-level cognitive and economic tasks (Kahneman and Tversky 1979) (Ariely and Jones 2008) (Thaler 2015). However, for low-level tasks, such as perception, it has been shown that we rely on probabilistic reasoning to make the best possible use of sensory information (Ernst and

[1] Unbounded rationality assumes unlimited information and time during the process of decision-making (Gigerenzer, G. and P. M. Todd (1999)).

[2] An economic term, used to measure payoffs, satisfaction or preferences https://en.wikipedia.org/wiki/Utility

[3] https://en.wikipedia.org/wiki/Homo_economicus

Banks 2002). Moreover, it seems that we take sensory uncertainty and costs into account when we execute movements (Kording and Wolpert 2004). This allows us to achieve close-to maximum utility in complex motor tasks (Maloney, Trommershäuser et al. 2007) (Trommershäuser, Maloney et al. 2008).

In this thesis I apply a basic version of probabilistic reasoning to sensorimotor decision-making of larva. Far from a final conclusion, I see it as a small contribution to an ongoing and exciting dialog. Thus, I consider it as one among many piles in the mud; to be driven deeper and maybe even built upon in the future.

Chapter 1: Introduction

Drosophila melanogaster is one of the most studied model organisms in biology (Stephenson and Metcalfe 2012) (Bellen, Tong et al. 2010). The fly is a small, fast-growing and short-lived animal that can be maintained in big populations in the laboratory. For this reasons it became the workhorse of genetic research in the beginning of the 20th century (Morgan 1911). Later, *Drosophila* played a mayor role when the field of behavioral neurogenetics was established (Benzer 1967). In the attempt to shed light on the link between neurons and behavior, the number of neurons in the brain is an obvious criterion for choice of a model organism. The average human brain consists of a staggering 86 billions neurons and a mouse brain still contains around 70 million neurons (Herculano-Houzel 2009). However, the brain of an adult fly only contains about 100 000 neurons (Masse, Turner et al. 2009) and the number of neurons in the brain of a larva is even an order of magnitude lower. The reduced number of neurons in the brain implies that neural circuits have not evolved many of the redundancies, probably important to improve the signal-to-noise ratio, typical for the organization of mammalian brains. In this view neural circuits in insects represent a simplified, or stripped down version of a brain close to the minimum necessary for function[4].

The early development of *Drosophila melanogaster* larvae progresses through three different larval stages (Tyler 2000). First instar larvae

[4] In another view nervous systems of insects have evolved to be small by multiplexing functions. Thus, the lower number of neurons does not necessarily correlate with lower complexity.
https://www.ted.com/talks/michael_dickinson_how_a_fly_flies

(L1) emerge from a fertilized embryo after one day. While feeding continuously, larvae grow and molt into second instar larvae (L2) on day two and third instar larvae (L3) on day three. With just 10 000 neurons (Nassif, Noveen et al. 2002), the central nervous system of larvae produces a range of complex and well defined behaviors (Louis, Phillips et al. 2012) and has to solve many of the basic perceptual problems that we face as well. Larvae respond to the same sensory modalities as humans and are able to form and retrieve simple memories (Gerber and Stocker 2006). The combination of a numerically simple brain, a wealth of genetic tools to manipulate larval behavior (Luo, Callaway et al. 2008), and a quickly growing body of information about neuroanatomy, is about to establish the larvae as a model organisms par-excellence to elucidate underlying mechanisms of fundamental questions of sensory perception, processing, and behavior.

Perception and Beyond

The olfactory system

Olfactory systems of vertebrates and invertebrates have evolved independently but they are organized according to structural common principles (Wilson and Mainen 2006). It is likely that commonalities have arisen from shared evolutionary constraints (Eisthen 2002). First-order olfactory sensory neurons (OSNs) project to a primary processing region, dedicated to olfactory signals (Fig. 1). These brain areas are called olfactory bulbs and antennal lobes (AL) in mammals and insects respectively. From there second-order neurons carry the information to higher brain centers (Masse, Turner et al. 2009).

The dorsal organ, the larval equivalent of the nose, is a bilateral, perforated dome-like structure at the tip of the larval head (Chu and Axtell 1971, Singh and Singh 1984). It houses the dendrites of 21 OSNs expressing a 'private' olfactory receptor (OR) as well as an *odorant receptor co-receptor* (*Orco*) (Python and Stocker 2002, Larsson, Domingos et al. 2004, Benton, Sachse et al. 2006). The cell bodies of OSNs are contained within the dorsal organ ganglion (DOG), located close to the dorsal organ (Python and Stocker 2002). Each OSN expresses just one out of 23 different types of private OR (Vosshall and Stocker 2007). The exceptions are the pairs Or33b/Or47a and Or94a/Or94b, which are co-expressed in the same OSNs (Fishilevich, Domingos et al. 2005). *Drosophila* ORs are seven-transmembrane proteins with an inverted topology when

compared to mammalian ORs (Benton, Sachse et al. 2006). Thus, the N-terminus resides within the cytoplasm and associates with *Orco*, which is necessary for signal transduction. Together, *Orco* and the OR, are thought to form a ligand-gated cation channel (Sato, Pellegrino et al. 2008).

Odorant molecules enter the dorsal organ by diffusion. There is evidence that olfactory binding proteins (OBPs) mediate the receptor-ligand interaction. In adult flies absence of the OBP lush abolishes responses to alcohol and the pheromone 11-*cis* vaccenyl acetate (cVA) (Kim, Repp et al. 1998, Xu, Atkinson et al. 2005, Ha 2006). Every odorant molecule activates a different subset of OSNs according to the binding affinity of the expressed OR. The structure of an OR is tuned to interact with a number of distinct odorant molecules over a range of concentrations. A tuning curve relates the average OSN firing rate of a specific OSN to a stimulus (Butts and Goldman 2006). Tuning curves of adult and larval ORs have been systematically probed by extracellular electrophysiological recordings (Hallem, Ho et al. 2004, Hallem and Carlson 2006) (Kreher, Kwon et al. 2005, Kreher, Mathew et al. 2008). Typically, tuning curves depend on both odor identity and intensity. At low concentrations, odorants only bind to ORs with which they share a high affinity. Increasing the concentration recruits additional OSNs. Some receptors are narrowly tuned and only respond to a few structurally similar molecules while others interact with a broad set of ligands. Overall, the observed responses were mostly excitatory. However, in a few cases firing was even reduced after exposure to a chemical stimulus (Hallem and Carlson 2006) (Kreher, Mathew et al. 2008).

The antennal lobe (AL) is the primary processing center for olfaction and consists of 19 glomeruli (Masuda-Nakagawa, Gendre et al. 2009). The axon of each OSN targets a different glomerulus and connects to projection neurons (PNs) arborizing within the same glomerulus (Masuda-Nakagawa, Gendre et al. 2009). OSNs and PNs are both excitatory neurons and use acetylcholine as a neurotransmitter (Liu and Wilson 2013). A network of local interneurons (LNs) couples the glomeruli with each other (Das, Sen et al. 2008). LNs are either excitatory (Shang, Claridge-Chang et al. 2007, Yaksi and Wilson 2010) or inhibitory (Olsen and Wilson 2008). Inhibitory LNs are mostly GABAergic and mediate mainly intraglomerular connectivity (Asahina, Louis et al. 2009). Glutamateric inhibitory LNs are mostly interglomerular and inhibit GABAergic LNs as well as PNs (Liu and Wilson 2013). The concerted action of the complex LN network is important for gain control and divisive normalization (Olsen, Bhandawat et al. 2010).

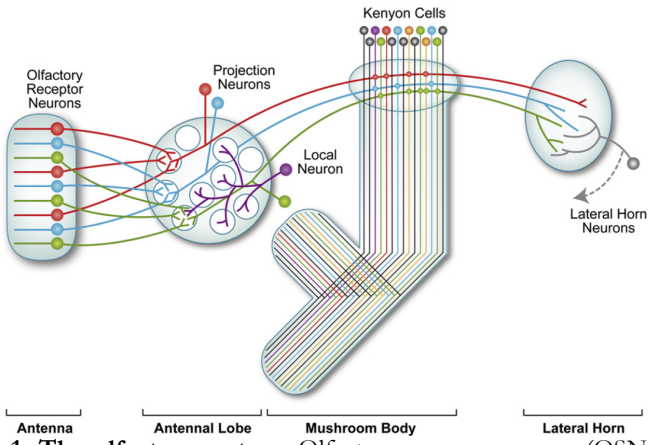

Figure 1: The olfactory system. Olfactory sensory neurons (OSNs) project to glomeruli in the antennal lobe. There, they make contact with projection neurons (PNs), which transmit the olfactory information to the Kenyon Cells (KCs) of the mushroom body (MB) and the lateral horn (LH). Figure taken from (Cachero and Jefferis 2008).

In the traditional view one OSN connects to one PN. However, recent evidence (Das, Gupta et al. 2013) as well as ongoing reconstruction of the antennal lobe reveals a more complicated picture (personal communication I. Tastekin). PNs project to higher brain centers, like the mushroom body (MB) and the lateral horn (LH).

The thermosensory system

Ectoderms, like *Drosophila melanogaster* are not able to regulate their body temperature (Stevenson 1985). Furthermore, with their low weight and small heat capacities the internal temperature matches the external temperature within seconds. Therefore, it is essential for larvae to respond to deleterious thermal stimuli as fast as possible (Garrity, Goodman et al. 2010).

Like mammals, *Drosophila* uses a number of different sensory pathways to sample the temperature in their surroundings. The terminal organ is a bilateral structure at the head of larvae and is located right next to the dorsal organ. Neurons in the terminal organ ganglion (TOG) are sensitive to stimulation by temperature (Liu, Yermolaieva et al. 2003). Depending on the neuron, a cold stimulus either inhibits firing, triggers oscillations, or increases firing in third instar larvae (Liu, Yermolaieva et al. 2003). Three neurons in the DOG also respond to cooling (Klein, Afonso et al. 2015). Interestingly these neurons differ in their reaction to temperatures changes. One of these thermosensing neurons has a higher baseline-calcium level and is more sensitive to the onset of warming than the other two neurons. Body wall neurons are also implicated in

thermosensation (Liu, Yermolaieva et al. 2003). Multidendritic neurons[5] express the *trp*[6] channels *pyrexia* (Lee, Lee et al. 2005) and *painless* (Tracey, Wilson et al. 2003, Xu, Cang et al. 2006, Sokabe, Tsujiuchi et al. 2008). Both, *pyrexia* and *painless* are implicated in noxious heat avoidance and are activated around 40 and 44°C respectively (Garrity, Goodman et al. 2010). Chordotonal neurons also express *painless* (Tracey, Wilson et al. 2003), as well as the ion channel *inactive*. *Inactive* is a member of the TRPV subfamily and implicated in choosing the preferred temperature (17.5°C) over slightly colder temperature (14-16°C) in third instar larvae (Kwon, Shen et al. 2010). Other members of the same family, TRP and TRPL, are also associated with cold sensing (Rosenzweig, Kang et al. 2008). TRPA1 and related signaling cascades (Kwon, Shim et al. 2008, Shen, Kwon et al. 2011) have been implicated in avoidance of slightly elevated temperatures in adults and larvae (Rosenzweig, Brennan et al. 2005, Hamada, Rosenzweig et al. 2008). It is noteworthy, that TRPA1 functions as an internal temperature sensor in the brain. This is made possible as a consequence of the rapid equilibration of internal and external temperatures in small animals.

[5] Multidendritic neurons and chordotonal neurons (later in the text) are sensory neurons of the peripheral nervous system. Both types are located in the body wall of *Drosophila melanogaster*, and have been often implicated in mechanosensory sensation (stretch sensors). They are distinguished by their morphology: chordotonal neurons have one dendrite while the other sets of neurons are characterized by multiple dendrites.
http://cuttlefish.bio.indiana.edu:7082/allied-data/lk/interactive-fly/aimorph/pns.htm

[6] Transient receptor potential (TRP) channels is a family about 30 related ion channels (Zheng, J. (2013)) , typically found in the walls of animal cells. They are subdivided in a number of subfamilies e.g. TRPA, TRPC, TRPV and TRPP. These channels are relatively non-selective and have been found to confer sensitivity to light, mechanosensation, temperature as well as chemicals.
https://en.wikipedia.org/wiki/Transient_receptor_potential_channel

In adult *Drosophila* the cells expressing internal TRPA1 heat sensors are called anterior cell (AC) neurons (Hamada, Rosenzweig et al. 2008). AC neurons have a sensory function and at the same time represent a first level of convergence of thermosensory information. They integrate their thermosensory information with signals from *pyrexia* expressed in the second antennal segment (Tang, Platt et al. 2013). While TRPA1 sensors detect shallow temperature gradients, GR28D-expressing heat sensing cells in the antenna mediate rapid warmth avoidance (Gallio, Ofstad et al. 2011, Mani, Mullainathan et al. 2013).

In larvae the circuits downstream from the sensors are mostly unknown at present, except for the thermosensors in the DOG that innervate a region posterior of the AL[7] (Klein, Afonso et al. 2015). In adults, a similar region in the brain[8] is innervated by heat and cold sensing cell from the third antennal segment innervate (Gallio, Ofstad et al. 2011). From there, projections are innervating the little studied lateral protocerebrum, the MB and the LH where further thermosensory processing takes place (Frank, Jouandet et al. 2015) (Liu, Mazor et al. 2015).

Higher brain centers

At present, studies on the mushroom body (MB) and the lateral horn (LH) have mainly focused on adult flies (Fig. 1). In addition most of these studies have investigated the role of higher brain

[7] The authors have not specified the exact region.

[8] Neurons from the third antennal segment innervate the proximal antennal protocerebrum.

centers in connection with olfaction, since the connectivity to temperature sensing system has only been described recently (Frank, Jouandet et al. 2015) (Liu, Mazor et al. 2015). The MB is associated with learned behavior (Keene and Waddell 2007) and representation of valence (Aso, Hattori et al. 2014, Aso, Sitaraman et al. 2014), while the LH is responsible for innate responses (Heimbeck, Bugnon et al. 2001, Masse, Turner et al. 2009, Ruta, Datta et al. 2010). On a computational level this is achieved by sparse connections between PNs and Kenyon cells (KCs) of the MB and selective connection between PNs and LH (Luo, Axel et al. 2010).

In addition to a selective connectivity, wiring of the LH is highly stereotyped (Marin, Jefferis et al. 2002, Jefferis, Potter et al. 2007). Neurons that run from the AL to the LH cluster into broadly and narrowly tuned groups (Fişek and Wilson 2013). The broadly tuned neurons receive input from multiple glomeruli, have a broad dynamic range, and are thought to be involved in stimulus generalization. Narrowly tuned lateral horn neurons might be necessary for discrimination and link specific cues directly to certain behavioral programs. The LH alone is sufficient for the generation of basic olfactory behaviors (de Belle and Heisenberg 1994).

By contrast connectivity of PNs to the KCs of the MB seems to be random and sparse (Caron, Ruta et al. 2013). In adult flies every single KC out of about 2000 cells, connects to only 10% of the glomeruli. KCs make up the main body of the three lobes (α/β, α'/β', and γ) of the MB (Fig. 2). The remainder consists of mushroom body output neurons (MBONs) and dopaminergic neurons (DANs). Each lobe of the MB is compartmentalized into

five subsections, with every MBON and DAN type innervating only certain compartments (Fig. 2). DAN axons converge onto the shared KC-MBON synapses, where they modulate neural processing (Fig. 2). The MBON axons terminate in the LH and four additional zones in the brains of adult *Drosophila*, (Aso, Sitaraman et al. 2014). Aso et al. showed that activation and inhibition of certain MBONs with genetic methods modulates attraction and avoidance or blocks memory retrieval for the behavior specific to this MBON. Thus, the authors concluded that the MB encodes valence and thus biases decision-making (Aso, Sitaraman et al. 2014). Furthermore, they showed that activation of multiple MBONs mediating the same behavior has an additive effect i.e. results in an improved behavioral performance in a certain task.

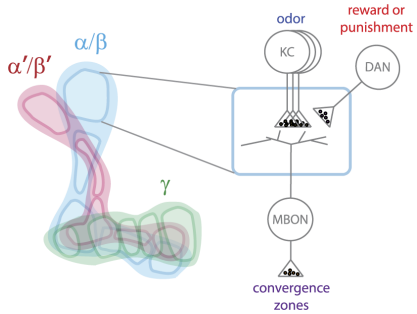

Figure 2: Schematic representation of the mushroom body circuitry. Each of the three mushroom body lobes (pink, blue and green) contains five compartments. In every compartment Kenyon cells (KCs) form synapses with mushroom body output neurons (MBONs). Dopaminergic neurons (DANs) modulate signal processing and thus influence the valence of a cue. Figure taken from (Griffith 2014).

Perception to Action

An animal has to process sensory information so it can be used to guide behavior. The process of converting sensory input into motor output is called sensorimotor integration. This process has to be flexible enough to incorporate a wide variety of internal and external (posture, timing, etc.) states (Huston and Jayaraman 2011). To navigate sensory gradients it is essential to disentangle the perception arising from self-generated movement, from the spatial quality of the gradient. Therefore, it is likely that sensorimotor integration is not only a feed-forward process but contains feedback loops at multiple stages (Huston and Jayaraman 2011).

Strategies to navigate chemical gradients

The term *kinesis* (Greek for movement or motion) describes the simplest forms of gradient navigation. *Escherichia coli* navigate chemical gradients by a biased random walk (Berg and Brown 1972). These bacteria are able to modulate the length of straight swimming bouts, called runs, depending on whether it is moving up or down the gradient. In addition to runs its trajectory also consists of tumbles in which the direction of a new run is chosen at random. Similar to bacteria, *C. elegans* is able to bias the length of its runs, whereas reorientation events, termed pirouettes, are random (Pierce-Shimomura, Morse et al. 1999). However, runs in *C. elegans* navigation are not completely straight. Instead, they are mostly bent towards the source of the chemical gradient. Therefore, *C. elegans* is able to continuously refine the direction of its runs in a process

called weathervaning (Iino and Yoshida 2009) (Izquierdo and Lockery 2010).

More sophisticated strategies to navigate sensory gradients are collectively termed *taxis*-behaviors (Greek for arrangement). The nature of the gradient is usually specified by a prefix e.g. chemotaxis for navigation of chemical gradients. *Drosophila* larvae are able to bias both run length and turn orientation towards the side of the stimulus location during chemotaxis (Gomez-Marin, Stephens et al. 2011, Gershow, Berck et al. 2012) (Gepner, Mihovilovic Skanata et al. 2015, Hernandez-Nunez, Belina et al. 2015, Schulze, Gomez-Marin et al. 2015). Therefore, larvae have to make two different types of decisions: when to turn (type 1) and where to turn to (type 2). While running, wild-type larvae monitor the perceived change of odor concentration over time. Turns are triggered by a prolonged experience of a negative slope of perceived odor concentration (Gomez-Marin, Stephens et al. 2011). In short, larvae are able to modulate their run length depending on their bearing with respect to the gradient (type 1 decision) (Gomez-Marin, Stephens et al. 2011) (Gershow, Berck et al. 2012). Larvae are able to chemotax even if the number of functional OSNs has been reduced with genetic methods (Fishilevich, Domingos et al. 2005) (Louis, Huber et al. 2008) (Asahina, Louis et al. 2009). Experiments with larvae with only one functional set of OSNs, showed that they relied on the same strategy as wild-type larvae in odor gradients (Gomez-Marin, Stephens et al. 2011) (Gershow, Berck et al. 2012) and virtual odor gradients (Gepner, Mihovilovic Skanata et al. 2015, Hernandez-Nunez, Belina et al. 2015, Schulze, Gomez-Marin et al. 2015).

Therefore, larvae need just one type of OSN to perform the necessary computations required for chemotaxis. This finding also extends to sensory neurons mediating aversion to odors such as Or45a (Hernandez-Nunez, Belina et al. 2015) or CO_2 (Gepner, Mihovilovic Skanata et al. 2015). In this scenario, however, runs are biased towards gradient descent. Consequently, turns are triggered by exposure of larvae to positive slopes of perceived stimulus over time.

Electrophysiological investigation of OSN firing showed that the activity of OSNs depends on stimulus intensity and its first derivative (Schulze, Gomez-Marin et al. 2015). An OSN is excited by an increase in odor concentration. A rise in OSN activity results in prolonged up gradient movement. A negative derivative of stimulus intensity, resulting from a decrease in odor concentration, inhibits OSN firing and increases the probability of turning. Consequently runs are shortened. Therefore the OSN activity correlates directly with the observed behavior. The type 1 decision has been modeled based on the behavior after reverse correlation with a linear-nonlinear model (Gepner, Mihovilovic Skanata et al. 2015, Hernandez-Nunez, Belina et al. 2015) or based on the OSN firing rates (Schulze, Gomez-Marin et al. 2015). The latter approach suggests a testable biophysical model employing incoherent feed-forward and feedback loop motifs (Alon 2006).

At the end of a run larvae stop and sample the odor environment by lateral head casts. The last head cast determines the direction of a turn (type 2 decision), which mostly points in the favorable direction (Gomez-Marin, Stephens et al. 2011, Gershow, Berck et al. 2012).

Typically, larvae are able to select the favorable direction over 70% of times after just two head casts (Gomez-Marin, Stephens et al. 2011). As in *C. elegans*, larvae are also able to weathervane and thus bias their runs towards the odor source (Gomez-Marin and Louis 2014, Ohashi, Morimoto et al. 2014).

Thermotaxis

Since larvae are not able to regulate their body temperature they have to rely on behavioral strategies to find suitable environmental conditions (Stevenson 1985, Heinrich 1993). Movement towards warm temperatures (up gradient) is called positive thermotaxis. Movement down gradient due to the avoidance of heat is referred to as negative thermotaxis. Thermal preferences change profoundly during development. First instar larvae are attracted to temperatures between 23-29°C (Luo, Gershow et al. 2010), third instar prefer around 18 °C (Kwon, Shen et al. 2010) and adult 24-26°C (Sayeed and Benzer 1996).

Positive and negative thermotaxis relies on the same behavioral strategy (Luo, Gershow et al. 2010). Similar as in chemotaxis, thermotactic behavior can be divided into a sequence of runs and turns. Run length is elongated if larvae move in the direction of preferred temperature and shortened if moving in the opposite direction (type 1 decision) (Luo, Gershow et al. 2010) (Klein, Afonso et al. 2015). After a run larvae stop and perform lateral head casts to choose the direction of the next run (type 2 decision). Larvae are able to modulate the amplitude of their casting movements. If larvae are heading towards the undesirable

temperature the amplitude of their head casts is bigger than when they are heading towards the direction of the preferred temperature (Klein, Afonso et al. 2015). Similar as in chemotaxis the outcomes of turns are biased towards the location of the preferred temperature. First instar larvae navigate gradients as shallow as 0.05 °C/mm (Luo, Gershow et al. 2010). Combining the speed of first instar larvae of approximately 0.1mm/s with the minimal slope leads to an estimation of a sensory sensitivity as low as 0.005°C/s (Luo, Gershow et al. 2010, Klein, Afonso et al. 2015). Klein et al. show that inactivation of the three cells in the DOG that respond to temperature changes, abolishes both positive and negative thermotaxis in their assay[9] (Klein, Afonso et al. 2015). This is possible because the thermosensory cells in the DOG respond to cooling by depolarization and warming by hyperpolarization (Klein, Afonso et al. 2015). In summary larvae are able to navigate temporally and spatially changing gradients by the implementation of two types of decisions. Thus, orientation behaviors can be seen as a sequence of low-level decisions.

Social Interactions

Drosophila larvae form modest aggregations during foraging (Wu, Wen et al. 2003, Durisko, Kemp et al. 2014). Aggregation behavior is slightly increasing during early development and peaks in second instar larvae (Durisko, Kemp et al. 2014). In addition, an aggregation

[9] However it is not clear how this would impact most of the other assays and thermosensors discussed in the section 'The thermosensory system'.

of larvae facilitates the onset of burrowing behavior (Rohlfs and Hoffmeister 2004, Durisko, Kemp et al. 2014).

These social interactions seem to be mediated by olfactory and visual cues. Justice et al. claim that larvae are attracted to the writhing movement of other larvae (Justice, Macedonia et al. 2012). The authors exclude the possibility that attraction is mediates by the olfactory system by presenting the larvae on top of a plastic lid, on the outside of the behavioral chamber. Furthermore, the attraction to the target is abolished in the absence of light or if the target lacks movement. In a follow-up paper the same group postulate that this form of visual attraction develops in a critical period and is defined by the density of larvae during rearing (Slepian, Sundby et al. 2015). Based on the observation that larvae tended to follow the tracks of other larvae, two novel larval pheromones that mediate attraction have recently been described (Mast, De Moraes et al. 2014). These pheromones are both long-chain fatty acids and bind to channel subunit genes of the pickpocket family. This family of receptors is also involved in detecting the male pheromone cVA.

Aggregation behavior and group burrowing might protect larvae from predators (Lefèvre, de Roode et al. 2011) or help break down and soften food (Durisko, Kemp et al. 2014). However, social burrowing is also observed on soft food, thus social behavior might be part of a general strategy to make use of social information (Durisko and Dukas 2013).

Nevertheless, experimental evidence suggests that group effects have only a minor impact on chemotaxis strategy, because larvae

have been reported to navigate chemical gradients as individuals (Monte, Woodard et al. 1989) (Kaiser and Cobb 2008). This conclusion is based on low resolution tracking of two groups of larvae. While one group is attracted to the odorant the other group is indifferent to the same cue. Mass assays with separate and mixed group populations do not influence behavioral performance (attraction vs. indifference) for both groups. However, comparison of mass assays with single larvae experiments reveals a slightly worse performance in the group condition. Although larvae cover similar distances in both conditions, performance declines in proportion to the number of larvae bumping into each other (Kaiser and Cobb 2008).

Decision-making

Decision-making is the process of selecting an action from several alternatives[10]. All animals constantly determine a course of action even though they do not have access to extensive cognitive resources (Kristan 2008, Webb 2012). Psychological research typically focuses on human-like decisions while the neuroethological/behavioral research is geared to reveal the neural mechanisms underlying decisions (Kristan 2008). This difference is revealed in the choice of model organisms. Organisms with numerically simple brains such as insects are used to elucidate the function of neural networks, while human or primate brains are chosen for cognitive studies. Clearly, complex brains are more suitable for research of cognitive tasks. However, I want to argue

[10] https://en.wikipedia.org/wiki/Decision-making

that the choice of model organisms was also influenced by the available technology. Recent progress in technology, such as the availability of cameras and improvements in machine vision and equipment makes it relatively easy to set up an assay to track behaviors of vertebrates and invertebrates alike. This facilitated the adaptation of concepts from psychological models and application to other organisms. Until recently it was assumed that many properties of decision-making are hallmarks of humans or primate brains. However, research into sensory perception has challenged this assumption. Rats are able to base their decisions on uncertainty present in the stimulus (Kepecs, Uchida et al. 2008) and accumulate evidence optimally when making decisions (Brunton, Botvinick et al. 2013). Moreover, rats use a similar strategy as humans when combining information from different sensory systems (Raposo, Sheppard et al. 2012) (Sheppard, Raposo et al. 2013). Could the brains of rodents and smaller animals follow the same principles of perception than our brains? For these reasons I want to argue here that at least in the field of perception, psychological and neuroethological approaches are beginning to converge. In this thesis I refer to decision-making at the level of sensorimotor integration as low-level decision-making[11]. Further, I allude to tasks involving advanced cognitive abilities as high-level decision-making.

[11] At this level of decision-making, information might be processed by elementary cognition, e.g. simulation of the surrounding environment (Webb, B. (2012)), or by neural circuits, shaped and specialized to perform these computations by evolution.

Multisensory Integration in Mammals and Insects

We can only navigate the world by using signals from multiple senses. Multisensory integration ensures that separate streams of information, originating from the same cause are combined to an unified perception. Interestingly, this does not only relate to objects in the external world but extends to everything we perceive. The different variations of the rubber hand illusion (Botvinick and Cohen 1998) and of laboratory induced out-of-body experiences (Ehrsson 2007, Petkova and Ehrsson 2008, Guterstam, Petkova et al. 2011) trick our body into believing that a foreign object, e.g. a rubber hand, is part of ourselves. To induce these illusions, typically, a haptic stimulation (touch) is applied synchronously to our real body and to a foreign body, while our gaze is manipulated in a way that we only perceive the foreign body (including the stimulation). In many cases this is enough to transfer our perception towards the foreign object. These experiments suggest, that a big part of what we label as the sense of self, namely our location in space and ownership of our bodies and limbs, result from an underlying process of multisensory integration.

Traditionally, sensory systems have been studied in isolation. It was assumed that incoming sensory information is first processed separately before being combined in dedicated multisensory brain areas (Penfield and Rasmussen 1950). The superior colliculus (SC) is one of the most studied multisensory areas in mammalian brains (Newell, Mamassian et al. 2010). This brain region is involved in orientation behaviors and receives visual, auditory, and somatosensory input. Receptive fields of multisensory neurons

overlap so that they respond to stimuli from different modalities at the same spatial location (Meredith and Stein 1990). This organization entails that sensory stimuli are more likely to be integrated into a common perception if they are co-localized in space or time (Meredith and Stein 1986, Meredith, Nemitz et al. 1987). In addition, it has been shown that the multisensory enhancement effect is greater for weak unimodal stimuli (Stein and Meredith 1993).

Recent evidence suggests that multisensory processes may activate brain regions formerly thought to be unisensory. Cross-modal interaction refers to the finding that signals from one modality may affect the detection of other modalities. In blind people the visual cortex (V1) is stimulated by Braille reading (Sadato, Pascual-Leone et al. 1996) and sounds (Röder, Stock et al. 2002). Therefore, it is not surprising that other cross-modal interactions have been observed too. It has been shown that the sensitivity to luminance detection is enhanced if a visual stimulus coincides spatially and temporally with an auditory stimulus (Frassinetti, Bolognini et al. 2002). However, in violation of the spatial principle, visual intensity is also enhanced by an accompanying sound regardless of the location of that sound (Stein, London et al. 1996). The improvement to detect visual stimuli with unrelated auditory cues has been confirmed by other groups (Spence and Driver 1997) (McDonald, Teder-Sälejärvi et al. 2000) and is believed to pertain to some type of cross-modal attention effect (McDonald and Ward 2000). Reversal of the experimental strategy also facilitates stimulus perception. This

way, the detection of auditory signals is improved if accompanied by a task-irrelevant light flash (Lovelace, Stein et al. 2003).

Multisensory cues also have an impact on the behavior of insects such as *Drosophila melanogaster*. Male courtship behavior in the fly is one of the most-studied multisensory processes (Krstic, Boll et al. 2009). Males initiate the behavior after favorable gustatory sampling of cuticular hydrocarbons on the bodies of females with their forelegs (Spieth 1974) (Ferveur 2005). Courtship is further mediated by olfactory cues, such as pheromones indicating the state of sexual availability (Brieger and Butterworth 1970) (Kurtovic, Widmer et al. 2007) and food derived odors (Grosjean, Rytz et al. 2011). Both gustatory and olfactory stimuli converge on P1 neurons (Kohatsu, Koganezawa et al. 2011) (Clowney, Iguchi et al. 2015). Activation of these neurons triggers courtship behavior even if there are no other flies present. Visual (Kohatsu and Yamamoto 2015) and auditory cues (Spieth 1974) (Coen, Clemens et al. 2014) are also important for courtship behaviors.

The host-seeking behavior of female mosquitos relies on gradients of CO_2, human scent, and heat (McMeniman, Corfas et al. 2014). CO_2 detection enhances attraction to human scent and is crucial for attraction to heat in the range of human body temperature. A mutation of the CO_2 receptor diminishes the host-seeking behavior but does not abolish it completely. Interestingly, the presence of wild-type mosquitos in a swarm of mosquitos that are unable to detect CO_2, does not rescue the host seeking behavior of all mosquitos. This finding is effectively ruling out the influence of group effects. The combination of CO_2 and odor gradients is

sufficient to trigger feeding from unheated blood. (Woke 1937) (McMeniman, Corfas et al. 2014). One study investigated the nature of cross-modal interactions in adult *Drosophila melanogaster* (Wasserman, Aptekar et al. 2015). It has been shown previously that pairing odors with visual stimuli increases the optomotor response, resulting in improved plume-tracking capability (Chow, Theobald et al. 2011). Wasserman et al. identified a cell in the visual system that responds stronger when visual and olfactory stimuli are presented at the same time. This modulation is mediated by octopaminergic neurons and is induced upon flight initiation (Suver, Mamiya et al. 2012). Even though the stimuli do not share the same spatial location, temporal synchrony alone can be sufficient to increase the robustness of perception.

In *Drosophila melanogaster* the mushroom body (MB) and subesophageal ganglion (SOG) are potential sites of information integration. Lewis et al. proposed that conflicting information is integrated in the MB (Lewis, Siju et al. 2015). During the fermentation of fruits, CO_2 is often released together with odors. The sensory information about ambient CO_2 levels is represented in Kenyon cells (KCs) in the MB and induces an innate behavioral avoidance response in flies (Bräcker, Siju et al. 2013). In the presence of food odors, however, a group of dopaminergic neurons modulates the neural response. This results in a reduction of innate aversion. Tastekin and Riedl et al. have shown that the SOG acts as a multisensory center for sensorimotor integration in *Drosophila* larvae (Tastekin, Riedl et al. 2015). In an attempt to dissect the circuits underlying chemotaxis, the authors have identified a number

of neurons in the SOG causing a defect in the transition from runs to turns during chemotaxis. The defect generalizes to thermotaxis and photophopic orientation behavior. Together with the evidence that the SOG is involved in gustation (Kwon, Dahanukar et al. 2011) they conclude that this area of the larval brain is a multimodal hub for action selection.

Ohyama et al. describe the circuitry of integration of mechanosensory and nociceptive stimuli in *Drosophila* larvae (Ohyama, Schneider-Mizell et al. 2015). Both sensory pathways originate in the body wall and are stimulated by an attack of a parasitic wasp (Hwang, Zhong et al. 2007), triggering a rolling escape response in *Drosophila* larvae. Mechanosensory chordotonal neurons are activated by the vibration of the wing beat and nociceptive multidendritic class IV neurons by stinging. The authors have identified four sites of first-level convergence in the ventral nerve cord (VNC). Half of these are unimodal and react to mechanosensory stimuli only, while the other two sites respond to both types of stimulation. A combined presentation of both stimuli at bimodal sites results in a super-additive enhancement of rolling behavior. Stimulation of bimodal and unimodal sites together further increases the probability of rolling. This is plausible because at a second level of convergence both unimodal and bimodal sites ultimately connect to a command-like neuron in the VNC, called 'Goro'. Activation of this neuron reliably triggers rolling behavior upon stimulation. From there, information ascends to the brain in a multi-step pathway and converges back onto the Goro neuron in a descending pathway. Finally the authors model the multi-level

architecture of convergence and conclude that this architecture improves action selection and therefore leads to a faster escape (Ohyama, Schneider-Mizell et al. 2015).

Ohyama et al. describe the circuitry for cue combination, where both causes point towards the same goal. However, cue conflict has also been studied. Gepner et al. induce photophobic behavior with blue light flashes and attraction behavior with red light flashes in larvae expressing a red light-activated ion channel in their OSNs (Gepner, Skanata et al. 2015). Following a Linear-Nonlinear-Poisson (LNP) approach the authors calculate the average sensory experience before a turn (turn triggered average) for each stimuli (blue and red light) separately. This reveals that larvae turn in response to increases of blue light (avoidance) and decreases of red light intensity (attraction). Next, the authors examined the larval behavior to fluctuating red and blue light at the same time. Turn frequency is highest if the red light intensity decreases and blue light intensity increases. This favored an LNP model assuming early linear integration over a model assuming independence. A recent paper illustrates that in ants the behavior of cue integration is close to optimal (Wystrach, Mangan et al. 2015). Foraging ants rely on a visual compass and path integration. Path integration maintains a home vector pointing towards the starting point of a foraging bout. Furthermore, the authors show that directional uncertainty in the path integrator is proportional to the distance travelled. Ants experience a conflict between path integration and the visual compass after capture on their way to the feeder and release at another location. In choosing their path, ants behave as if the

conflicting cues are weighted by their uncertainty in accordance with Bayesian cue integration (this is the topic of the next section). However, an additional experiment suggests that ants only approximate the Bayesian solution by using the length of the home vector as proxy for uncertainty (Wystrach, Mangan et al. 2015).

The Brain and the Environment

Probabilistic inference: The brain as a statistical machine

Brains are evolutionary products of our interaction with the environment[12]. External stimuli are intrinsically noisy and our sensors are imperfect as well (Faisal, Selen et al. 2008). It has been argued that the variability in the brain is a proxy of the uncertainty in our surroundings (Ma, Beck et al. 2006). How the brain deals with uncertainty lies at the heart of many problems in perception, decision-making and action (Körding 2007). We would perform best if our brains captured and exploited the uncertainty present in the sensory stimuli from our surroundings. In this view the brain is akin to a statistical machine[13]. This refers to the idea that the brain handles information in accordance with statistical principles. Thus, every stimulus should be encoded as a probability distribution and defined by a mean and variance. By contrast, the standard or non-probabilistic approach assumes that the brain encodes just one value - the mean - of the stimulus.

Probabilistic inference is the process of formulating a hypothesis about the surroundings based on incomplete or uncertain evidence (i.e. sensory input) of a hidden cause (hidden variable). To achieve this, the brain should represent every parameter as a probability distribution. This way every possible value is associated with a

[12] Daniel Wolpert: The real reasons for brains
https://www.ted.com/talks/daniel_wolpert_the_real_reason_for_brains
[13] Adam Kepecs: The brain is a statistical engine
http://bigthink.com/videos/the-brain-is-a-statistical-engine

corresponding probability at every time point (Knill and Pouget 2004).

Bayes' rule (Bayes 1763) is a mathematical rule to relate two conditional probabilities with each other. However, it can also be seen as "a law of logical rational inference in the face of uncertainty" (Gallistel and King 2011). It describes how uncertain information can be combined to a probability distribution:

$$p(hypothesis|sensory\ input) = \frac{p(sensory\ input|hypothesis) * p(hypothesis)}{p(sensory\ input)} \quad (1)$$

The numerator consists of the likelihood, p(sensory input|hypothesis) and the prior, p(hypothesis). Together, the likelihood and the prior form a generative model, thereby determining the statistical structure of the task (Pouget, Beck et al. 2013). Further, it establishes how the probabilities of observable variables depend on hidden variables. The likelihood expresses the probability of the observed sensory input with respect to the hypothesis about the state of the world. The prior, or prior experience represents the information already known before the combination with the likelihood. There are a number of examples for very strong priors in humans, causing persistent illusions (Shams, Kamitani et al. 2000) (Vilares and Kording 2011). One of them is a strong assumption, that light comes from above. At times this can impact our spatial perception, such as in figure 3. Due to the orientation of the gradients, we perceive the left circle as a groove and the right circle as a bump. The denominator of Bayes' rule, p(sensory input), is called the marginal likelihood and acts as a scaling factor. The result of Bayes' rule is the posterior distribution,

p(hypothesis|sensory input). This distribution has some special properties. Its mean is shifted towards the narrower probability distribution and its variance is smaller than the variance of the prior and the variance of the likelihood distribution.

Figure 3: An example of a visual illusion caused by a prior. The assumption that light comes from above results in perception of a groove on the left circle and a bump on the right circle. The gradient in the left circle is interpreted as a groove because a light source from the top generates a shadow in the upper half and only illuminates the bottom half. Reversing the gradient leads to a bump, where the upper half is illuminated and the bottom half is in the shadow.

Bayes' rule formulates how the prior information of a hypothesis should be updated with new information. The posterior of the previous step is the prior of the next step of iteration. These concepts have been expanded to a number of applications, e.g. to allow inference over space (Ma, Navalpakkam et al. 2011) and time[14]. Causal inference is another application of Bayes' rule to infer the structure of the world. A typical example is a perception that arises from multiple separate and independent causes or relates to a common cause. Therefore, the Bayes' approach compares the probability of different and ultimately exclusive scenarios, by

[14] Hidden Markov models (HMM) describe the change of latent variables over time. The Markov property states that the conditional probability of the future is only dependent on the present state and independent from the past. HMMs with continuous variables and Gaussian distributions are called Kalman filter Kalman, R. E. (1960)).

combining the prior probability with likelihood for each scenario (Knill 2003, Tenenbaum, Griffiths et al. 2006, Körding, Beierholm et al. 2007).

In many interesting scenarios the shape of the prior can be neglected. This is either because the effect of a prior is eliminated by the design of the experiment[15] or the prior is very broad and hence it is not informative. For instance, if the prior covers several orders of magnitude of a physical variable, then the likelihood given an observation can be considered as very narrow compared to the prior. Therefore, in these cases the prior can be safely assumed to be flat[16] over the entire range of possible stimulus values.

Cue integration: a way to test probabilistic inference

Instead of combination of a prior and likelihood, cue integration usually combines the information of two distributions of sensory cues. A graphical model (Pearl 2000) represents this scenario (Fig. 4). The graphical model shows no direct connection between two cues in the model because the sensory inputs are assumed to be independent.

[15] If the experiment is designed as a two-alternative forced choice (2AFC) task the effect of the prior is eliminated.

[16] Flat priors have a uniform probability across the entire range of values. For this reason every possibility is equally likely.

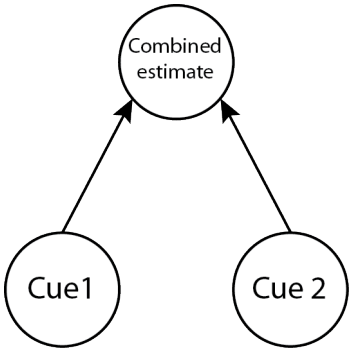

Figure 4: Cue integration. The graphical model depicts the integration of two independent cues to a combined estimate according to Bayes' rule.

The idea that sensory perception implements some form of probabilistic inference can be dated back to Ernst Mach (Mach 1886) and Hermann von Helmholtz (Helmholtz 1891). However, solid evidence in favor of the probabilistic nature of sensory integration was only added during the last two decades.

A typical cue combination experiment starts with a separate assessment for each cue[17]. Next, the combined experiments are performed with different levels of uncertainty for one cue[18]. If the brain represents probabilities and combines them according to Bayes' rule, the brain should weight each cue according to its reliability (Knill and Pouget 2004). The theoretical weight of each cue can be calculated and these predictions are compared with the experimental results. If the fit of the prediction is good it is concluded that the behavior follows Bayes' rule, i.e. that it is Bayes optimal. This is only possible if the brain has access to the reliabilities of the cues (Ma and Pouget 2008).

[17] This is usually assessed with a psychometric curve.

[18] The manipulation of stimulus uncertainty depends on the nature of the cue. It is easiest to corrupt visual stimuli e.g. by adding noise to a cue shown on a screen.

In a study testing cross-modal integration between the visual and haptic (touch) system, subjects estimate the width of a bar. Humans have been found to integrate cues in a statistical optimal fashion. (Ernst and Banks 2002). Optimality can be described with respect to the mean (μ) and the variance (σ^2) of the posterior distribution. To be optimal the cues have to be weighted (w_v weight for the visual cue, w_t weight for the touch cue) so that each cue contributes to the mean of the combined estimate (μ_{vt}) according to its reliability (eq. 2, Fig. 5).

$$\mu_{vt} = \frac{1/\sigma_v^2}{1/\sigma_v^2 \, 1/\sigma_t^2} w_v + \frac{1/\sigma_t^2}{1/\sigma_v^2 + 1/\sigma_t^2} w_t \quad (2)$$

In addition, the variance (σ_{vt}^2) of the combined distribution has to be smaller than the variance of each of the unimodal distributions (eq. 3, Fig. 5).

$$\sigma_{vt}^2 = \frac{\sigma_v^2 \sigma_t^2}{\sigma_v^2 + \sigma_t^2} \quad (3)$$

This property of the posterior distribution is connected to the increase of information (Pouget, Beck et al. 2013). The peak of the posterior distribution reflects the most likely value of the stimulus, while the width takes the uncertainty into account (Fig. 5).

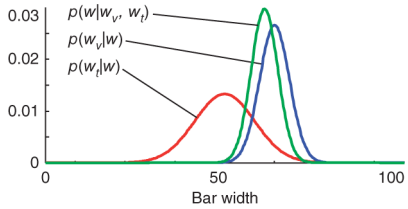

Figure 5: Bayesian cue integration between the visual and haptic system. Subjects estimate the width of bar by vision and touch. Every sensory cue is represented as a probability distribution: touch (red) $p(w_t|w)$; vision (blue) $p(w_v|w)$; posterior (green) $p(w|w_t,w_v)$. The peak of a distribution represents its mean, the width its reliability. The mean of the posterior is computed by weighing each cue according to its reliability (eq. 2). Therefore, the distribution is shifted towards the narrower (visual) probability distribution. The variance of the posterior distribution is smaller than the variance of the haptic and the variance of the visual probability distribution (eq. 3). Figure taken from (Pouget, Beck et al. 2013)

Ernst et al. show that integration of information only takes place under certain conditions. Normally (e.g. daylight), the detection threshold of the visual system is markedly lower than the threshold for the haptic system. In this case, the haptic information is ignored and the perception is captured by the visual system. The addition of noise to the visual scene elevates the visual detection threshold. If the visual detection threshold is above the haptic threshold, perception is captured by the haptic system instead. Thus, integration of information only takes place when both cues have similar detection thresholds [19]. The predictions of the model matched the captured conditions as well as the case of cross-modal integration.

Ventriloquism is a prime example for a visual-capture effect (Alais and Burr 2004). Typically we perceive voices as emanating from

[19] In psychophysics detection thresholds are defined as the difference of a property when it is judged 84% of the time higher than the same property at the point of subjective equality.

moving lips. Astonishingly, this is also the case when the only moving lips in sight are from a puppet[20] or pictured on a screen. Similarly, subjects estimating the azimuthal location of simultaneous short light flashes and brief sounds perceive this visual capture effect. Crucially, subjects have been primed to perceive both signals as a combined event, such as a ball hitting the screen. High uncertainty in the visual signal leads to an "inverse ventriloquist effect" where sound captures vision. Although we rarely experience this effect, it means that the position of a blurred dot is perceived close to the position of the sound. For noise levels in-between these extremes, the bimodal data follows the rules of Bayesian sensory integration.

Bayesian cue combination also happens within the same modality (Knill 2003) (Jacobs 1999). When subjects infer the depth of a cylinder from visual motion and texture cues, their behavior can be described with a Bayesian model. In the latter study (Jacobs 1999) the author tested two Bayesian models with different assumptions. The first model assumed uniform prior distributions and let to a good fit. In nature however, cylinders e.g. trees, tend to have a circular base. Thus, the second model incorporated the prior, that all participants assumed that the cylinders were circular. This model resulted in an even better fit to the data. This illustrated that differences in initial assumptions can bias the modeling approach.

[20] It could be argued that the knowledge that a puppet cannot speak can also be considered a prior knowledge. Indeed, this illusion is so common that no adult believes that the puppet is speaking. However, it seems that this additional prior at the cognitive level does not change the illusion itself or at least does not interfere with the perception when we know that the setting is artificial. We are happy to exploit this illusion when we are watching television.

The next section describes the potential impact of incorrect assumptions on the inference process.

The limits of probabilistic inference

Optimal inference is only possible if the structure of the generative model[21], that is the distribution of the likelihood and the prior, are fully known. Any deviations from the natural distributions of the prior or the likelihood, either introduced through assumptions or due to the experimental setup, result in suboptimal inference (Ma 2012). Especially scenarios of cue conflict are often artificial. For example, the McGurk effect (McGurk and MacDonald 1976) introduces a subtle dissonance into the visual and auditory stream of information and thus violates the underlying prior of synchrony (Ma 2012). For this reason it may not be possible to observe optimal cue combination under these conditions.

The level of suboptimality in the inference process depends on the extent the generative model deviates from what is encountered in the world (Ma 2012). For severe deviations from reality, suboptimality impacts behavior more than the effects of internal and external noise (Beck, Ma et al. 2012). Due to the complexity of the generative model of some real world tasks, suboptimal behavior might be inevitable in the long run. Especially high-level decision-

[21] The generative model defines the assumed underlying statistical structure of a task. It describes a probabilistic model based on hidden variables that creates data for a specific set of the parameters. In our case the generative model is made up of the likelihood and the prior
https://en.wikipedia.org/wiki/Generative_model

making is influenced by psychological biases (Kahneman and Tversky 2000) and might follow other decision strategies such as heuristics (Hutchinson and Gigerenzer 2005).

However, the distinction between optimal and suboptimal behavior is not connected with assumptions about the probabilistic nature of a computation. Even if an inference process is suboptimal it can still be probabilistic (Ma 2012). This is important because the essence of the probabilistic approach is not that behavior should be Bayes optimal: it is about the representation of information in the form of probability distributions and how the brain uses this information (Griffiths, Chater et al. 2012) (Pouget, Beck et al. 2013). This reverses the current reasoning from "optimality implies probabilistic representations" to "use of a probabilistic decision rule entails encoding of probability distributions in the brain" (Ma 2012).

Representations and encoding of probability distributions in the brain

There are a number of possibilities of how uncertainty and probability distributions can be represented in the brain. The probabilistic and non-probabilistic approaches agree that neurons represent the mean of a sensory signal. Thus, what is left for the probabilistic approach to show is how uncertainty is represented in the brain. Since this topic is not the focus of this thesis I am restricting myself to highlight a few key concepts.

In principle, uncertainty can be encoded in the same neuron as the mean or in separate neurons. As for the latter possibility, it has been shown that populations of neuromodulators represent uncertainty in

different brain areas. For example, dopaminergic neurons represent the uncertainty of reward in the midbrain of primates (Fiorillo, Tobler et al. 2003). In all this and similar studies, however, representations of uncertainty relate to high-level tasks and not to low-level tasks such as uncertainty in sensory perception. To study the representation of uncertainties together with the mean in sensory systems, the encoding of the stimulus is an obvious starting point. The theory of probabilistic population codes (Ma, Beck et al. 2006) proposes that the uncertainty in the environment is represented by the variability of signals in the brain (Mainen and Sejnowski 1995). A stimulus is captured by the activity of the subset of neurons tuned to respond to it. Its mean and reliability can be extracted from the population activity if the statistical process underlying the variability is known. If the underlying probability is Poisson-like (Tolhurst, Movshon et al. 1983, Graf, Kohn et al. 2011, Berens, Ecker et al. 2012), population codes can perform Bayesian inference by summing activity over neural populations even though tuning curves are completely different (Chater, Tenenbaum et al. 2006).

Bayesian Decision Theory

Perception alone is enough to form a decision. To execute the decision, however, action is needed. Activation of muscles is one of the few ways we can affect the world around us. Every action has a cost. This consists partly of the energy spent on the movement itself, but also includes the potential rewards and setbacks of the consequences the action entails. To calculate the expected costs of

actions the probabilities of the world states are multiplied with a cost function. In the final step of Bayesian decision-making an optimal behavior is a behavior that minimizes the costs. As a consequence decision-making can only be called optimal with respect to the cost function (Ma 2012).

Cue integration and motor control are both fields where Bayesian statistics are applied. Movement planning follows Bayesian principles to minimize the variance and thus expected cost (Kording and Wolpert 2004). In contrast to high-level economic tasks it has been shown that sensorimotor tasks can be optimal in a way that they minimize cost and maximize expected utility (Trommershäuser, Maloney et al. 2008).

About this study

Aims of the study

In this study I show that (i) larvae are able to combine information within and across sensory modalities. In collaboration with theorists I work towards (ii) developing a model that predicts the increase in behavioral performance when larvae are exposed to multiple cues as compared to just one cue. By manipulating uncertainty associated with one cue I aim to show that (iii) the behavior of sensory integration follows Bayes' rule and establish that even numerically simple brains are able to encode probability distributions.

Scenarios for sensory integration and experimental strategy

Larvae encounter an abundance of sensory information in their environment. In the cue combination paradigm, information can be combined within the same modality (olfaction) or across modalities (olfaction and thermosensation). I refer to these as intramodal and intermodal integration, respectively.

In this study I investigate both categories of sensory integration. I chose to study the thermosensory and olfactory system as the modalities of interest, because larvae are able to navigate both thermosensory and odor gradients in a similar way. (Luo, Gershow et al. 2010) (Gomez-Marin, Stephens et al. 2011).

Information should be combined in a way that represents the causal structure of the world (Tenenbaum, Griffiths et al. 2006). Therefore,

I defined scenarios larvae encounter in their natural habitat, where it is beneficial to combine sensory information within or across modalities. Every smell is composed of a multitude of different chemical compounds (Tressl and Drawert 1973) activating different subsets of OSNs. Thus, I assume that larvae are able to integrate information within the same modality. I test intramodal integration by presenting two congruent odor gradients to larvae (Fig. 6 A). For intermodal integration, I imagined a scenario where a potential food source (indicated by an odor gradient) is partially exposed to sunlight. This results in a thermal gradient across and around a batch of food. Ectotherms, like *Drosophila* larvae, have to use behavioral strategies to regulate their temperatures (Stevenson 1985). Therefore, larvae have to avoid excessive heat to survive. In such a scenario larvae are expected to aggregate on the side of the food with the preferred (cooler) temperature (Fig. 6 B).

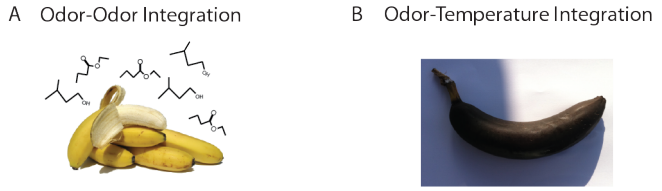

Figure 6: Scenarios to study multisensory integration. (**A**) Odor-Odor Integration. A banana smell consists of multiple odorants (pictured). I picked two of these odorants and presented them during the unimodal and combined experiments. (**B**) Odor-Temperature Integration. A food source, like a ripe banana (pictured) could be partially in exposed to the sun. Larvae should aggregate at the side of tolerable temperature. Thus, I exposed larvae to odor gradients and temperature gradients at the same time.

Chapter 2: Materials and Methods

Fly stocks and animal preparation

Fly stocks were raised in a 12h light- dark cycle and kept at 22°C. An exception was made for the comparison of chemotaxis between different developmental stages. These flies were kept at 25°C according to a protocol shared between various labs. Moreover, larvae containing light gated opsins, were raised in the dark. For first instar L1 larvae adult flies were held in fly cages and egg laying was allowed for 2h on molasse plates with yeast paste. L1 larvae were collected at 30h AEL +/- 2h hour and used for experiments. Third instar (L3) larvae were reared for 120 hours in tubes on conventional cornmeal-agar fly food.

In this study I tested the behavior of three strains considered as wild-type: w^{1118}, CantonS and CantonS-Magdeburg[22]. The Gal4-UAS expression system (Brand and Perrimon 1993, Luo, Callaway et al. 2008) was used to generate larvae with a single functional OSN (Fishilevich, Domingos et al. 2005). This was achieved by restoring the co-receptor *Orco* in a single OSN in an *Orco* null mutant background. Thus, I generated larvae with just the *Or42a*-expressing OSN functional by crossing: *w*;*Or42a*-Gal4;UAS-*Orco*,$Orco^{-/-}$ with *w*;+;$Orco^{-/-}$ (both stocks were a gift from Vosshall Lab), *Or42b* OSN functional: *w*;*Or42b*-Gal4;UAS-*Orco*,$Orco^{-/-}$ (gift from Vosshall Lab) with *w*;+; $Orco^{-/-}$, and *Or13a* OSN functional: w;*Or13a*-Gal4;UAS-Orco,$Orco^{-/-}$ (generated by Mariana Lopez Matas) with *w*;+;$Orco^{-/-}$.

[22] Collaborators shared this stock with us. It was used exclusively to compare between different developmental stages. Unfortunately it was shown later that it might be contaminated.

For experiments involving the use of Channelrhodopsin I used flies with the genotype: Or42a-Gal4,GMR>hid/UAS-Orco, UAS-ChR2-H134R;*dtrpA[1]*,*Orco*$^{-/-}$ (Schulze, Gomez-Marin et al. 2015). The Chrimson stock (*w*;+;UAS-CsChrimson-mVenus) was a gift from the Jayaraman lab. I used *w*;+;*Or67b*-Gal4 and *w*;*Or42a*-Gal4;+ to drive the expression of Chrimson in single OSNs.

All behavioral experiments were performed between 22-24°C and 50-60% humidity. Due to their small size, first instar larvae were selected under a dissecting microscope and transferred to a 3% agarose plate prior to testing. Following a protocol established elsewhere (Hutchinson and Gigerenzer 2005, Louis, Huber et al. 2008), third instar larvae where separated from the food by rinsing with a 15% (w/V) sucrose solution. Testing occurred between 30 to 120 minutes after the introduction of the sucrose.

Optogenetics, virtual odor realities and noise

Optogenetics is defined as the use of genetic tools to deliver light sensitive microbial opsins to target cells, thus making them amenable to optic manipulation (Deisseroth 2011). This allows for precise control of spiking in neurons, by millisecond control of a light stimulus (Boyden, Zhang et al. 2005). In neuroscience this approach was pioneered in the early 2000s by a small number of labs (Zemelman, Lee et al. 2002, Boyden, Zhang et al. 2005, Lima and Miesenböck 2005) and its use has been increasing ever since (Boyden 2015, Deisseroth 2015).

Channelrhodopsin, a non-selective cation channel gated by blue light, was the first opsin adopted by a wide audience (Boyden, Zhang et al. 2005). However, *Drosophila* larvae were sensitive to blue light (Hassan, Iyengar et al. 2005, Sprecher and Desplan 2008) (Keene and Sprecher 2011). This response was mediated by the photoreceptors of the larval bolwig's organ (Sprecher and Desplan 2008) and light class IV multidendritic neurons in the body wall (Xiang, Yuan et al. 2010). Photoreceptors were inactivated by the expression of an apoptosis-inducing protein hid (Haining, Carboy-Newcomb et al. 1999) in the Bolwig's organ (GMR>hid). Furthermore, the photophobic response of body wall neurons was abolished after the deletion of the *dtrpA1* gene, thus rendering the larvae insensitive to light (Schulze, Gomez-Marin et al. 2015). The latter mutation also abolished the ability of larvae to thermotax, although it was not clear if that was due to the mutation or genetic background effects (see section 'Different strains show different ability to thermotax' for more information). Efforts to preserve

thermotaxis while inactivating the photophobic response by deletion of the gene for gustatory receptor *Gr28b* as described in (Xiang, Yuan et al. 2010) were not successful. This strategy kept thermotactic behavior intact but failed to abolish the avoidance of blue light at high intensities (data not shown).

These problems were solved by the introduction of Chrimson (Klapoetke, Murata et al. 2014), an opsin gated by light in the red range. Since larvae are not sensitive to red light at low intensity no further mutations were necessary to make larvae blind (Salcedo, Huber et al. 1999, Xiang, Yuan et al. 2010).

I used optogenetics to mimic input to the olfactory system for three purposes: the generation of virtual odor realities guiding behavior (Bellmann 2010, Gepner, Mihovilovic Skanata et al. 2015, Hernandez-Nunez, Belina et al. 2015, Schulze, Gomez-Marin et al. 2015), for electrophysiology (Schulze, Gomez-Marin et al. 2015) and for the generation of noise.

The light gradient and noise were generated by LEDs mounted above the setup. The intensity of the light gradient was assessed with a photodiode at different voltages. I chose to perform experiments at 12.5% of total power. This corresponded to 0.625V and a light intensity of 1.37 W/m^2. (see 'An assay to test sensory integration' for more details on the gradient geometry and placement of LEDs). To test the effect of noise I added light flashes on top of a light gradient (positive noise) or flashed the light gradient itself (negative noise). The duration of each light flash was fixed to 100 ms while the inter-flash interval was randomly drawn

from a Poisson distribution (Tolhurst, Movshon et al. 1983, Graf, Kohn et al. 2011, Berens, Ecker et al. 2012). However, the minimal interval in Labview was set to ten milliseconds. Therefore, all the interspike intervals presented were the minimal- or multiples of the minimal interval. Importantly, I used the same temporal noise sequence for all experiments (frozen noise). For experiments in the light gradient I extrapolated the voltage input to achieve 50% of the peak intensity of the gradient. This corresponded to 0.294V and a light intensity of 0.69 W/m^2. For noise in odor gradients I exposed larvae to 11.15 W/m^2 (4V).

Tracking of Animal Posture and Movement

Behavioral arena

To compare behavior between different developmental stages I used an established assay (Gomez-Marin, Stephens et al. 2011) (Fig 7). First, I reproduced the results of the previous analysis with wild-type w^{1118} larvae. Afterwards, I tested the difference between L1 and L3 with CantonS-Magdeburg larvae.

To create the behavioral arena, a rectangular lid (Falcon 353071 lid for 96 well plates, Corning Inc., USA) containing an odor droplet in the center was inverted and placed on top of a slab of 3% agarose (Falcon 353958 rectangular plate lid, Corning Inc., USA). After waiting approximately 15 seconds for the odor gradient to establish itself, the lid was slightly tilted and a single larva was introduced into the center of the arena. Tracking lasted for a maximum of five minutes for L3 larvae and six minutes for L1 larvae. Tracking automatically ceased whenever the larva left the field of view. The behavioral arena was illuminated from above by a flat light pad (Slimlite Lightbox, Kaiser).

Sensory Orientation Software

Behavior was recorded at five frames per second (fps) with a video camera (scA1390-17fc, scout series, Basler) placed under the setup. Tracking and image processing were performed with the *SOS-track* software (Gomez-Marin and Louis 2012, Gomez-Marin and Louis 2012, Gomez-Marin, Partoune et al. 2012). This software package

was used to extract the positions of head, tail, centroid and midpoint from every frame and calculated all kinematic variables. The sensory gradient was mapped onto these positions to determine the sensory experience of the larvae.

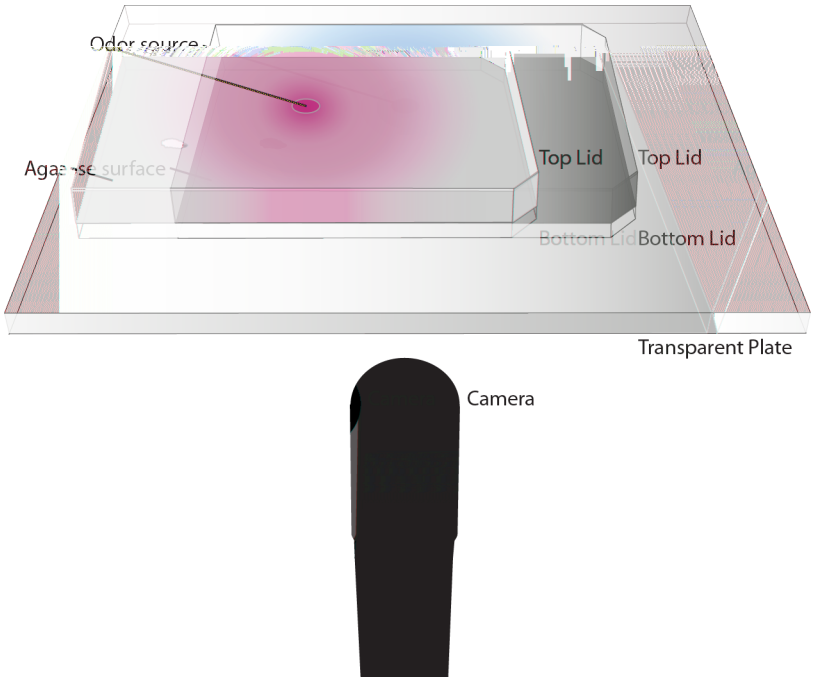

Figure 7: Behavioral Setup for the SOS-Tracker. At the start of every experiment a rectangular cover (bottom lid), which was coated with a layer of 3% agarose, was placed on top of a transparent plate. Next, 10 µL of an odor dilution was pipetted into a single well of a second lid, which was inverted onto the agarose surface (top lid). After the odor gradient was established, the top lid was tilted and a larva was introduced into the center of the behavioral arena. Larval movement was recorded with a camera, mounted below the setup. The behavioral arena was illuminated from above (not shown).

Definition of Turns and Weathervaning

Larval trajectories were decomposed into runs and turns by fitting small linear segments (segment length: 0.2 and 0.5 mm for L1 or L3, respectively) to the trajectories and calculating the angle between these fragments (Schulze, Gomez-Marin et al. 2015). If this angle passed a threshold of 20 degrees the reorientation movement was scored as a turn. We relied on a bootstrap strategy to estimate the errors in the turn probabilities. The represented estimate of the standard error was calculated as described in (Martinez and Martinez 2012). Weathervaning was quantified as described in (Gomez-Marin and Louis 2014).

Multisensory integration

An assay to test sensory integration

To test the intermodal and intramodal scenarios, I built a custom-made behavioral assay, to record the larval response to chemical and thermal gradients (Fig. 8 A). Two Peltier elements[23] (CPP-065, TE Technology Inc., USA) were attached to a rectangular copper plate via thermo-conductive paste (Céramique, Arctic Silver, USA). Between the Peltier elements, two temperature sensors (Thermistor: MP-2444, TE Technology Inc., USA) were embedded (Thermo-conductive glue, Arctic Aluminia, Artic Silver) into the metal plate. Each sensor was positioned next to a Peltier element, and just outside of the behavioral arena. Both sensors were connected to a control unit (TC-48-20, TE Technology Inc, USA; powered by: PS-24-6.5 ,TE Technology Inc., USA), which was regulating the output of the Peltier elements. The temperature at each sensor was recorded with a software package provided by the supplier (TC-48-20, TE Technology Inc., USA). For an independent temperature assessment, I used a thermometer with a surface probe (MM2000, TME Electronics, UK, and TS01-S, Surface/Immersion Probe Backfilled, TME Electronics, UK) and an infrared thermometer (Fluke 561, Fluke, USA). By controlling the temperature at each sensor I was able to generate linear temperature gradients between the sensors. In the same way I created a "neutral" background, i.e.

[23] A Peltier element is a thermoelectric heating device using the Peltier effect for heating or cooling. A DC current passes through an alternate array of n-type and p-type semiconductors transports heat from one side to the other.
https://en.wikipedia.org/wiki/Thermoelectric_cooling

without a temperature gradient, by setting the same temperature at each sensor. I visualized temperature gradients with Liquid Crystal Display sheets (NT61-161, Edmund Optics, USA).

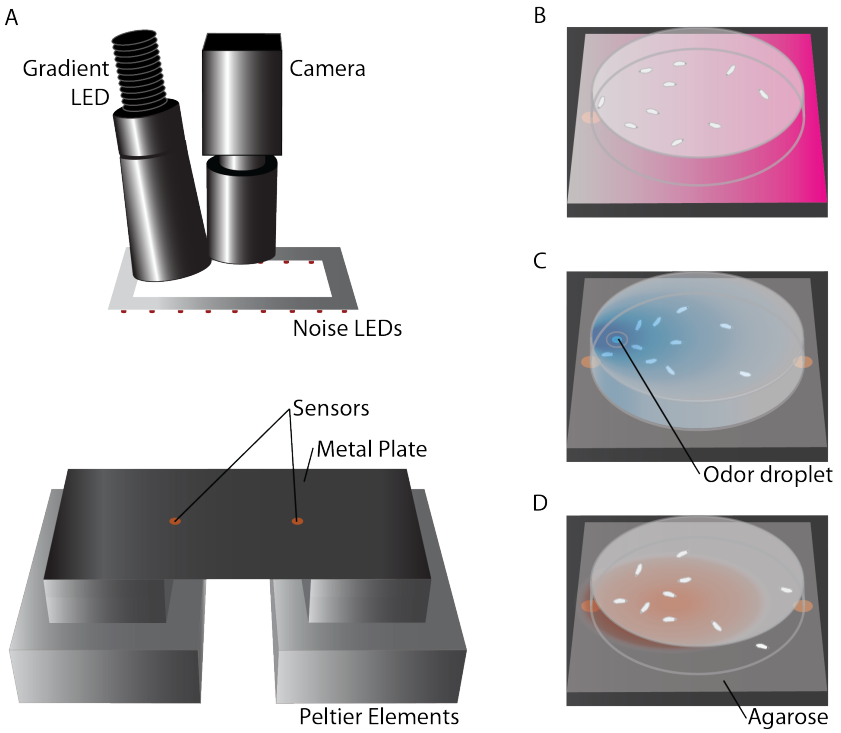

Figure 8: An assay to test sensory integration. (**A**) Two Peltier elements were attached to a metal plate. Next to each Peltier element, a temperature sensor was embedded into the metal plate. The temperature of every sensor was monitored by a separate control unit, which regulated the Peltier element (not shown). Red light gradients and noise were generated by LEDs (625nm) mounted above the assay. A camera recorded larval behavior. (**B**) Linear temperature gradients were established by setting different target temperatures at each sensor. Before the start of every experiment a slab of agarose was placed above the metal plate between both sensors. After larvae were exposed to the established gradient, they tended to avoid the hot side (magenta) and accumulate on the half with the preferred temperature. (**C**) An odor gradient emanated from a droplet of odor presented at the roof of an inverted petridish. (**D**) Light gradients were generated by the gradient LED mounted above the setup. A mask in front of the LED modulated the light. Larvae were attracted towards the peak of the odor and light gradient.

At the start of an experiment the temperatures of the sensors were set to the desired values and a quadratic slab of agarose (SeaKem, LE Agarose, Lonza, Switzerland) was placed in the middle of the copper plate. After the temperature gradient was established I placed ten third instar larvae on the agarose surface in a way that five larvae started at either side of the midline. Next, a Petridish was inverted and placed on top of the agarose between the temperature sensors. Thus, the behavioral arena was enclosed (Fig. 8 B). When odor- or light gradients were presented without a temperature gradient, both sensors where set to 22 °C (neutral background) instead. To create odor gradients I pipetted 5 µL of an odorant dilution into a transparent reinforcement ring stuck to the bottom of a Petridish with a diameter of 90 mm, before placing larvae on the agarose. (Fig. 8 C). To elicit chemotaxis in a red light gradient (625nm), a LED was placed above the setup (PLS-0625-030-S, Mightex Systems, Canada). The emitted light passed through a mask (exponential cone r=16.5mm diameter, Leicrom, Spain) in front of the LED resulting in a light gradient in the behavioral arena (Fig. 8 A, D). The geometry of this gradient was assessed by averaging images and mapping them onto the petridish (Fig. 9 A, B). In noise experiments, light flashes illuminating the behavioral arena evenly, were added on top of the presented gradients. These flashes originated from a custom built rectangular contraption lined with red LEDs (Flexible LED strip red 30 x SMD-LED, 850 nm, 12 V, Lumitronix, Germany) facing towards the behavioral area (Noise LEDs, Fig. 8 A). After the start of the experiment a camera (Stingray F145B ASG, Allied Vision Technologies GmbH, Germany) recorded the behavior of the group of ten larvae for 300

seconds at seven frames per second. An infrared filter (Optical Cast Plastic IR Longpass Filter, Edmund Optics, USA) was placed in front of the camera to exclude any light artifacts. The assay was illuminated by a circle of infrared LEDs (SMD5050-IR InfraRed Tri-Chip Flexible LED strip, 850 nm, Ledlightworld LTD, UK), placed on the outside of the behavioral arena (not shown). This LED ring was not in contact with the copper plate and did not interfere with the temperature gradient.

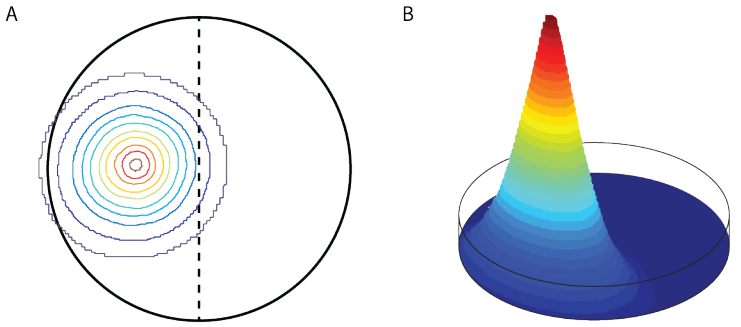

Figure 9: Assessment of light gradient. (**A**) A contour plot of light intensities was mapped onto a representative location of the petridish. (**B**) A 3D reconstruction of the light gradient, approximately mapped onto the model of a petridish

Quantification of behavior

Larvae were tracked with a custom-written software in MATLAB. Tracking was performed offline and the analysis was usually restricted to the approach phase, i.e. the first 180 seconds of the experiment. First, I applied a black-and-white threshold to every acquired gray scale frame. The resulting picture was subtracted from a background image. The background image was not the same over

the course of the whole experiment. Rather, I computed separate background images for time bins of thirty seconds, over all available frames (7 fps), to improve the quality of tracking. After subtraction I used a size threshold to identify big objects in the image and deleted them if necessary. Afterwards, all remaining blobs were labeled and sorted by size in descending order.

In the first frame of an experiment, the initial positions of larvae had to be labeled. This task could be performed by hand or automatically. A requirement for automatic recognition was that all larvae could be identified as separate blobs (i.e. were not touching). In this case, the algorithm was looking for a predefined number of blobs in a designated starting area. After identification of larvae in the first picture, their change of positions was tracked over time. For this, all the distances between every identified larva in the present frame, and every blob in the next frame were computed. Subsequently, the blob closest to the present position was assigned the 'best match' to represent the same larva in the next frame. Moreover, the distance of displacement had to be below a predefined threshold of maximal possible displacement. If the same blob was identified as the best match by two or more larvae, this issue was resolved by ranking all the following matches in an ascending order. The larva with the longest distance to the second best match was granted its preferred match, while the others were assigned to their secondary choices. This algorithm was continued until multiple tags of the same blobs were resolved. In case this was not possible because the distances exceeded the threshold maximal possible displacement it was assumed that the larvae were touching

each other, and the positions of these larvae were assigned to the closest blob. If this happened, the surroundings of multiple tags were monitored for free blobs in subsequent images. An untagged blob below the threshold of maximal distance of displacement usually meant that larvae had separated and would be tagged accordingly. Sometimes a larva could not be assigned to candidate blob in the following picture. This was mostly due to tracking errors of larvae at the edge of the behavioral arena. Errors of the tracking algorithm, e.g. retagging of larva when they reappeared, were corrected manually.

Unlike more sophisticated tracking solutions (Pérez-Escudero, Vicente-Page et al. 2014) this strategy did not conserve identity of the animals. Consequently, I did not have direct access to the complete trajectories but merely to the centroid positions over time. Therefore, I decided to quantify the observed behavior with a preference index (PI). This index was calculated as the number of larvae on the half circle of the preferred site of aggregation (e.g. odor source or preferred temperature) divided by the total number of larvae on the plate (Fig. 10). Thus, I deemed it sufficient to analyze just one frame per second.

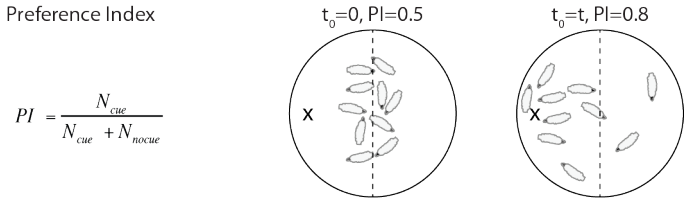

Figure 10: Preference Index (PI). The preference index was calculated by dividing the number of larvae on the side of the cue (peak of odor- and light gradient, preferred temperature) by the number of larvae on the plate. In the beginning of an experiment larvae were uniformly distributed across the two halves of the behavioral arena. Later, during the experiment the PI rose due to attraction of larvae towards the stimulus.

The preference index over the course of an experiment could be quite variable from one experiment to the next. Accordingly, multiple experiments were performed to compute a representative progression of the PI over time for every condition. Therefore the behavior of larvae in absence of a stimulus (Fig. 11) resulted in an average PI around 0.5.

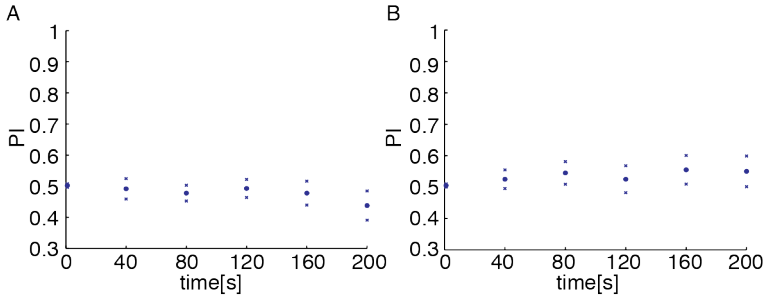

Figure 11: Larvae behaved randomly in absence of a directional stimulus. (**A**) Temperature control. The distribution of larvae on agarose without a temperature gradient was random (neutral temperature background: both sensors were set to 22˚C). Note: The full dataset was analyzed at 1, 40, 80, 120, 160 and 200 seconds and plotted accordingly. Experimental conditions: *Or42a*-Chrimson n=10, *Or67b*-Chrimson n=10 (**B**) Noise Control. The addition of noise (light-flashes) did not cause a bias in the distribution of larvae. Experimental conditions: *Or42a*-Chrimson n=20, RT23˚C. The red LEDs above the behavioral area were on during the whole experiment (intensity: 11.15 W/m²).

Experimental strategy

To test sensory integration in larvae I followed a simple behavioral strategy. Every dataset consisted of three conditions: two sets of unimodal experiments, where just one cue was presented, and the combined condition, where both cues were present. During odor-odor integration I investigated the integration effect between two congruent odor gradients (Fig. 12 A). In the odor-temperature integration scenario I presented an odor gradient and a one-dimensional temperature gradient, in a way that the preferred sites of aggregation (the peak of odor intensity and the preferred temperature) were overlapping (Fig. 12 B).

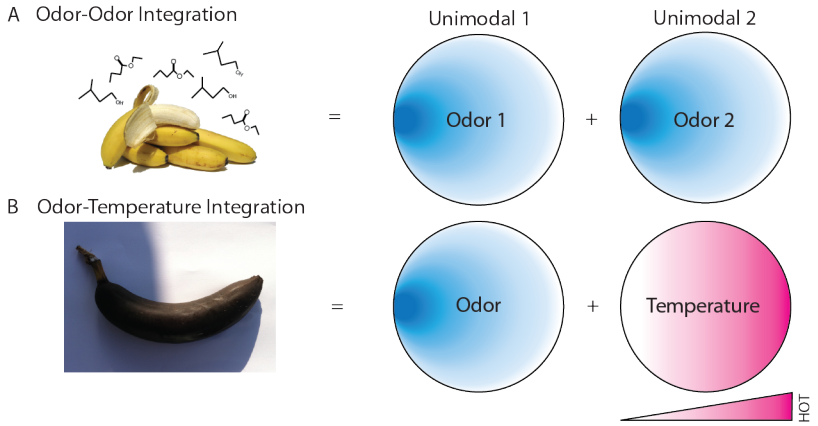

Figure 12: Experimental strategy. Every scenario consisted of two unimodal and the combined condition. First, larval behavior was tested with each unimodal cue (Unimodal 1 and 2) separately. Second, both cues were presented together. (**A**) Odor-Odor Integration. (**B**) Odor-Temperature Integration

When the effect of noise was tested it was necessary to repeat these three conditions in the presence of noise. Therefore, the total

number of conditions was augmented to six. If larvae were able to combine information from different sources we expected to see improved behavioral performance in the combined case. Except for the initial experiments in wild-type, all experimental conditions were interleaved.

A probabilistic framework for sensory integration in larvae

To test the hypothesis of optimal sensory integration, a theoretical framework was developed together with Ruben Moreno and Alexandre Pouget. This framework predicted the performance of larvae exposed to two sensory gradients (combined condition) as a function of their performance in the single-gradient conditions. A Bayesian model predicted the combined behavior according to the principles of probabilistic inference. In a second, fixed-weight model the information was combined in a suboptimal manner.

Two experimental conditions were considered: the scenarios of intramodal and intermodal integration. The first tested integration of information between two odor gradients, the second between an odor and a temperature gradient. Mathematically these two conditions were described with the same formalism. Instead of referring to either temperature- or sensory gradients I will use 'cue 1' and 'cue 2' during this derivation. The two sensory gradients were congruent and thus always pointed in the same direction.

The Bayesian model: defining an optimal decision rule

The Bayesian model tested the hypothesis of optimal cue integration. To guide behavior, larvae had to estimate the direction of favorable gradient change. This direction was described by a hidden variable s, which was set to s=1 if larvae where heading in the favorable direction and s= -1 if they heading away from it. After larvae were introduced in the middle of the agarose surface, they were exposed to well controlled sensory gradients. Larvae sampled

their surroundings to gather information about the sensory gradients. Δc_1 and Δc_2 represented the accumulated evidence from the sensory gradients of cues 1 and 2 at time *t* from all larvae. These mean-field values corresponded to the local gradients, Δc_1^0 and Δc_2^0, which were corrupted by Gaussian noise. The local gradients were expressed as a function of the hidden variable s: $\Delta c_1^0 = s\Delta C_1$ and $\Delta c_2^0 = s\Delta C_2$, where $\Delta C_i >= 0$ represented the absolute values of the true gradients Δc_i^0, i=1,2. The sampled gradients Δc_1 and Δc_2 followed:

$$\Delta c_1 = s\Delta C_1 + \sigma_1 n_1 \quad ; \quad \Delta c_2 = s\Delta C_2 + \sigma_2 n_2 \quad (4)$$

where n_i (i=1,2) were independent normal random variables and σ_i represented the inverse reliability of the i-th cue. Errors occurred when sampled gradients were assigned a different direction than their true location (e.g., when $\Delta c_1 < 0$, $\Delta c_1 < 0$ and s=1).

In a probabilistic framework larvae should build a probability distribution over the hidden variable and local gradients given the observations of Δc_1 and Δc_2. This probability distribution was computed with Bayes' rule:

$$p(s, \Delta C_1, \Delta C_2 | \Delta c_1, \Delta c_2) = \frac{p(\Delta c_1, \Delta c_2 | s, \Delta C_1, \Delta C_2)\, p(s)\, p(\Delta C_1)\, p(\Delta C_2)}{p(\Delta c_1)\, p(\Delta c_2)} \quad (5)$$

The prior information was represented by p(s), $p(\Delta C_1)$ and $p(\Delta C_2)$. I assumed that a larva dropped in the behavioral arena had no prior expectations of the favorable direction of both gradients. Similarly, I did not expect any preference for a certain odor or temperature difference. Rather I reasoned that, in the light of the ability of larvae

to navigate gradients varying on the order of magnitudes, a very broad distribution of possible values of Δc_1 and Δc_2 made biological sense. For this reason, I concluded that all priors were flat and could be ignored. I also assumed that the fluctuations of the sensory gradients are independent of each other. This led to the following simplification of Bayes' rule:

$$p(s, \Delta C_1, \Delta C_2 | \Delta c_1, \Delta c_2) \propto p(\Delta c_1, \Delta c_2 | s, \Delta C_1, \Delta C_2) \propto p(\Delta c_1 | s, \Delta C_1) p(\Delta c_2 | s, \Delta C_2) \quad (6)$$

Using equation (4) $p(\Delta c_i | s, \Delta C_i) = N(\Delta c_i | s\Delta C_i, \sigma_i^2)$ for i=1,2 that was, a Gaussian probability density with mean $s\Delta C_i$ and variance σ_i^2. Inserting this expression into Eq. (6), I found:

$$p(s, \Delta C_1, \Delta C_2 | \Delta c_1, \Delta c_2) \propto e^{\left(-\frac{(\Delta c_1 - s\Delta C_1)^2}{2\sigma_1^2} - \frac{(\Delta c_2 - s\Delta C_2)^2}{2\sigma_2^2} \right)} \quad (7)$$

To guide behavior, larvae needed to determine the orientation of favorable gradient change regardless of the absolute values of true concentration gradients. Therefore, they marginalized the absolute values of the gradients to obtain the posterior over the hidden variable s,

$$p(s | \Delta c_1, \Delta c_2) \propto \int_0^\infty d\,\Delta C_1 \int_0^\infty d\,\Delta C_2 p(\Delta c_1, \Delta c_2 | s, \Delta C_1, \Delta C_2) \quad (8)$$

Using equation (6), (7) and the definition of cumulative Gaussian, $\Phi(x) = \int_{-\infty}^{x} dy\, N(y|0,1)$, I found

$$p(s | \Delta c_1, \Delta c_2) \propto \Phi\left(\frac{s\Delta c_1}{\sigma_1}\right) \Phi\left(\frac{s\Delta c_2}{\sigma_2}\right) \quad (9)$$

Next I approximated the cumulative Gaussians by sigmoid functions, known to be an excellent approximation for the best fit

parameters ($\Phi(x)$ was approximated by $\Phi^{-1}(x)$:$1/(1+\exp(-\alpha x))$, where α was the best fit parameter). Therefore, within this approximation, I rewrote the probability over s as

$$p(s|\Delta c_1, \Delta c_2) = \frac{1}{1 + e^{(-\alpha(\frac{\Delta c_1}{\sigma_1} + \frac{\Delta c_2}{2})s}} = \frac{1}{1 + e^{(-\alpha d s)}} \quad (10)$$

where I defined the decision variable '*d*'

$$d = \frac{\Delta c_1}{\sigma_1} + \frac{\Delta c_2}{\sigma_2} \quad (11)$$

The decision variable weighted the sampled gradients with the reliability of each gradient. In summary, the decision rule reads:

"choose s= 1" if $d > 0$ or "choose s= -1" if $d < 0$ (12)

To behave in accordance with Bayes' rule larvae followed the decision rule outlined in equation (11) and (12). However, this did not mean that larvae were computing equations (5)-(10) explicitly. These computations could be bypassed if the larval nervous system evolved to represent the inverse reliabilities in some other way and hard-wired the decision-rule in the brain. Although the decision rule was deterministic given the measurements in Δc_1 and Δc_2 I did not have access to the measurements made by the larvae. Thus the value of the decision variable *d* is unknown. However by quantifying the behavior of larvae it was possible to determine its statistical properties given the knowledge of the local gradients $\Delta c_1^0 = s\Delta C_1$ and $\Delta c_2^0 = s\Delta C_2$. The decision variable *d* was the sum of two Gaussian variables, and therefore it was a Gaussian variable. Its mean and variance were respectively

$$\langle d \rangle(\Delta C_1, \Delta C_2) = \frac{\Delta C_1}{\sigma_1} + \frac{\Delta C_2}{\sigma_2} \quad ; \quad Var(d)(\Delta C_1, \Delta C_2) = 2 \quad (13)$$

Next I established the link between the decision rule and the experimental measurement, the preference index (PI). The PI was defined as the fraction of larvae on the side of preferred aggregation[24] of the behavioral arena at time *t*. Using equation (13), the PI was calculated as the fraction of times that the decision variable *d* was above zero.

$$\mathrm{PI}(\Delta C_1, \Delta C_2) = p(d > 0 | \Delta c_1^0, \Delta c_2^0) \quad (14)$$

$$\mathrm{PI}(\Delta C_1, \Delta C_2) = \Phi\left(\frac{\Delta C_1}{\sqrt{2}\sigma_1} + \frac{\Delta C_2}{\sqrt{2}\sigma_2}\right) \quad (15)$$

This equation provided a prediction of the preference index when the two gradients are present. I used the same expression to find expressions for the preference indexes for the single-gradient conditions as

$$\mathrm{PI}(\Delta C_1) = \mathrm{PI}(\Delta C_1, \Delta C_2 = 0) = \Phi\left(\frac{\Delta C_1}{\sqrt{2}\sigma_1}\right) \quad (16)$$

$$\mathrm{PI}(\Delta C_2) = \mathrm{PI}(\Delta C_1 = 0, \Delta C_2) = \Phi\left(\frac{\Delta C_2}{\sqrt{2}\sigma_2}\right) \quad (17)$$

Finally, I used the equations (15)-(17) to derive the 'combination rule'

$$\mathrm{PI}(\Delta C_1, \Delta C_2) = \Phi\left(\Phi^{-1}\big(PI(\Delta C_1)\big) + \Phi^{-1}\big(PI(\Delta C_2)\big)\right) \quad (18)$$

[24] The side of preferred aggregation is the side a larva reaches when following the favorable gradient change i.e. the side with the odor source and the preferred temperature.

where $\Phi^{-1}(x)$ is the inverse cumulative normal. Using the same sigmoidal approximation of the cumulative Gaussian employed above, we showed that the PIs were related through the 'multiplicative rule'

$$\mathrm{PI}(\Delta C_1, \Delta C_2) = \frac{\mathrm{PI}(\Delta C_1)\mathrm{PI}(\Delta C_2)}{\mathrm{PI}(\Delta C_1)\mathrm{PI}(\Delta C_2) + (1 - \mathrm{PI}(\Delta C_1))(1 - \mathrm{PI}(\Delta C_2))} \quad (19)$$

It was shown that these two predictions for combined PIs were identical (Moreno-Bote, Knill et al. 2011). To predict the combined behavior I plugged the experimental results in the multiplicative rule (19).

The fixed-weight model: a suboptimal decision rule

Next I compared the predictions of the optimal behavior to predictions of suboptimal decision-making. Thus, I derived a general model for suboptimal performance in detail, and showed how these differ from the optimal model. In the fixed-weight model suboptimal behavior consisted in weighting the cues in a way that did not depend on the reliability of the cues, that is,

$$d_{fw} = w_1 \Delta c_1 + w_2 \Delta c_2 \quad (20)$$

where w_1 and w_2 are fixed weights. These weights established a fixed relative preference for the sensory gradients of cue 1 and cue 2. Therefore, this model can be considered as belonging to the family of "preference-based" models, or "economic-like" models, in which animals are assumed to make decisions based on the relative preference for different items or qualities of the environments.

More complex, non-linear, rules can be used, but here we restrict our analysis to these linear combination rules because our data seem to fitted well by linear models.

Next I determined the statistical properties of the fixed-weight decision rule d_{fw}, using the model described in equation (4),

$$\langle d_{fw} \rangle (\Delta C_1, \Delta C_2) = w_1 \Delta C_1 + w_2 \Delta C_2 \quad (21)$$

$$Var(d_{fw})(\Delta C_1, \Delta C_2) = w_1^2 \sigma_1^2 + w_2^2 \sigma_2^2 \quad (22)$$

As before I predicted the preference index for the combined gradients and single-gradients,

$$\mathrm{PI}(\Delta C_1, \Delta C_2) = \Phi\left(\frac{w_1 \Delta C_1 + w_2 \Delta C_2}{\sqrt{w_1^2 \sigma_1^2 + w_2^2 \sigma_2^2}}\right) \quad (23)$$

$$\mathrm{PI}(\Delta C_1) = \mathrm{PI}(\Delta C_1, \Delta C_2 = 0) = \Phi\left(\frac{w_1 \Delta C_1}{\sqrt{w_1^2 \sigma_1^2 + w_2^2 \sigma_2^2}}\right) \quad (24)$$

$$\mathrm{PI}(\Delta C_2) = \mathrm{PI}(\Delta C_1 = 0, \Delta C_2) = \Phi\left(\frac{w_2 \Delta C_2}{\sqrt{w_1^2 \sigma_1^2 + w_2^2 \sigma_2^2}}\right) \quad (25)$$

In the fixed-weight model a change in reliabilities in one the cues affected the two cues simultaneously and by the same factor. This model also results in the the combination rule (18), and the multiplicative rule (19). Although these rules could used to predict cue integration, the predicion of the combined behavior was not sufficient to distinguish between optimal and suboptimal behavior.

Model comparison

Since it was not possible to distinguish the optimal and the fixed-weight model based on the combination rules, I developed a strategy to distinguish the two models based on their behavior in single-gradients with and without the presence of additional noise.

In single gradients the preference indices of cue 1 and cue 2 were denoted as $PI(\Delta C_1)$, eq. (16), and $PI(\Delta C_2)$, eq. (17). The presence of additional noise in the sensory gradient of cue 1 increased the noise from σ_1 to σ_1' by a factor η resulting in a preference index with noise denoted as $PI(\Delta C_1)$'. If the additional noise in cue 1 corrupted behavioral performance, it followed that $PI(\Delta C_1)' < PI(\Delta C_1)$ and $\eta > 1$. Thus,

$$PI(\Delta C_1)' = \Phi\left(\frac{\Delta C_1}{\sqrt{2}\sigma_1'}\right) = \Phi\left(\frac{\Phi^{-1}(PI(\Delta C_1))}{\eta}\right) \quad (26)$$

Next I derived the prediction for the preference index for behavior in a single gradient of cue 2 and pure noise in the channel of cue 1 σ_1'. In the optimal model an increase of noise of cue 1 did not impact the behavior because σ_1' was not part of the equation (17). Therefore,

$$PI(\Delta C_2) = \Phi\left(\frac{\Delta C_2}{\sqrt{2}\sigma_2}\right) = PI(\Delta C_2)' \quad (27)$$

However, for the fixed-weight model an increase of the noise in cue 1 changed the prediction of $PI(\Delta C_2)$' as seen in equation (24) because $\sqrt{w_1^2\sigma_1'^2 + w_2^2\sigma_2^2} = \eta\sqrt{w_1^2\sigma_1^2 + w_2^2\sigma_2^2}$. Therefore

$$\mathrm{PI}(\Delta C_2)' = \Phi\left(\frac{w_2 \Delta C_2}{\sqrt{w_1^2 \sigma_1'^2 + w_2^2 \sigma_2^2}}\right) = \Phi\left(\frac{\Phi^{-1}(\mathrm{PI}(\Delta C_2))}{\eta}\right) \quad (28)$$

$$\mathrm{PI}(\Delta C_1 \Delta C_2)' = \Phi\left(\frac{\Phi^{-1}(\mathrm{PI}(\Delta C_1, \Delta C_2))}{\eta}\right) \quad (29)$$

In other words, the PI(ΔC_2)' was related to PI(ΔC_2) by the same factor η than PI(ΔC_1)' and PI(ΔC_1). This prediction contrasts to the optimal prediction, for which PI(ΔC_2)' was equal to PI(ΔC_2). This way I can distinguish the Bayesian and fixed-weight model.

However, these predictions assumed the absence of any other cross-modal interactions. In the presence of cross-modal interactions the factor eta could be different for both modalities η_i, i=1,2. In this scenario the preference indices predicted by the **Bayesian model** for the single gradient conditions in the presence of noise were

$$\mathrm{PI}(\Delta C_1)' = \Phi\left(\frac{\Delta C_1}{\sqrt{2}\eta_1 \sigma_1}\right) = \Phi\left(\frac{\Phi^{-1}(\mathrm{PI}(\Delta C_1))}{\eta_1}\right) \quad (30)$$

$$\mathrm{PI}(\Delta C_2)' = \Phi\left(\frac{\Delta C_2}{\sqrt{2}\eta_2 \sigma_2}\right) = \Phi\left(\frac{\Phi^{-1}(\mathrm{PI}(\Delta C_2))}{\eta_2}\right) \quad (31)$$

Therefore the combined condition in the presence of noise can be written as

$$\mathrm{PI}(\Delta C_1, \Delta C_2)' = \Phi\left(\frac{\Delta C_1}{\sqrt{2}\eta_1 \sigma_1} + \frac{\Delta C_2}{\sqrt{2}\eta_2 \sigma_2}\right) \quad (32)$$

This resulted in the combination rule, which was already described in equation (18)

$$\mathrm{PI}(\Delta C_1, \Delta C_2)' = \Phi\left(\frac{\Phi^{-1}\left(PI(\Delta C_1)\right)}{\eta_1} + \frac{\Phi^{-1}\left(PI(\Delta C_2)\right)}{\eta_2}\right)$$
$$= \Phi\left(\Phi^{-1}\left(PI'(\Delta C_1)\right) + \Phi^{-1}\left(PI'(\Delta C_2)\right)\right) \quad (33)$$

The preference indices predicted by the **fixed-weight model** for the single gradient conditions in the presence of noise were

$$\mathrm{PI}(\Delta C_1)' = \Phi\left(\frac{w_1 \Delta C_1}{\sqrt{w_1^2 \sigma_1'^2 + w_2^2 \sigma_2'^2}}\right) \quad (34)$$

$$\mathrm{PI}(\Delta C_2)' = \Phi\left(\frac{w_2 \Delta C_2}{\sqrt{w_1^2 \sigma_1'^2 + w_2^2 \sigma_2'^2}}\right) \quad (35)$$

The combined preference indices in the presence of noise

$$\mathrm{PI}(\Delta C_1, \Delta C_2)' = \Phi\left(\frac{w_1 \Delta C_1 + w_2 \Delta C_2}{\sqrt{w_1^2 \sigma_1'^2 + w_2^2 \sigma_2'^2}}\right) \quad (36)$$

also resulted in the combination rule if eta is defined as $\eta = \sqrt{w_1^2 \sigma_1'^2 + w_2^2 \sigma_2'^2} \Big/ \sqrt{w_1^2 \sigma_1^2 + w_2^2 \sigma_2^2}$.

$$PI'(\Delta C_1, \Delta C_2) = \Phi\left(\frac{\Phi^{-1}\left(PI(\Delta C_1)\right)}{\eta} + \frac{\Phi^{-1}\left(PI(\Delta C_2)\right)}{\eta}\right)$$
$$= \Phi\left(\Phi^{-1}\left(PI'(\Delta C_1)\right) + \Phi^{-1}\left(PI'(\Delta C_2)\right)\right) \quad (37)$$

Thus both the predictions for the combined preference for the Bayesian model and the fixed-weight model resulted in the same combination rule already derived in equation (18). Therefore I was not able to distinguish the Bayesian model from the fixed-weight model in the case of cross-modal interactions. In this scenario it was also impossible to make predictions based on the single gradient condition because the eta was different for both gradients. If the

additional noise in cue 1 led to an increased performance in cue 2 the factor eta was $\eta_1>1$ and $\eta_2<1$.

Computing the fit of a model with the likelihood

To compare the fit of a model to the experimental data I computed the likelihood (L) for the last time-bin in the combined condition. The likelihood (L) of the data given the model is computed as

$$\mathrm{L} = \left(\frac{N}{n}\right) PI_{model}^{n}(1 - PI_{model}^{n})^{N-n} \quad (38)$$

The preference index described the fraction of larvae for which *n* out of *N* larvae moved to the side of preferred aggregation ($PI=n/N$). PI_{model} was the preference index at the last time bin predicted by the model, which was compared to the experimental data. Given that the two models had no free parameters, direct comparison of the LL was sufficient to decide which model fitted best. Thus, the model with the best fit had the highest likelihood. Computing the LL in this way assumed that larvae were independent.

Optimality in group decision-making

The Bayesian model was derived under the assumption that larvae behaved independently. Here, I applied the same formalism assuming interactions between animals in the group. Larvae *i* follows the Bayesian decision rule of equation (11). However, its behavior is influenced by the behavior of other larvae:

$$d = \frac{\Delta c_1}{\sigma_1} + \frac{\Delta c_2}{\sigma_2} + \lambda \sum_{i \neq i} d_j \quad (39)$$

The last term of eqaution (38) describes group effects. The factor λ represented the strength of the interactions between animals. I supposed that the decision variables for all animals were distributed identically, and their covariance was $Cov(d_k, d_l) = \rho Var(d_i)$, where ρ was the correlation coefficient. I found that the mean and variance of d_i were,

$$\langle d_i \rangle = \frac{\Delta C_1}{\sigma_1} + \frac{\Delta C_2}{\sigma_2} + \lambda(n-1)\langle d_i \rangle \quad (40)$$

$$Var(d_i) = 2 + \lambda^2 Var(d_i)(1 + (n-2)\rho \quad (41)$$

where n is the number of the larvae in the group. I assumed that the fluctuations of the local estimates of the gradients made by one larva were independent from the local estimates made by other larvae. Therefore the decision variables on the last term were independent of the sampled gradients. Using the previous equations, I obtained that

$$\langle d \rangle(\Delta C_1, \Delta C_2) = \frac{\Delta C_1}{(1-\lambda)\sigma_1} + \frac{\Delta C_2}{(1-\lambda)\sigma_2} \quad (42)$$

$$Var(d)(\Delta C_1, \Delta C_2) = \frac{2}{1 - \lambda^2(1 + (n-2)\rho)} \quad (43)$$

The equations (42) and (43) had the same structure as the corresponding equations for the Bayesian model. Consequently these expressions resulted in the same combination rule (18) as the Bayesian model with the assumption of independent larvae. The inverse reliabilities and the variance of the decision variable were normalized by constant factors that did not depend on the tested

conditions. Therefore, under the assumption that interaction were weak (i.e., $\lambda^2(1+(n-2)\rho<1)$, interactions between larvae did not affect the predictions of the optimal model.

Chapter 3: Integration within the olfactory system

Chemotaxis

Comparison of chemotaxis ability of different developmental stages

Previous work showed that third instar larvae navigate chemical gradients using a set of stereotypical sensorimotor responses (Gomez-Marin, Stephens et al. 2011). Using the same methodology, I compared the behavior of first instar (L1) and third instar (L3) larvae. After starting close to an odor source, both L1 and L3 larvae responded in a similar manner: they remained in the vicinity of the odor source, resulting in 'ball-of-wool-like' trajectories (Fig. 13 A-A"). I described trajectories as sequences of runs and turns, as shown in illustrative trajectories in (Fig. 13 B-B"). A comparison of these trajectories with the respective sensory experiences (Fig. 14 A-A") revealed that turns are mainly triggered after a preceding decline in sensory experience, as well as for fine adjustment of the trajectories close to the odor source.

Note that the spatial scale of the trajectories is different between L1 and L3, which is to be expected considering the differences in size and speed of these two developmental stages (Fig. 15 A, B). L1 larvae were slower than L3 larvae, even after normalization by the relative difference in body length (Fig 15 B, C). In spite of these differences, the overall pattern of motor output was similar between L1 and L3 larvae (Fig. 16 A-A"). Before turning, larvae reduced the speed of their forward movement ($v^{centroid}$). This deceleration was mild in L1 and strong in L3. At the same time, both L1 and L3

initiated a head cast, which was associated with an increase of the head speed (v^{head}). The average sensory experience preceding a turn (turn-triggered average) illustrated that turns are elicited upon detection of prolonged negative changes of odor concentration (Fig. 17 A-A"). Implementation of a turn resulted in an increase in the turn-triggered average of perceived odor concentration as larvae mostly turned towards higher odor concentrations.

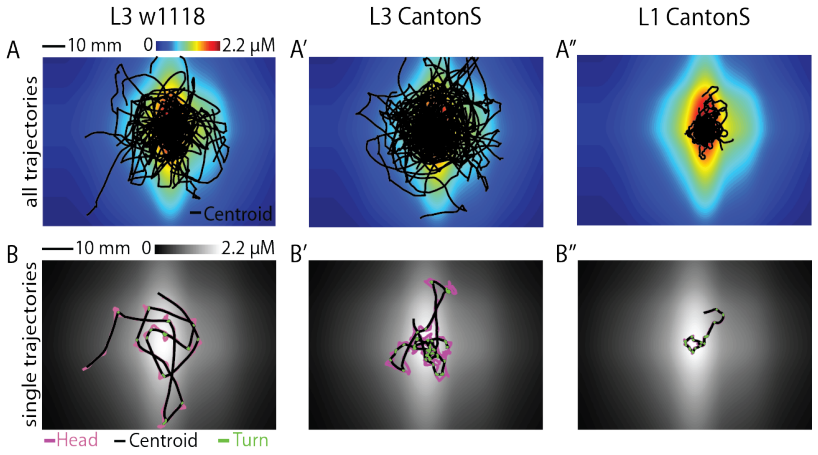

Figure 13: Trajectories of first (L1) and third (L3) instar larvae. (**A-A"**) Trajectories of the centroid positions of all L3 w^{1118} (A, 23 trajectories 417 turns), L3 CantonS (A', 29 trajectories, 444 turns) and L1 CantonS (A", 38 trajectories, 647 turns) used in the study. Trajectories were superimposed onto the reconstructed odor gradient. Larvae aggregated close to the peak of the gradient. (**B-B"**) Illustrative trajectories for the three experimental conditions: W^{1118} at L3 and CantonS at L3 as well as L1. The trajectory of the centroid position is shown in black and the head position in magenta. Turns were marked as green segments. For L1 and L3 larvae, trajectories featured an alternation of runs and oriented turns. However, the spatial scale of the motion differed markedly between the two developmental stages. Larvae were plotted on the same gradient as in (A-A").

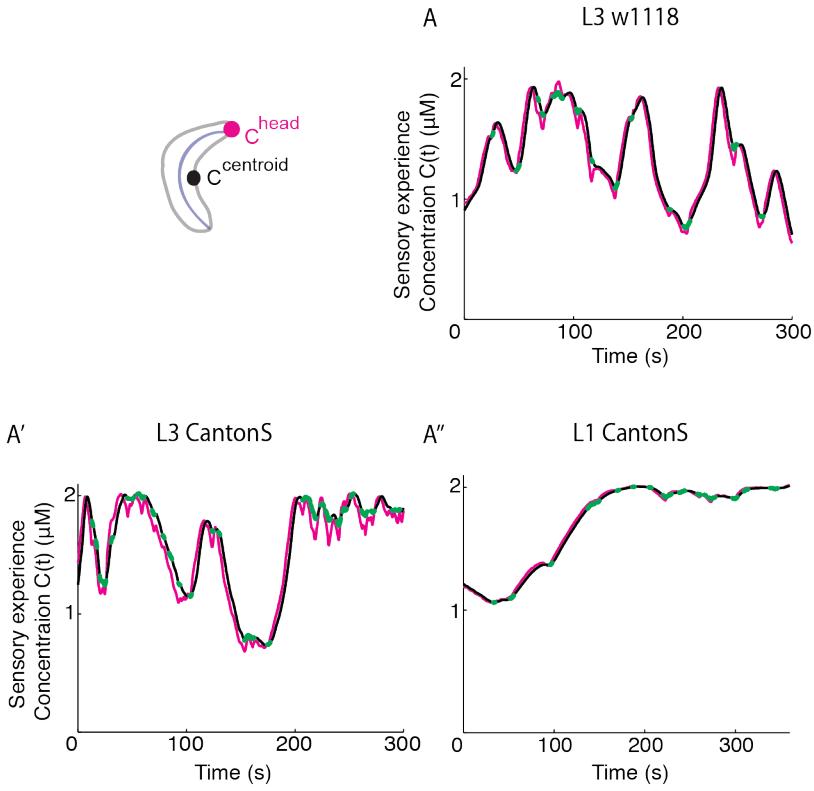

Figure 14: Sensory experience of first (L1) and third (L3) instar larvae. (**A-A"**) The difference between the concentrations measured at the head (magenta), and at the centroid (black), was more pronounced in L3 larvae due to their larger size and range of their head casts. Turns were marked as green segments and typically occurred after prolonged exposure to negative slopes of sensory experience or reorientations close to the odor source. The sensory experience corresponded to the illustrative trajectories in Fig. 13 B-B".

The motor output (speed) of L1 larvae was more than one order of magnitude lower than those of L3 larvae. Similarly, the decrease in speed after turn initiation is much smaller in L1 than in L3. It is possible that the absolute decrease of centroid speed in L1 was masked because the centroid was dragged along during the head movement due to the small size of these larvae.

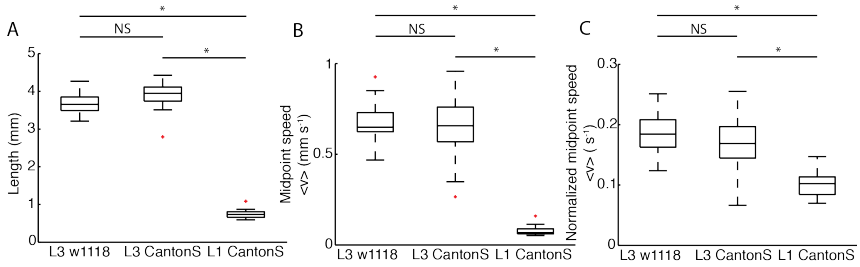

Figure 15: Comparison of first (L1) and third (L3) instar larvae sizes and midpoint speeds. (**A**) Average sizes (in mm) of L3 w^{1118}, L3 CantonS and L1 CantonS larvae. L1 were about four times smaller than L3 larvae. (**B**) Average speed of the midpoint for the same genotypes as in (A). L1 moved approximately ten times slower than L3 larvae. (**C**) Midpoints speeds after normalization by the body length. In accordance with (A) and (B) the normalized midpoint speed of L1 was roughly half of that of L3 larvae. *: statistically significant difference ($p<0.05$)

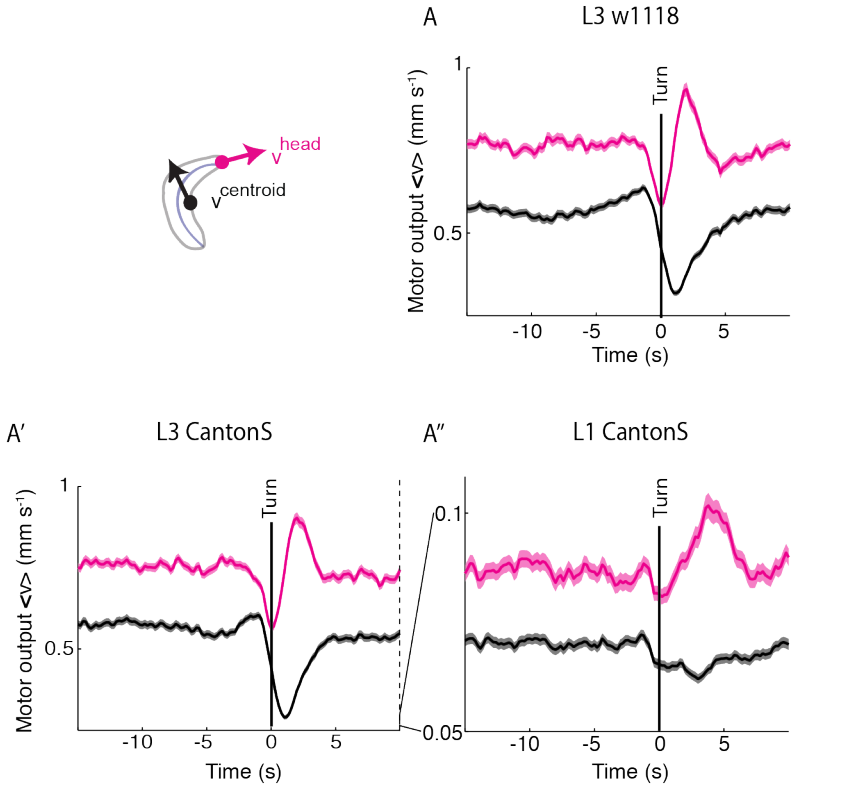

Figure 16: Turn-triggered averages of motor output. (**A-A"**) Turn-triggered averages of speed of the centroid (black) and head (magenta). The speed of the centroid declined upon turn initiation, while the speed of the head increased while a head cast took place.

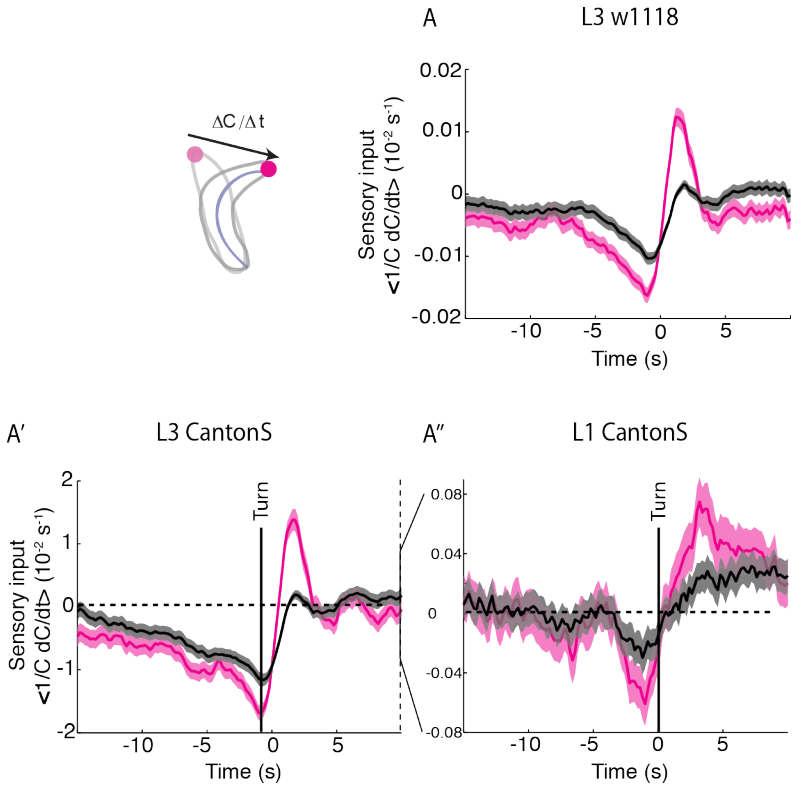

Figure 17: Turn-triggered averages of sensory perception. (**A-A"**) Turn-triggered averages of the odor concentration perceived by the larva at the centroid (black) and at the head (magenta). Turns were preceded by a prolonged exposure to a negative slope of sensory experience. The implementation of a turn was followed by a sharp rise in the concentration measured at the head position: this surge was due to head casts, which tended to be oriented towards the direction of increasing odor concentration.

The small size of L1 also explained differences in the sensory input of L1 and L3 larvae. Head casts of L1 larvae had reduced amplitudes as compared to L3. Therefore, they sampled a smaller concentration difference. Since accurate sampling of the odor space was crucial during reorientation events, I speculated that L1 larvae might be prone to errors in gradient assessment, thereby showing a reduction

in chemotactic performances compared to L3 larvae. The turning precision of larvae towards the odor gradient depended on the bearing between the direction of motion (body axis) and the direction of the local odor gradient (Fig. 18 A-A"). Maximum reorientation performances were observed for larvae oriented perpendicular to the odor gradient (bearing of ± 90 degrees). Even though the modulation of the reorientation performance as a function of the bearing was reduced for L1 larvae, the data indicated that L1 larvae were able to bias the direction of their turns.

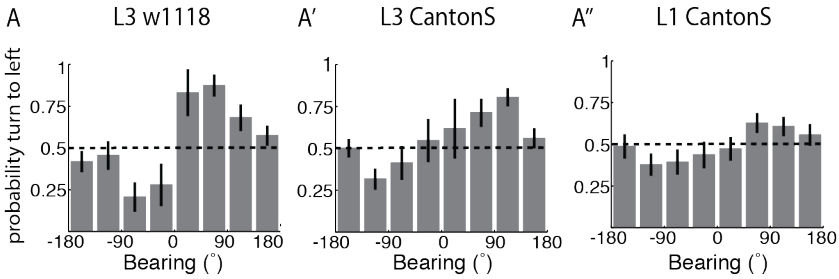

Figure 18: Turn performances of first (L1) and third (L3) instar larvae. (**A-A"**) The turn performance is the relationship between the probability of turning towards increasing odor concentration and the bearing before turn initiation. Positive bearing angles were defined according to anticlockwise convention; thus left turns reoriented the larva towards the odor source. Turning performances were highest for bearing angles around 90° (motion perpendicular to the local odor gradient). The bearing angle is represented in 8 bins of 45°. Error bars represent an estimate of the standard error calculated based on a bootstrap procedure (Martinez and Martinez 2012).

Larvae have been shown to reorient through abrupt turns. In addition, chemotaxis also results from the continuous deflection of runs toward the local odor gradient — a mechanism termed weathervaning (Gomez-Marin and Louis 2014). I found that both

L1 and L3 larvae were able to bias their runs with respect to the local odor gradient. This aspect of the orientation behavior was established through the correlation between the instantaneous reorientation rate and the bearing angle associated with the direction of motion (Fig. 19 A-A").

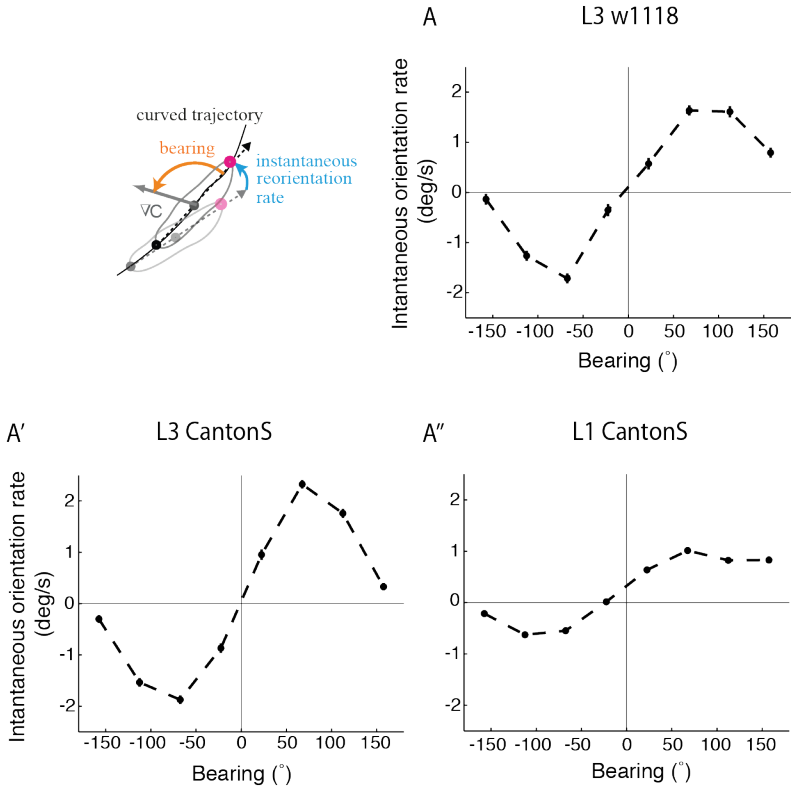

Figure 19: Weathervaning performance of first (L1) and third (L3) instar larvae. (**A-A"**) Weathervaning was quantified as average instantaneous reorientation rate during runs as a function of the local bearing angle. The bearing angle is the angle between the body axis and the direction of the local odor gradient. The instantaneous orientation rate is quantified as the change of the body angle during a run. Larvae bent their runs most strongly toward the source when they were oriented perpendicular to the local odor gradient. Error bars show SEM.

Chemotaxis in w^{1118} larvae assessed with the Preference Index

After showing that chemotaxis ability was conserved across different strains and developmental stages, I proceeded to quantify this behavior with the preference index (PI). For this analysis I used only L3 larvae. To collect more data, every experiment was performed with a group of, usually, ten larvae.

Figure 20 shows the progression of the PI over time, in an odor gradient with four different source concentrations of ethyl butyrate (EtB). EtB was chosen because it activated only a small subset of OSNs (Kreher, Mathew et al. 2008). Initially, larvae were equally distributed on both sides of the midline resulting in a PI of 0.5. Any deviations from this PI at the beginning of the experiments were due to incorrect placement, or larvae crossing the midline before the start of the recording. If exposed to a high concentration of EtB, larvae quickly accumulated in the vicinity of the odor source. This resulted in a PI above 0.9 for a concentration of 10^{-2} M EtB. For the other gradients the process of accumulation was slower, in a manner consistent with the decrease of the source concentration. The gradient with lowest concentration of EtB, did not lead to any attraction towards the side of the odor droplet. This indicated that the odor concentration was below the detection threshold. Furthermore, the distribution across the arena was equal, illustrating that the assay was free of systematic bias.

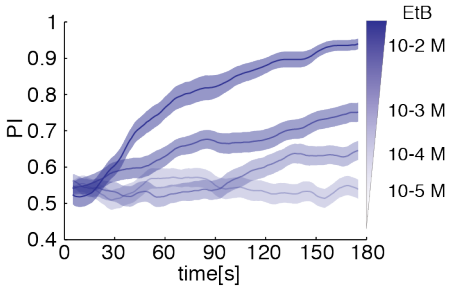

Figure 20: Chemotaxis in odor gradients with different concentrations. Behavioral performance, as assessed with the PI, improved with increasing EtB concentration. To test sensory integration I chose a source concentration, resulting in a gradient with medium attraction (10^{-3} M EtB). Number of repetitions per condition: 10^{-2} M n=21, 10^{-3} M n=26, 10^{-4} M n=16, and 10^{-5} M n=20

Group size influences chemotactic behavior

The impact of group size on chemotactic behavior was assessed by chemotaxis experiments with single larva and groups of 5, 10 or 15 larvae. This analysis revealed that group size was inversely correlated with behavioral performance (Fig 21 A).

To distinguish between social interactions and detrimental secondary effects I compared the experimental SEM to the binomial error. The binomial error, or normal approximation interval, assumes statistical independence between all larval decisions. Initially the SEM and binomial errors are quite different, but the values converge after the first 60-80 seconds (Fig. 21 B). Therefore, I concluded that larvae behave virtually independent with respect to chemotactic behavior.

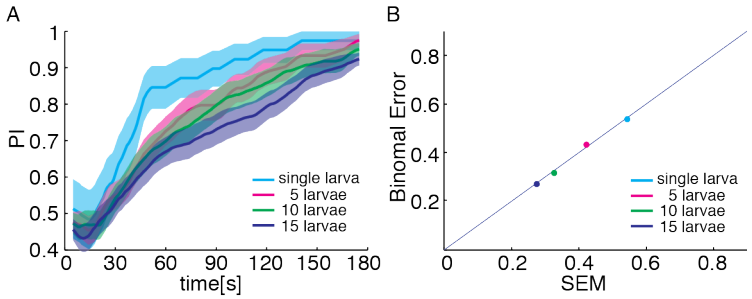

Figure 21: Group size influences chemotaxis. (**A**) The behavioral performance decreased with group size. Placement effects, like initial orientation with respect to the gradient and manipulation time, contributed to this effect. Odor dilution: $5*10^{-3}$ M EtB; Number of repetitions: single larva n=39, 5 larvae n=18, 10 larvae n=19, and 15 larvae n=21; (**B**) Comparison of the SEM with the binomial error 80 seconds into the experiment. Every dot represents a set of experiments with a different number of larvae. All conditions aligned at the 45° degree line. This illustrated that, the SEM and the binomial errors, which assumed independence, were equivalent.

Specificity of odors and independence of channels

To test the combination of sensory information it would be ideal to work with independent stimuli. The literature suggested a number of ways how different odorants could be combined to achieve independent stimulation of the olfactory system. Previously, the tuning curves of larval OSNs were investigated by means of behavior (Fishilevich, Domingos et al. 2005, Mathew, Martelli et al. 2013) and electrophysiology (Kreher, Mathew et al. 2008). Therefore, it was shown that every odorant activates a number of specific OSNs. I refer to the subset of OSNs activated by an odorant as an input channel. I tried to verify the independence of the channels experimentally. To this end I generated larvae with a single functional OSN (Fishilevich, Domingos et al. 2005). In doing

so I tested the attraction of every odorant with two different larvae, each with a different single functional OSN.

I was not able to identify a single pair of odorants, which fulfilled the condition of independence completely. Most of my observations fell into one of two categories: (i) either the odorant did not lead to any significant chemotaxis in larvae with single functional OSN, or (ii) the odorant eliciting chemotaxis in one channel could cause significant attraction in the other channel as well.

Acetal is a typical example for the first category. It was shown to be specific to *Or42b* (Mathew, Martelli et al. 2013). Nevertheless, larvae with just the *Or42b* neuron active (*Or42b*-functional) showed no attraction to a gradient of acetal at a dilution of 10^{-2} M (data not shown). Increasing the odor concentration to 1 M resulted in a minor attraction to acetal (Fig. 22 A). However, at this concentration, attraction was indistinguishable from chemotactic behavior of *Or42a*-functional larvae (Fig. 22 A). 3-Octanal and 1-octen-3-ol were further examples of category one odorants. Both were reported to activate *Or13a* (Kreher, Mathew et al. 2008). Testing *Or13a*-functional larvae in dilutions ranging up to one or two molar did not reveal any attraction (Fig. 22 B).

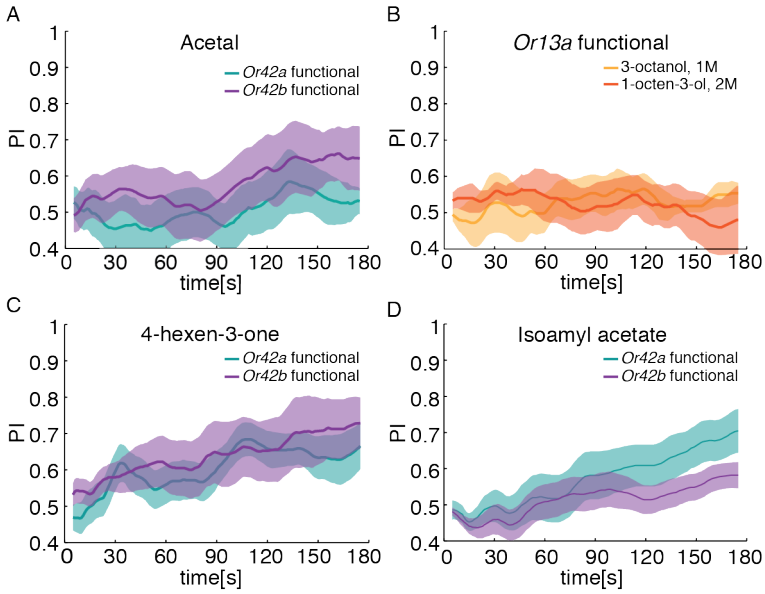

Figure 22: Specificity of odors. (**A**) *Or42a*- and *Or42b* functional larvae were chemotaxing in an acetal gradient. Although the dilution was high (1M), attraction was weak. Number of repetitions *Or42a* n=7, *Or42b* n= 8 (**B**) *Or13a* functional larvae were not attracted to 3-Octanol (n=6) and 1-octen-3-ol (n=5). (**C**) A 4-hexen-3-one gradient (10^{-2} M) elicits attraction from *Or42a*- but also from *Or42b* functional larvae. Number of repetitions: *Or42a* n=9 and Or42b n=7 (**D**) Isoamyl acetate leads to attraction in *Or42a* (n=11) but not in *Or42b* functional larvae (n=19).

4-hexen-3-one, an odorant of the second category was less specific than reported. Instead of binding to *Or42a* only (Mathew, Martelli et al. 2013) it also elicited chemotaxis in *Or42b*-functional larvae at a concentration of 10^{-2} M (Fig. 22 C). Lowering the odor concentration to 10^{-3} M abolished chemotaxis for *Or42a*-functional larvae (data not shown).

Although my screen was not exhaustive, in practice it was very difficult to identify a pair of odors with complete independence between their channels. If a certain odor dilution resulted in chemotaxis in one channel, the same odor should not be allowed to

elicit attraction in the other channel, even though its concentration was much higher. Thus, I established partial independence, a scenario with less rigid criteria. Odor pairs were accepted if an odor causing chemotaxis in one channel resulted in indifference in the other channel at the same concentration. I identified two odorants complying with the criteria of partial independence. I showed that isoamyl acetate (IAA) caused attraction through the *Or42a* but not in the *Or42b* neuron (Fig. 22 D). Similarly, 1-Hexanol led to chemotaxis via *Or42a*, weak chemotaxis through *Or13a*, and no chemotaxis with *Or42b* neurons (data not shown). This was consistent with the evidence from electrophysiological recordings (Kreher, Mathew et al. 2008).

Chemotaxis elicited by light gradients

Optogenetics was another way to achieve complete independence of inputs. Expression of a microbial opsin in an OSN rendered this neuron sensitive to light (Boyden, Zhang et al. 2005). Hence, one neuron could be activated completely independent of other neurons. This technique also proved efficient to introduce sensory noise into the olfactory system.

After expression of Channelrhodopsin (Pulver, Pashkovski et al. 2009) in the *Or42a* neuron, larvae were able to navigate gradients of blue light (Schulze, Gomez-Marin et al. 2015) (Fig. 23). Furthermore, the addition of light flashes on top of the light gradient corrupted larval chemotaxis (Fig. 23). However, the mutations needed to abolish the photophobic response to blue light, caused serious problems (see 'Optogenetics, virtual odor gradients

and noise' for more details). Therefore, I did not continue to use Channelrhodopsin.

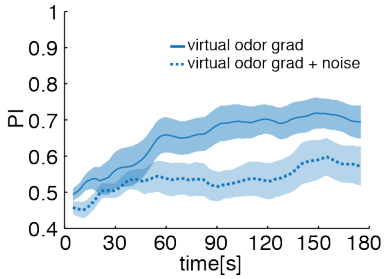

Figure 23: Chemotaxis in virtual odor gradients with Channelrhodopsin. Chemotaxis performance decreased when light flashes were on top of a sensory gradient. Experimental conditions: virtual gradient, n=17, virtual gradient+noise, same light gradient as before, randomized light flashes, n=16

The use of Chrimson (Klapoetke, Murata et al. 2014) solved this problem. Chrimson turned out to be more efficient in navigating light gradients in my setup. This means that the macroscopic behavior in the light gradient was quite similar to chemotaxis in odor gradients. Moreover, it was easier to regulate the strength of accumulation by changing the amplitude of the light gradient. Thus, stronger gradients resulted in an increased precision of chemotaxis. Noise was added in the form of randomized light flashes on top of a sensory gradient (Fig. 24 A). Randomizing the availability of the directional information was another strategy to increase the uncertainty. (Fig. 24 B). This was achieved by flashing the light gradient in a randomized way. Both strategies corrupted chemotactic behavior. The decrease in behavioral performance correlated with increasing distortion of the gradient due to noise (Fig. 24 B). Although both types of noise had an impact on behavior, I used only the first strategy (randomized light flashes) when I tested

sensory integration. The presentation of additional light flashes had the advantage that it could be used to corrupt behavior of larvae behaving in odor gradients and light gradient alike. In addition, the noise was uniformly distributed over the behavioral arena and did not just affect larvae in the light gradient.

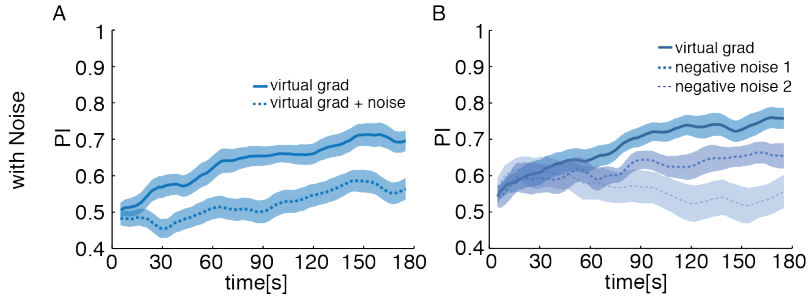

Figure 24: Chemotaxis in virtual odor gradients with Chrimson. (**A**) Chemotaxis performance decreased when light flashes were on top of a sensory gradient. Experimental conditions: virtual gradient, light intensity at the peak of the gradient 1.39 W/m^2, n=30, virtual gradient+noise, same light gradient as before, randomized light flashes, light intensity 0.69 W/m^2, n=30 (**B**) Chemotaxis performance was correlated with the time the gradient information was available; Attraction behavior decreased from when the gradient information was accessible constantly (virtual grad, n=30), 42% of the time (negative noise 1, flashed with 4.2Hz 100ms, n=13) or just 30% of the time (negative noise 2, flashed with 3Hz, flash duration 100ms, n=17).

Odor-Odor Integration

Odor-odor integration refers to the integration of information within the olfactory system. Therefore, I presented two different olfactory cues to every animal. Cues were presented separately (single-gradient condition) and then together at the same side of the behavioral arena (combined condition). To avoid capture effects I exposed larvae to odor concentrations leading to attraction in the low or medium range. If some form of multisensory integration was taking place I expected to observe an improvement in chemotaxis performance.

Odor-odor integration in wild-type larvae

Wild-type w^{1118} larvae were exposed to gradients of 1-hexanol or ethyl butyrate. Both odors elicited a similar level of attraction, when presented alone (Fig. 25 A). When odors were combined, larvae accumulated quicker on the side of the odor source and mostly stayed there until the end of the experiment (Fig. 25 A). Since behavioral performance improved, I concluded that larvae were able to integrate information from two congruent odor sources. Subsequently, I inserted the preference indices of the single conditions into the multiplicative rule (equation (19)) and predicted the combined behavior for every timepoint of the combined condition. This resulted in a good fit of the optimal prediction (Fig. 25 B).

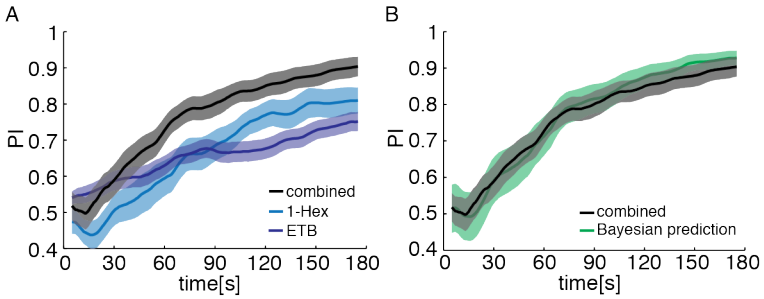

Figure 25: Sensory integration in w^{1118} larvae. (**A**) Behavioral performance improved upon combined presentation of two odor gradients as compared to exposure to a single gradient. Experimental conditions: 1-hexanol, 10^{-2} M, n=20; EtB, 10^{-3} M, n=26; combined n=19 (**B**) The Bayesian prediction fitted the experimental data well.

However, another possibility could also account for the observed improvement. A subset of OSNs was activated by both 1-hexanol and ethyl butyrate. Therefore, it was possible that the improvement was due to stronger activation of these OSNs by two types of molecules. To exclude this hypothesis, I aimed to test sensory integration by (i) lowering the odor concentration so it does not cause attraction in both channels, or (ii) with independent channels.

Integration with partially overlapping channels

Previously I showed that isoamyl acetate resulted in attraction mediated by *Or42a*, but not by *Or42b*-functional larvae (Fig. 22 D). However, I did not identify a suitable odor, which activated *Or42b* without activating *Or42a*. Therefore I presented isoamyl acetate and ethyl butyrate to larvae, with only to two active OSNs (*Or42a* and *Or42b*). Ethyl butyrate interacted with both receptors, while isoamyl acetate activated just *Or42a*. In this scenario, the channels were partially overlapping. Presentation of a single gradient resulted in

stronger attraction to ethyl butyrate than to isoamyl acetate (Fig. 26 A). In the beginning the slope of the preference index of the combined condition was steeper than the slope of either single-gradient condition, before leveling off at around 90 seconds (Fig. 26 A). Overall, its shape was remarkably similar to the combined condition for wild-type larvae. However, there was a dip in the combined condition at around 150 seconds into the experiment. This dip was not captured by the prediction of the model with optimal behavior (Fig 26 B).

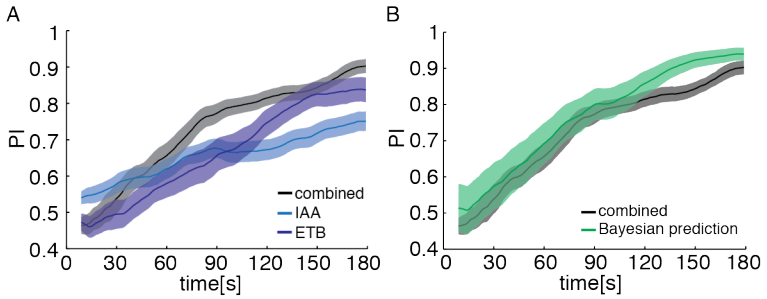

Figure 26: Sensory integration with partially independent channels. (**A**) The experimental data showed an improvement when larvae were chemotaxing in two congruent odor gradients as compared to a single gradient. Experimental conditions: Isoamyl acetate (IAA), 1/3 M, n=19; EtB, 10^{-3} M, n=26; combined n=20 (**B**) The prediction fitted the data well for the first 120 seconds. Beyond this timepoint, the prediction deviated slightly from the experimental data.

Integration with independent channels

Optogenetics made it possible to control the activity of an OSN with light. This fulfilled the criteria of complete independence of input for one channel. Even though light stimulation guaranteed independent input, it was still possible to stimulate the same channel with an odor. To achieve complete independence the odor

stimulation had to be uncoupled as well. *Or67b* was insensitive to stimulation by ethyl butyrate. This was shown by electrophysiology (Kreher, Mathew et al. 2008) and verified by behavioral experiments (Fig. 27). Thus, ethyl butyrate activated a small subset of OSNs sensitive to this odor (Kreher, Mathew et al. 2008), while *Or67b* was stimulated exclusively by light. Since no other odor gradients were present during the experiments, cross-activation of *Or67b* could be excluded.

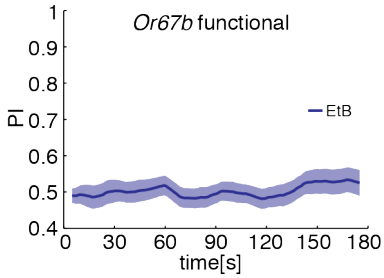

Figure 27: Uncoupling of the peripheral perception of two olfactory stimuli. Larvae with just the *Or67b* OSN functional were not attracted to the side with the sensory cue. Source concentration 10^{-3} M EtB; n=20

Figure 28 shows the results of sensory integration with independent channels. The preference indices of the conditions with a single gradient were similar. The slope of the combined condition was higher than the slopes of the single-gradient condition over the whole course of the experiment (Fig. 28 A). Therefore, I concluded that larvae integrated sensory integration from two independent inputs. Although the prediction deviated slightly between 30 and 90 seconds, at no time did it differ significantly from the experimental data (Fig. 28 A).

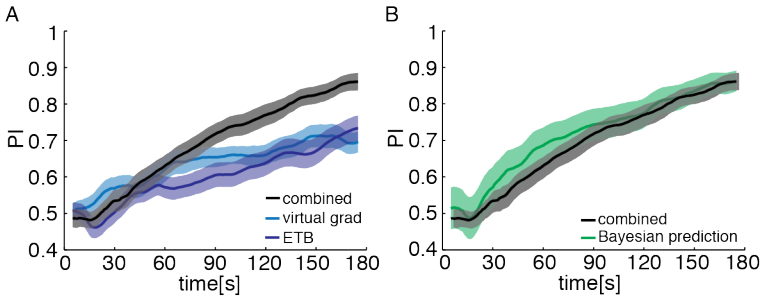

Figure 28: Sensory integration with independent channels. (**A**) The combined condition outperformed both single-gradient conditions. Experimental conditions: EtB, $2.5*10^{-4}$ & $5*10^{-4}$ M, n=30 M; virtual gradient, light intensity at peak 1.39 W/m², n=30; combined n=30 (**B**) There was no significant difference between the prediction and the data over the whole experiment.

Testing the model: integration with sensory noise

Building on the scenario of complete independence, I added noise on top of the sensory gradients. Noise was presented in both single-gradient conditions as well as during combined experiments. Larvae navigated single ethyl butyrate gradients better than the light gradient. Chemotaxis improved when larvae were exposed to both cues, although this increase of the PI was not significant for most of the time (Fig. 29 A). However, the prediction fit the data perfectly (Fig. 29 B), because light gradient contributed weakly to the combined performance.

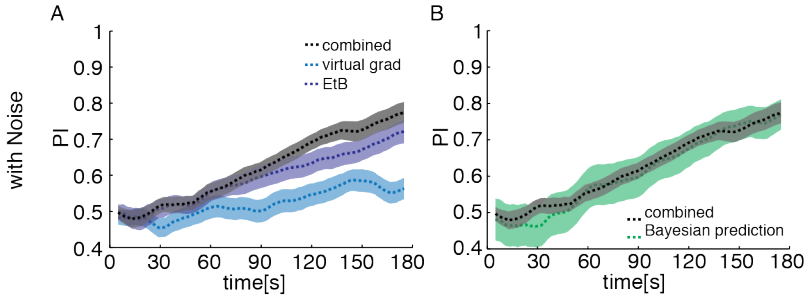

Figure 29: Odor-odor integration with additional sensory noise. (**A**) Chemotaxis in the combined condition was slightly better than the exposure of larvae to EtB gradients alone. This was mainly due to the weak contribution of the light gradients corrupted by noise. Experimental conditions: EtB, $2.5*10^{-4}$ & $5*10^{-4}$ M, n=30 M; virtual gradient, light intensity at peak 1.39 W/m², n=30; combined n=30; sensory noise was present in all conditions, intensity of a light flash: 0.69 W/m² (**B**) The prediction for Bayesian sensory integration fitted the data well.

A comparison between the single-gradient conditions with and without noise revealed the effect of sensory perturbation in the different channels. The additional light flashes corrupted the taxis behavior in the light gradient (Fig. 30 A), without affecting the behavior in the odor gradient (Fig. 30 B).

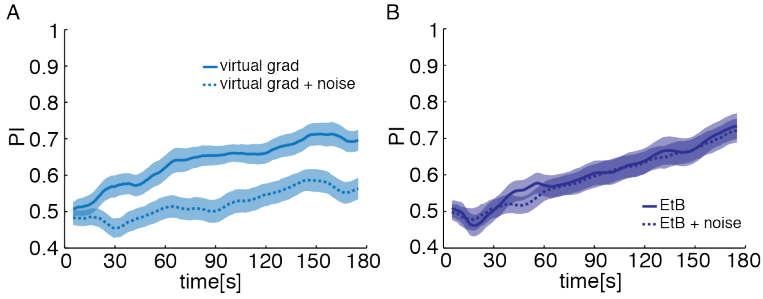

Figure 30: The impact of noise on behavior. (**A**) *Or67b* mediated chemotaxis in a light gradient with and without noise. The addition of randomized light flashes (0.69 W/m²) on top of the light gradient had a negative impact on chemotaxis performance within the same channel. (**B**) Chemotaxis in an odor gradient with and without noise in *Or67b*. Noise in another channel had no impact on the chemotaxis performance. Single-gradient conditions for (A) and (B) are the same as in Fig. 28 A and Fig. 29 A.

As a next step, I predicted the performance of a fixed-weight model of sensory integration. In this model the weights were not adjusted according to reliability, as in the Bayesian prediction, but were independent of noise (Fig. 31). To compare these models the likelihood to fit the combined condition for every model were computed at 180 seconds. These were 0.0558 and $5.45*10^{-9}$ for the Bayesian and fixed-weight model, respectively. Thus, I concluded that the odor-odor integration was implemented as a Bayesian strategy.

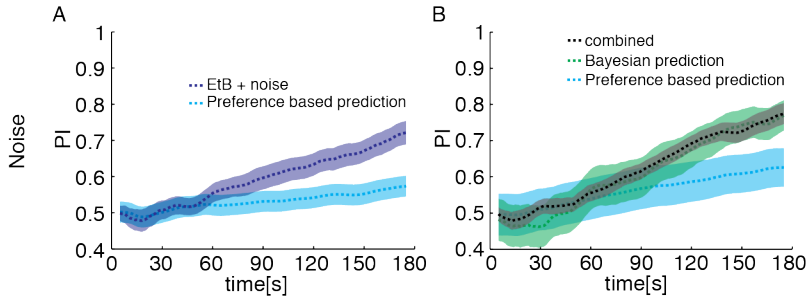

Figure 31: Predictions for the fixed-weight model with noise. (**A**) Comparison between the PI of the behavior in an odor gradient with noise, and the corresponding prediction for the fixed-weight model. The prediction deviated significantly from the observed behavior. (B) Prediction of the combined PI for the fixed-weight model under noise conditions. The prediction was significantly lower than the experimental results. In contrast, the prediction for the Bayesian model fitted well. Experimental data and predictions were taken from Fig. 29.

Chapter 4: Cross-modal integration

Thermotaxis

Thermotaxis of w^{1118} larvae

First, I assessed thermotactic behavior of w^{1118} larvae in a number of different, one-dimensional, gradients. The tested gradients formed two groups (Fig. 32). A neutral gradient, with the same temperature on each side (16-16˚C), resulted in an equal distribution between both halves of the behavioral arena. A similar distribution was observed for the gradient from 16-26˚C. Thus, the detection threshold in this assay was above 0.105˚C/mm. Increasing the gradient by two degrees, from 16-28˚C resulted in a movement towards the side of preferred temperature. A further increase from 16-30˚C resulted in a mild improvement of thermotaxis.

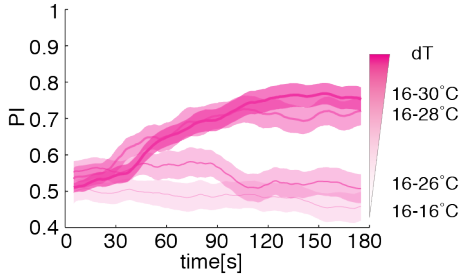

Figure 32: Thermotaxis of w^{1118} larvae in different gradients. Thermotaxis performance correlated with the slope of the temperature gradients. The temperature difference (ΔT) is the difference between the temperatures set at the sensors at the extremity of the behavioral arena. Experimental conditions: ΔT 16-16˚C, n=33; ΔT 16-26˚C, n=20; ΔT 16-28˚C, n=20; ΔT 16-30˚C, n=35

Different strains show different abilities to thermotax

Thermotaxis was more sensitive than chemotactic behavior. In contrast to w^{1118} larvae, many strains were not able to navigate the thermal gradients presented in the previous section (Fig. 32). To induce thermotaxis I shifted the gradients to higher temperatures and increased the steepness of the gradient. Thus, CantonS wild-type larvae did not thermotax in the shallow 16-30°C gradient, but were able to navigate a 20-40°C temperature gradient (Fig. 33 B). Similarly, thermotaxis was induced in the Chrimson line (Fig. 33 B), *Or42a* driver lines and other genetically modified stocks.

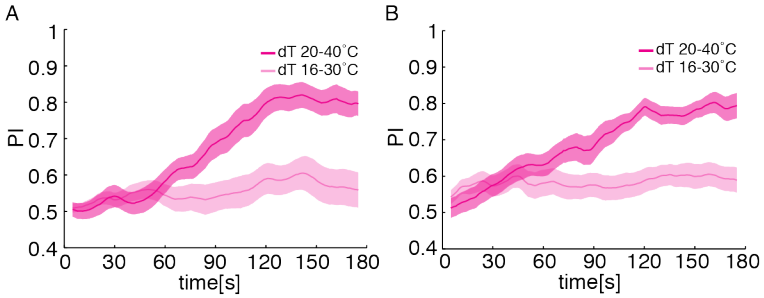

Figure 33: Thermotaxis was not conserved across different genetic backgrounds. (**A**) CantonS wild-type larvae did not thermotax properly in a gradient from 16-30°C. Only an increase of the temperature gradient to 20-40°C resulted in proper thermotaxis. Experimental conditions: ΔT 16-30°C, n=21; ΔT 20-40°C, n=18 (**B**) Same observation as in (A) with the Chrimson line (*w*;+;UAS-CsChrimson-mVenus). Experimental conditions: ΔT 16-30°C, n=25; ΔT 20-40°C, n=30

Odor-Temperature Integration

For intermodal integration, I assumed independence between sensory inputs. As before, I chose unimodal conditions that led to medium attraction to exclude capture effects and observed a similar progression of the preference index over time. Since thermotaxis ability was not conserved across genotypes, I varied the temperature gradient accordingly. I also introduced slight changes to the odor concentration if it seemed better suited for a certain experiment.

Odor-temperature integration in wild-type larvae

Both groups and single w^{1118} larvae were able to integrate information across sensory modalities. Larvae improved their performance when they were exposed to an odor and a temperature gradient as compared to the presence of just one sensory gradient (Fig. 34). In general the Bayesian prediction fitted well. The fit was worse for single-larva experiments (Fig. 34 C-D). This was probably due to the different number of larvae in group-experiments versus single-larvae experiments. Although I conducted around 80 single-larva experiments for every condition, I could not obtain smoother plots. This was not surprising considering that this number of larvae was the equivalent of eight group experiments with ten larvae in every experiment.

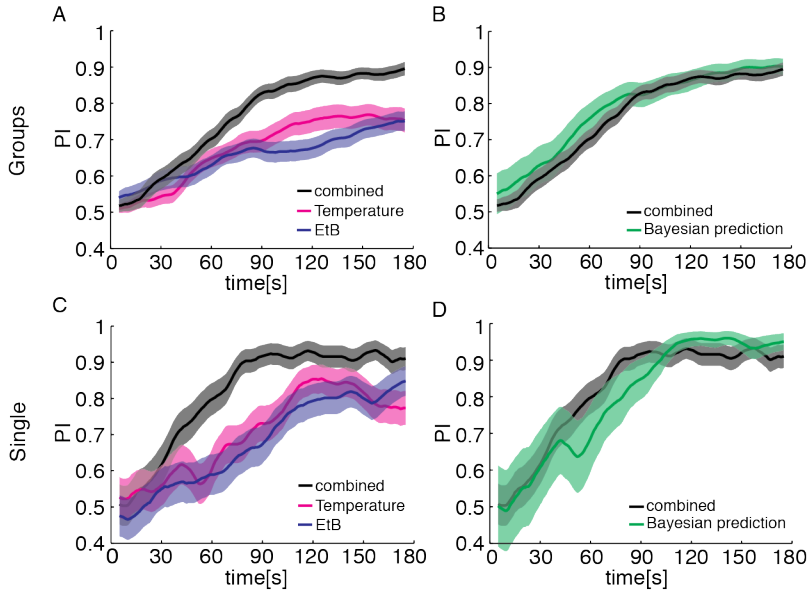

Figure 34: Multisensory integration in w^{1118} larvae. (**A**) Groups of wild-type larvae were able to combine information across different modalities. The preference indices of combined condition were higher than the preference indices of either unimodal condition. Experimental conditions: EtB, 10^{-3} M, n=26; ΔT 16-30˚C, n=35; combined, n=27 (**B**) The Bayesian prediction matched the experimental data. (**C**) The preference indices of single w^{1118} larva also improved when exposed to the combined gradients. Experimental conditions: EtB, 10^{-3} M, n=79, ΔT 16-30˚C, n= 81, combined n=83 (**D**) The trend of the Bayesian prediction followed the experimental data. However, the prediction was more variable than for groups of larvae, because the total number of larvae was much lower.

Testing the nature of odor-temperature integration with noise

I performed a number of different experiments to test the impact of noise on odor-temperature integration. Chrimson was expressed either in the *Or42a* or the *Or42b* neuron. Since these larvae were less sensitive to temperature (Fig. 33 B), I shifted gradients towards higher temperatures.

In the first set of experiments larvae navigated a temperature gradient from 20-40°C and an odor gradient emanating from a droplet of 10^{-3} M ethyl butyrate. The boost in behavioral performance in the combined condition indicated sensory integration. Overall, the results without the presence of noise (Fig. 35) were similar to the behavior of wild-type larvae (Fig. 34 A, B).

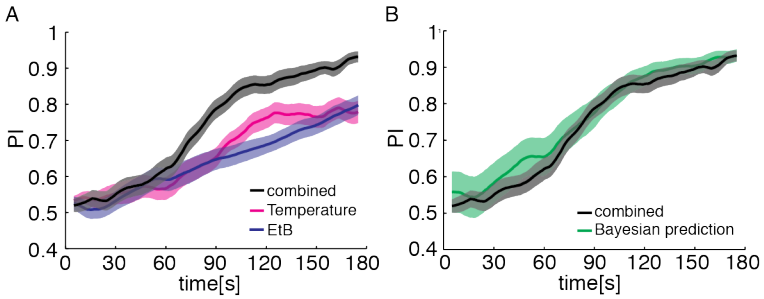

Figure 35: Multisensory Integration in *Or42a*-functional larvae. (**A**) Larvae expressing Chrimson in the *Or42a* OSN performed better when exposed to both gradients at the same time than in any of the unimodal condition. With the exception of the temperature gradient, the experimental conditions and results were quite similar to wild-type experiments. Experimental conditions: EtB, 10^{-3} M, n=30; ΔT 20-40°C, n=30; combined, n=30 (**B**) The experimental preference index over time is very similar to the prediction of the Bayesian framework.

The experiments were repeated with the addition of noise on top of the sensory gradients. However, the noise was always injected into the olfactory system. To corrupt chemotaxis in an odor gradient higher-intensity light flashes had to be used than in the presence of light gradients. Most likely this was necessary because noise was injected via one single OSN, while the odorant activated multiple OSNs. As expected, noise led to a reduction of chemotaxis

performance (Fig 36 A, C). Surprisingly thermotaxis performance increased with noise in the olfactory channel (Fig 36 A, D).

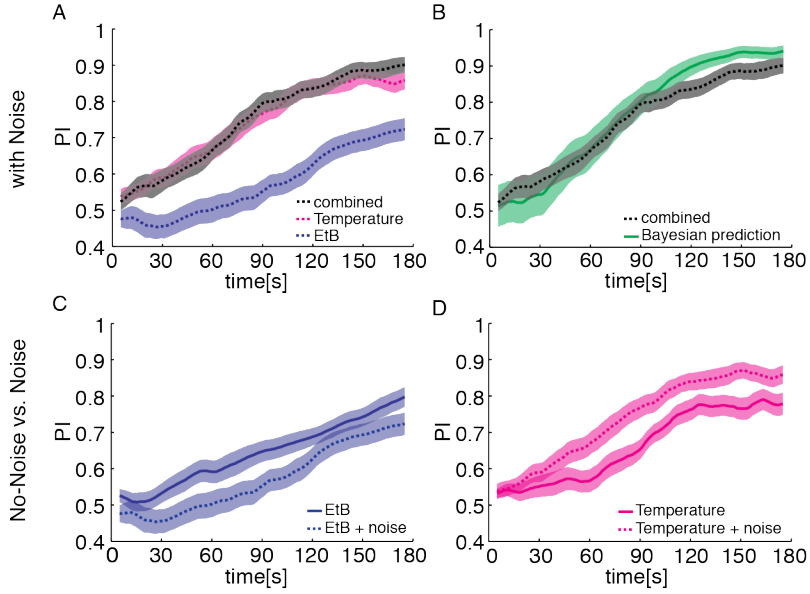

Figure 36: Multisensory integration in *Or42a*-functional larvae with noise. (**A**) *Or42a* larvae navigated EtB and temperature gradients while noise was injected into the olfactory system via the *Or42a* neuron. The combined condition was equal to the unimodal temperature condition. Experimental conditions: EtB, 10^{-3} M, n=30; ΔT 20-40°C, n=30; combined, n=30; sensory noise was present in all conditions, intensity of a light flash 11.15 W/m² (**B**) The Bayesian prediction matched the experimental data for the 90 seconds. It deviated slightly from the experimental data in the second half of the experiment. (**C**) Comparison of the chemotactic behavior with and without noise. Noise corrupts the chemotaxis performance. Experimental conditions from Fig. 35 A and Fig 36 A (**D**) Thermotaxis performance increases with noise in the olfactory system. Experimental conditions from Fig. 35 A and Fig. 36 A.

For the second set of experiments I used the same genotype but replaced the odor gradient with a virtual gradient of red light. Thus, the gradient information and noise were transmitted through the same channel (*Or42a*). Independent of the presence of noise, the behavior of the combined condition improved as compared to the behavior of larvae exposed to only one sensory gradient (Fig. 37 A,

C). Furthermore the experimental results matched the theoretical predictions (Fig. 37 B, D). However, as in the previous dataset the thermotactic behavior navigated gradients more efficient in the presence of noise in the olfactory system.

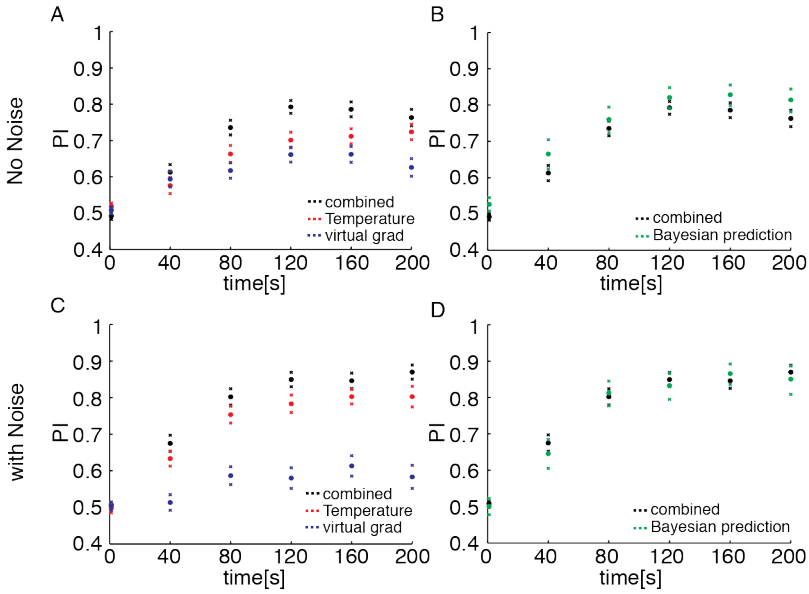

Figure 37: Multisensory integration between an *Or42a*-mediated virtual odor gradient and a temperature gradient. (**A**) The behavioral performance of larvae expressing Chrimson in the *Or42a* OSN, improved when exposed to light gradients and temperature gradients at the same time. Experimental conditions: ΔT 20-36˚C, n=49; virtual gradient, light intensity at peak 1.39 W/m², n=49 combined condition, n=49, Note: The full dataset was analyzed at 1, 40, 80, 120, 160 and 200 seconds and plotted accordingly. (**B**) The Bayesian prediction is not significantly different from the experimental results, although the PI of the prediction was a bit higher than the experimental PI. (**C**) Same experiments as in (A) with the presence of noise in all conditions. In the combined condition taxis behavior improved slightly. Experimental conditions: ΔT 20-36˚C, n=30; virtual gradient, light intensity at peak 1.39 W/m², n=30; combined, n=30, sensory noise was added by randomized light flashes with an intensity of: 0.69 W/m² (**D**) The Bayesian prediction fitted the experimental data well.

Finally, these results were verified with another genotype. Expression of Chrimson in the *Or67b* OSN resulted in the same observations (Fig. 38).

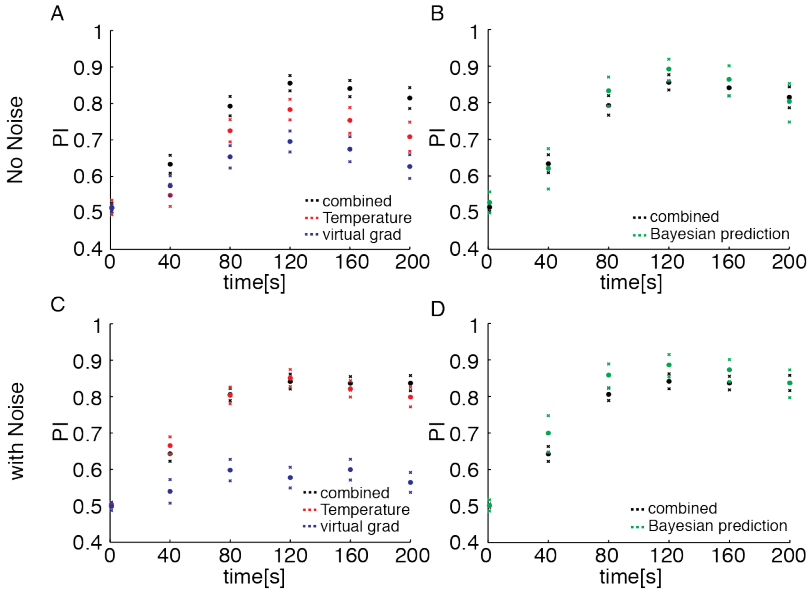

Figure 38: Multisensory Integration between an *Or67b*-mediated virtual odor gradient and a temperature gradient. (**A**) Larvae expressing Chrimson in the *Or67b* OSN navigated red light gradients and temperature gradients. The behavioral performance improved when larvae were exposed to both gradients at the same time. Experimental conditions: ΔT 20-32˚C, n=27; virtual gradient, light intensity at peak 1.39 W/m², n=28; combined condition, n=27, Note: The full dataset was analyzed at 1, 40, 80, 120, 160 and 200 seconds and plotted accordingly. (**B**) The Bayesian prediction is not significantly different from the experimental results. (**C**) Same experiments as in (A) although with the presence of noise in all conditions. In the combined condition taxis behavior improved slightly. Experimental conditions: ΔT 20-32˚C, n=27; virtual gradient, light intensity at peak 1.39 W/m², n=27; combined, n=27, sensory noise was added by randomized light flashes with an intensity of: 0.69 W/m² (**D**) The experimental PI was not significantly different from the predicted PI.

Chapter 5: Discussion

Behavioral strategy and variability

All organisms have to use strategies to deal with changes in their environments. Chemotaxis and thermotaxis follow a similar navigational strategy. Both modalities rely on a process of biasing run time and turns towards the favorable gradient direction (Gomez-Marin, Stephens et al. 2011, Gershow, Berck et al. 2012, Gepner, Mihovilovic Skanata et al. 2015, Hernandez-Nunez, Belina et al. 2015). It has been speculated that this similarity in behaviors might reflect an underlying limitation of the nervous system of *Drosophila* larvae to modulate behavior (Frye and Dickinson 2004)}(Gepner, Mihovilovic Skanata et al. 2015). However, I argue here that there is sufficient evidence to conclude that larval behavior is flexible enough to adapt to environmental contingencies. One behavior that larvae can adjust are head casts, which are an integral part of thermotactic and chemotactic strategies (Gomez-Marin and Louis 2012). Presumably, larvae use these lateral head movements to sample the environment such as odor and temperature gradients. The frequency of initial head casts decreases in the presence of food (fructose) (data not shown). This decrease is probably mediated by gustatory signals, which suppress motor programs (Schoofs, Hückesfeld et al. 2014) and is a good example of the adaptive nature of larval behavior to its environment. Ongoing efforts to screen and find the neurons underlying navigation behaviors of different sensory systems (e.g. collaborative projects like the larval Olympiad) yielded separate hits for different modalities (personal communication M. Louis). This suggests that larvae possess

sufficient neural capabilities to process information for every sensory system separately. It is not clear where the information arising from different modalities converges, but it has been shown recently that the subesophageal ganglion (SOG) acts as a premotor hub combining information from various modalities (Tastekin, Riedl et al. 2015).

I have just argued that *Drosophila* larvae are flexible enough to modulate their behavior in different situations. Thus, larval behavior is can be influenced by to many internal and external factors. A lack of proper control of developmental, genetic and external influences during experiments can enhance pre-existing behavioral variability. During my experiments I have tried to control the behavioral variability of thermotaxis. It is well documented that larvae exhibit different temperature preferences during first (L1), second (L2) and third instar (L3) stages (Garrity, Goodman et al. 2010). By contrast, odor-search behavior is more robust during larval development. I showed that L1 and L3 larvae rely on very similar strategies during chemotaxis (Fig. 13-19). However, a few differences remained: L1 larvae were still considerably slower when size was taken into account (Fig. 15 C) and turning performances were worse for L1 larvae (Fig. 15 D). This might have also been due to the fact that the assay and odor gradient had been optimized for L3 larvae (Gomez-Marin, Stephens et al. 2011). Therefore, developmental effects seem to have a bigger impact on behavioral variability during thermotaxis than chemotaxis. The genetic background also plays a role. The ability to chemotax does not differ strikingly between L3 larvae from the w^{1118} and CantonS strain (Fig. 13-19). By contrast

thermotaxis ability strongly varies between these different genotypes (Fig. 32 and 33). Small genetic differences such as a mutation of the *white* gene have been shown to affect behavioral variability via a serotonin dependent pathway (Kain, Stokes et al. 2012). w^{1118} larvae harbor this mutation while CantonS larvae do not. In theory the *white* mutation could cause the observed thermosensory differences because neither CantonS (Fig. 33 A) nor the Chrimson line, (Fig. 33 B), were able to navigate the shallow thermal gradient. In addition to the 'internal' developmental and genetic factors there are also external factors that can influence behavior. It is likely that observed differences in behavioral performance are partly due to the different gradient geometries. Odor gradients in my experimental setup were 2-dimensional and partly non-linear, while thermotaxis was restricted to 1-dimensional linear gradients. Humidity, the presence of food (Dillon, Wang et al. 2009), and the cultivation temperature (Krstevska and Hoffmann 1994) also affect the temperature preference of larvae and adult flies. However, in laboratory conditions these environmental factors are can be reasonably well controlled. Are there other plausible explanations for the variability of thermotaxis?

It is possible that behavioral variability might not only be due to changes in internal and external conditions but might be inherent to certain behaviors. In this respect variability might be the outcome of an evolutionary strategy to counter unpredictable environmental changes. This strategy is called bet-hedging; it is thought to shape behavioral preferences together with plasticity and inheritance of behavioral traits (adaptive tracking). The finding that thermotactic

and phototactic behavior of recently domesticated adult flies was more variable than predicted by chance alone supports bet-hedging (Kain, Zhang et al. 2014). Bet-hedging produces a distribution of phenotypes with "preset" differences in preferred temperatures (Hopper 1999, Simons 2011). Thus, a fraction of animals are always suited to the actual conditions, at the expense of the remainder of the population (Kain, Zhang et al. 2014). Neural plasticity conditions the temperature preference in response to external temperature, in nematodes like C. elegans (Hedgecock and Russell 1975) but has less impact in adult flies (Krstevska and Hoffmann 1994). Adaptive-tracking proposes that temperature preferences are inherited and adapted slowly to the present condition (Kain, Zhang et al. 2014). However, it seems that individual preferences are not transmitted to the progeny (Kain, Zhang et al. 2014). The life cycle of *Drosophila* is too short to transmit the temperature development over various seasons to its offspring by adaptive-tracking. Therefore, flies following this strategy will always be adapted to the conditions of the past generation. This might be disadvantageous in environments with abrupt temperature changes due to seasonal transitions. In these circumstances the bet-hedging strategy could be successful, because individual animals might not be able to transmit sufficient information to their offspring to adapt them for the next season. Thus, this mechanism provides a convincing explanation for why different orientation behaviors exhibit higher levels of variability. This strategy suggests that an experimenter can decrease variability by controlling experimental conditions, but it can never be abolished completely. I conclude that the high level of

variability during thermotaxis might have its origin in a strategy like bet-hedging while chemotaxis probably follows a different strategy.

Group behavior

The contribution of social cues in larval navigation could confound the interpretation of my experiments because the theoretical framework assumes the absence of strong interactions between larvae. Therefore, I review the evidence for collective decision-making to evaluate the of social information contributing to the observed behavior. Models for collective decision-making have been successfully applied to zebrafish and a number of other species (Pérez-Escudero and De Polavieja 2011, Arganda, Pérez-Escudero et al. 2012). In larvae, social information could presumably be relayed by vision, olfaction or mechanosensation. At the start of each behavioral experiment larvae were mostly separated from each other. The behavioral arena is illuminated with infrared light, which larvae are not able to perceive. This precludes the possibility that larvae "see" each other. In principle, orientation decisions could be biased by a pheromone gradient resulting in larval aggregation (Mast, De Moraes et al. 2014). I assume that larval behavior improves in the presence of such a gradient. This is because the majority of larvae are on the side of the cues and a pheromone gradient should reinforce this aggregation. Nevertheless, it is unlikely that a pheromone gradient could be established during the duration of the experiment[25]. This conclusion is supported by my

[25] Mast et al. show that a single larva chooses agarose with pheromone depositions over plain agarose. However, prior to this test several hundred larvae were crawling on the agarose for 20 minutes to deposit the pheromones.

results and the results of previous studies, which show that larval chemotaxis performance decreases with increasing group size (Monte, Woodard et al. 1989, Kaiser and Cobb 2008) (Fig. 21 A). This finding suggests that larvae do not rely on social information during this type of sensorimotor decision-making in laboratory conditions. On the contrary, the authors of previous studies concluded that the reduction of behavioral performance was associated with higher frequencies of disadvantageous interactions (e.g. bumping) due to increased larval density (Kaiser and Cobb 2008). I speculate that negative interactions are not the only reason for decreased performance in the group assays I conducted. I base my speculations on the fact that errors (SEM) from my experiments are very similar to theoretical binomial errors, which assume that larvae behave independently form each other (Fig. 21 B). This agrees with behavioral observations from the past (Monte, Woodard et al. 1989, Kaiser and Cobb 2008) and suggests that other explanations are also responsible for the observed difference in performance.

I was for example able to control the larval orientation at the start of single-larvae experiments, but I could not achieve a similar control for groups of larvae. Therefore, a single larva was placed perpendicular to the olfactory gradient while the orientation at the onset of group experiments was random, due to larval movement during the delay caused by the sequential placement of larvae. High-resolution analysis of chemotaxis shows that perpendicular orientation to the gradient leads to the best results for decision-making (Fig. 18) (Gomez-Marin, Stephens et al. 2011). Handling

time of larvae could also have a negative influence on behavior. Prior to an experiment, single larvae were isolated using a brush and transferred one by one into a Petridish coated with agarose. At the start of the experiment all larvae were placed together in the behavioral arena. Bigger groups required longer manipulation times, especially during the placement onto the agarose surface of the arena. Consequently larvae in bigger groups of experiments are more agitated at the start of an experiment. The state of agitation influences thermotactic and phototactic behaviors (Lewontin 1959, Rockwell and Seiger 1973, Seiger, Seiger et al. 1983). Thus, it is conceivable that it also has an impact on chemotactic behavior. Together, these two effects, initial orientation and manipulation time, probably account for most of the differences seen in the behavioral assay although negative interactions certainly affect overall behavior as well. Taken together, I conclude that behavioral performance did not rely on social information or strong social interactions.

Sensory integration and probabilistic inference

One of the principal conclusions from this study is that larvae are able to combine information from multiple cues. Combination is achieved within and across modalities as outlined in the scenarios of intramodal (odor-odor) and intermodal (odor-temperature) integration. Importantly, the favorable direction of both gradients pointed towards the same side of the assay. This way I avoid dealing with unknown issues of hierarchy that might arise from conflicting information between different sensory systems in the intramodal scenario. In general, information should be combined in accordance with the causal structure of the world (Tenenbaum, Griffiths et al. 2006). This statement is relies on the assumption that sensory information is only combined if it originates from the same perceptual object (e.g. multiple odor gradients emanating from a ripe banana) However, I argue that larvae integrate sensory information even though it might not originate from the same perceptual object, providing that the scenario resembles their natural environment. (Gepner, Mihovilovic Skanata et al. 2015).

Intramodal integration refers to the combination of information from two different odor gradients. The performance of wild-type w^{1118} larvae improved when exposed to two odor gradients (Fig. 25) as compared to the behavior in a single gradient. However, I was not able to identify a pair of odorants that activated completely separate subsets of OSNs. For this reason, I resorted to an optogenetics approach. After identifying a receptor, which is not activated by EtB (Fig. 27) I expressed Chrimson in this OSN and transformed it into an independent input channel. This way I was

finally able to test sensory integration without any cross-activation at the levels of the ORs (Fig. 28). These results confirmed my initial assumptions, that the larval nervous system is able to combine independent information from different channels within the same modality.

The scenario of intermodal integration investigates the combination of information between the olfactory and thermosensory systems. Both w^{1118} and larvae expressing Chrimson in the *Or42a*-OSN, increased their performances when exposed to an odor and temperature gradient, as compared to behavior in the unimodal condition (Fig. 34 A, B; Fig. 35). However, odor and temperature gradients are not completely independent since thermal convection could potentially distort the odor gradient. To exclude such influences I used optogenetics to repeat these experiments with virtual odor gradients in which the odorant had been substituted by red light (Fig. 37, 38). These conditions offer a paradigm where complete independence of the inputs is assured. As observed earlier, the behavioral performance improved when both cues were presented at the same time. I concluded that larvae are integrating information between different modalities even though they do not arise from the same perceptual object.

Improved sensorimotor decision-making in the presence of multiple cues has been shown before in *Drosophila* larvae (Gepner, Mihovilovic Skanata et al. 2015). My study goes one step further and examines whether the rules of probabilistic inference apply to larval decision-making. Bayesian probabilistic inference has recently been applied to a cue conflict situation in ants (Wystrach, Mangan et al.

2015). Wystrach et al. show that ants behave similarly to the optimal solution but might only use a proxy of uncertainty instead of implementing the full Bayesian model. Together with collaborators I derived a model describing larval behavior based on a Bayesian framework. The model uses the preference indices of the behavior in two single sensory gradients as an input and predicts the preference index of the behavior in the combined condition. This prediction resulted in a good fit for all experimental conditions shown in this thesis. However, in a number of conditions the prediction did not yield a satisfactory fit. Such conditions were usually associated with experiments that did not result in behavioral improvements upon combination of two sensory gradients (data not shown). I speculate that the absence of behavioral improvements was due to a 'capture effect' in which the orientation response was purely guided by one sensory gradient, while the other was ignored. Capture effects are common in human psychophysics, e.g. humans usually experience a visual capture effect, due to the low sensory threshold of the visual system (Ernst and Banks 2002). Studies testing sensory integration in vertebrates rely on sophisticated psychophysical methods to avoid capture effects (Ernst and Banks 2002, Alais and Burr 2004, Raposo, Sheppard et al. 2012). Unfortunately, such methods have not yet been adapted for insects.

I tested the validity of the Bayesian model in a number of ways. The hallmark of Bayesian inference is that information is combined in proportion to its reliability. Manipulation of the uncertainty of a cue leads to a change in weighting of the cues but, importantly, the prediction of the Bayesian framework should still match the

observed behavior. I manipulated the reliability of olfactory cues by adding randomized light flashes on top of sensory gradients. Thus, I injected noise into the nervous system by expressing Chrimson in different OSNs. The temporal sequence of the light flashes was conserved in all experiments (frozen noise) although the amplitude (light intensity) varied depending on whether the odor gradient was odor or light (virtual odor gradient). Noise with a high amplitude (strong noise) was injected via the *Or42a*-neuron if larvae were chemotaxing in an EtB gradient (Fig. 36). In this condition only a fraction of the sensory input is corrupted by noise because EtB activates two to four OSNs[26] while Chrimson is only expressed in one of them (*Or42a).* For chemotaxis in a virtual odor gradient noise was injected with a lower light intensity (weak noise) via the *Or42a* or *Or67b*-OSN (Fig. 29, Fig. 37 C, D; Fig. 38 C, D). In accordance with the assumptions of the Bayesian framework the predictions matched the behavior of the combined condition even though the olfactory behavior was significantly reduced by the noise (Fig. 29, Fig. 36 A, B; Fig. 37 C, D, Fig. 38 C, D). Surprisingly, the unimodal thermotaxis improved when pure noise was injected in the olfactory system (Fig. 36 A,D; Fig. 37 C; Fig. 38 C). It seems that the improvement correlated with the amplitude of the light flashes. The increase was mild for weak noise (Fig. 37 C; Fig. 38 C) and high for strong noise (Fig. 36 A, D). The observed improvement of thermotaxis with noise in the olfactory system was probably due to cross-modal interactions. As described in the introduction, cross-modal interaction facilitates the detection of a cue by a task-

[26] Ethylbutyrate (EtB) activates two OSNs at a concentration of 10^{-4} M and four OSNs at a concentration of 10^{-2} M (Kreher, S. A., et al. (2008)).

irrelevant signal in another modality (Stein, London et al. 1996, Spence and Driver 1997) (McDonald, Teder-Sälejärvi et al. 2000, Lovelace, Stein et al. 2003). However, a similar effect was not observed during intramodal integration. Addition of noise to the virtual odor gradient corrupted chemotaxis in this gradient without improving chemotaxis in an odor gradient with pure noise in the other channel (Fig. 30). Such differences between intermodal and intramodal conditions have been predicted by psychophysical studies (Newell, Mamassian et al. 2010). The presence of cross-modal interactions is not expected to affect the Bayesian model in any way. To test whether larvae implement Bayesian inference I compared the predictions of the Bayesian model to predictions from a suboptimal fixed-weight model. In contrast with the Bayesian model, the fixed-weight model does not combine their cues according to their level of reliability. This model is in line with preference-based models of the economic tradition. Without the presence of sensory noise the prediction of both models are equivalent (equation (19)). The presence of external noise in the olfactory system allows the distinction between these models based on the behavior in a single sensory gradient and pure noise in the sensory other channel. However, this strategy to distinguish between the Bayesian and the fixed-weight model is only valid in the absence of cross modal interactions. For the intramodal condition the fixed-weight model failed to predict the behavior of larvae in a single olfactory gradient with only pure noise in the other sensory channel and the behavior of the combined condition. Since the Bayesian model predicted the behavior well, I concluded that larvae follow a

near-optimal Bayesian strategy when integrating cues from different sensory gradients.

The theoretical framework developed for this study focuses only on perceptual tasks. This is partly because the metabolic cost of turning is symmetrical i.e. independent of the direction. All other associated factors of the cost function are taken into account by the assumptions of the model. Thus, a larva is minimizing its cost if it is moving in the favorable direction of the combined gradients. The derivation of the model shows that slight interactions between larvae, like bumping into each other, do not affect the proposed way larvae combine information. This has also been verified experimentally. Both single and groups of larvae follow the predictions of the Bayesian model (Fig. 34 C, D).

The Bayesian model does not make any assumptions about the neural implementation. Recent findings started to reveal an astonishing wealth of data about sensory integration in *Drosophila* larvae. A mechanism for integration of conflicting information in the mushroom body (MB) has been proposed (Lewis, Siju et al. 2015). It has also been shown that both OSNs and thermosensory neurons are located in the same ganglion (Klein, Afonso et al. 2015). Co-localization of OSNs and thermosensory neurons allows for direct neuron-to-neuron communication by ephaptic coupling[27] (Katz and Schmitt 1940). In this process the electric field generated by the activity of a neuron interferes with the activity of neighboring neurons. Ephaptic coupling is causing non-synaptic inhibition in

[27] https://en.wikipedia.org/wiki/Ephaptic_coupling

sensilla of the olfactory system of adult flies (Su, Menuz et al. 2012) and might play a similar role in the dorsal organ ganglion (DOG) of larvae. This might explain cross-modal interactions or even constitute the first level of cue combination between sensory signals. Based on these observations, I propose a circuit of multilevel convergence similarly as described recently in the larvae (Ohyama, Schneider-Mizell et al. 2015). The authors used an optimization procedure, constrained by experimental data, to show that such a circuit is more sensitive to weak bimodal inputs. A multilevel convergence approach is compatible with diverging and converging motifs described for olfactory processing (Jeanne and Wilson). Theories of neural encoding like probabilistic population codes (Ma, Beck et al. 2006) specify the requirements for the encoding of probabilities. Although these models have been developed to process information at the level of peripheral sensory neurons, in principle they could also be implemented at later stages such as in the MB or lateral horn (LH). The LH is another region of potential importance for multisensory integration. This can be deduced from ongoing efforts to reconstruct of the connectivity of this region, which reveals sensory convergence (personal communication A. Khandelwal).

Future directions

At the moment, we ignore the type of noise larvae experience in the their natural environments. In contrast to adult flies which track the olfactory signal in odor plumes one can assume that graded olfactory stimuli as experienced by larvae are less noisy. In accordance with present convention I assumed that the noise in the nervous system is Poisson-like (Tolhurst, Movshon et al. 1983, Graf, Kohn et al. 2011, Berens, Ecker et al. 2012). I conducted a number of electrophysiological experiments to show that noise can indeed interfere with spiking activity induced by deterministic stimuli[28] (data not shown). Short flashes of light can trigger excitation followed by a short inhibition of OSNs. Presentation of stochastic stimuli corrupts neural firing markedly as compared neural activity in response to deterministic stimuli. However a detailed study of how noise impacts decision-making is still lacking.

All forms of orientation behavior in this thesis have been quantified with a preference index. This discrete measurement of the position of each larva represents a coarse way to quantify behavior. However, a low-resolution assessment of the movement of groups of larvae also has advantages. This type of assessment is more robust to differences in geometric shapes (1-dimensional temperature gradients vs. 2-dimensional odor gradients) and slight incongruences in sensory gradients (odor gradient vs. light gradient) than other, more refined behavioral metrics (e.g. distance form the odor source). In addition it is relatively easy to model the evolution of the

[28] These experiments were conducted with Channelrhodopsin (blue light).

preference index over time, without the need of any free parameters. Nevertheless the model described in this thesis generalizes easily to single decisions (e.g. type 1 and type 2 decisions as outlined in the introduction). High-resolution tracking or quantification of single turns is undoubtedly the gold standard of behavioral quantification and would be the next logical step of this project. In addition it would make sense to embed the decision-rules in an agent-based model and compare the behavior for different levels of environmental noise. This would provide a great way to test ideas about the implementation of Bayesian inference in larvae *in-silico*.

At present, research in sensory decision-making in insects still lacks a unifying theoretical framework and methodology. The ethological tradition has yielded powerful methods to discover the underlying neural substrate of behaviors, but it lacks the tools to access the wealth of information about decision-making that the psychological approach has amassed. During psychophysical experiments monkeys and rats perform hundreds of two-alternative forced choice (2AFC) decisions in a row and are rewarded with fruit juice or water for correct decisions. The recent development of closed-loop trackers and "virtual sensory realities" might help to close this gap. However, it is still not possible to perform 2AFC in insects and generate psychometric curves, because it is not possible to reward animals after single decisions. With the rise of optogenetics it would be possible to stimulate reward centers in the brain directly after a larvae performed a decision in a closed loop tracker. If this operant learning based approach turns out to be effective it would finally be possible to apply the psychophysics toolbox to *Drosophila* larvae.

Conclusion

In this study I aimed to show that larvae are able to combine sensory information from different sources according to Bayesian probabilistic inference. Larvae were tested in two-dimensional arenas comprising two odor gradients. These were either two odor gradients or an odor gradient and a virtual odor gradient. The virtual odor gradient was created by optogenetic stimulation of a single olfactory sensory neuron insensitive to the real odor. I manipulated the reliability of the virtual-odor cue by superimposing random light flashes to a static light gradient. I considered two models: an optimal Bayesian model in which cues are weighted according to their respective reliabilities and a suboptimal model in which cues are assigned fixed weights. I worked with collaborators, to derive behavioral predictions for the combination of both cues with and without noise. The fixed-weight model fails to accurately predict the combined behavior and the performance of a single cue when noise is present in the other channel. In contrast, the Bayesian model predicts the behavior well when both cues are combined. I found similar results, after I applied the same paradigm for the combination of a temperature and an odor (real odor or virtual odor) gradient. These findings demonstrate that near-optimal inference is not restricted to, integration within a single modality but also applies to multisensory integration. This study provides a basis for further research into Bayesian decision-making in Drosophila larvae.

Abbreviations

AC (neuron)	anterior cell neuron
AEL	after egg laying
AL	antennal lobe
cVA	11-*cis* vaccenyl acetate
DAN	dopaminergic neuron
DOG	dorsal organ ganglion
EtB	ethyl butyrate
fps	frames per second
IAA	isoamyl acetate
KCs	Kenyon cells
L1	first instar larvae
L2	second instar larvae
L3	third instar larvae
LH	lateral horn
LN	local interneuron
MB	mushroom body
MBON	mushroom body output neurons
OR	olfactory receptor
OSN	olfactory sensory neuron
PI	preference index
PN	projection neuron
PSTH	peristimulus time histogram
SC	superior colliculus
SEM	standard error of the mean
SOG	subesophageal ganglion
TOG	terminal organ ganglion
VNC	ventral nerve cor

Bibliography

Alais, D. and D. Burr (2004). "The Ventriloquist Effect Results from Near-Optimal Bimodal Integration." Current Biology **14**(3): 257-262.

Alon, U. (2006). An introduction to systems biology: design principles of biological circuits, CRC press.

Arganda, S., et al. (2012). "A common rule for decision making in animal collectives across species." Proceedings of the National Academy of Sciences **109**(50): 20508-20513.

Ariely, D. and S. Jones (2008). Predictably irrational, HarperCollins New York.

Asahina, K., et al. (2009). "A circuit supporting concentration-invariant odor perception in Drosophila." Journal of biology **8**(1): 9.

Aso, Y., et al. (2014). "The neuronal architecture of the mushroom body provides a logic for associative learning." eLife **3**.

Aso, Y., et al. (2014). "Mushroom body output neurons encode valence and guide memory-based actionselection in Drosophila." eLife **3**.

Bayes, T. (1763). "An Essay towards solving a Problem in the Doctrine of Chances." Philosophical Transactions (1683-1775) **53**: 370-418.

Beck, J. M., et al. (2012). "Not Noisy, Just Wrong: The Role of Suboptimal Inference in Behavioral Variability." Neuron **74**(1): 30-39.

Bellen, H. J., et al. (2010). "100 years of Drosophila research and its impact on vertebrate neuroscience: a history lesson for the future." Nature Reviews Neuroscience **11**(7): 514-522.

Bellmann, D. (2010). "Optogenetically induced olfactory stimulation in Drosophila larvae reveales the neuronal basis of odor-aversion behavior." Frontiers in Behavioral Neuroscience **4**.

Bentham, J. (1780). "An Introduction to the Principles of Morals and Legislation."

Benton, R., et al. (2006). "Atypical Membrane Topology and Heteromeric Function of Drosophila Odorant Receptors In Vivo." PLoS Biology **4**(2): e20.

Benzer, S. (1967). "Behavioral mutants of Drosophila isolated by countercurrent distribution." Proceedings of the National Academy of Sciences of the United States of America **58**(3): 1112.

Berens, P., et al. (2012). "A fast and simple population code for orientation in primate V1." The Journal of Neuroscience **32**(31): 10618-10626.

Berg, H. C. and D. A. Brown (1972). "Chemotaxis in Escherichia coli analysed by three-dimensional tracking." Nature **239**(5374): 500-504.

Botvinick, M. and J. Cohen (1998). "Rubber hands /`feel/' touch that eyes see." Nature **391**(6669): 756-756.

Boyden, E. S. (2015). "Optogenetics and the future of neuroscience." Nature neuroscience **18**(9): 1200-1201.
Nature Neuroscience 18, 1200 (2015). doi:10.1038/nn.4094

Boyden, E. S., et al. (2005). "Millisecond-timescale, genetically targeted optical control of neural activity." Nat Neurosci **8**(9): 1263-1268.

Bräcker, L. B., et al. (2013). "Essential role of the mushroom body in context-dependent CO_2 avoidance in Drosophila." Current biology : CB **23**(13): 1228-1234.

Brand, A. H. and N. Perrimon (1993). "Targeted gene expression as a means of altering cell fates and generating dominant phenotypes." Development **118**(2): 401-415.

Brieger, G. and F. M. Butterworth (1970). "Drosophila melanogaster: identity of male lipid in reproductive system." Science **167**(3922): 1262-1262.

Brunton, B. W., et al. (2013). "Rats and Humans Can Optimally Accumulate Evidence for Decision-Making." Science (New York, NY) **340**(6128): 95-98.

Butts, D. A. and M. S. Goldman (2006). "Tuning curves, neuronal variability, and sensory coding." PLoS Biology **4**(4): 639.

Cachero, S. and G. S. Jefferis (2008). "Drosophila olfaction: the end of stereotypy?" Neuron **59**(6): 843-845.

Caron, S. J. C., et al. (2013). "Random convergence of olfactory inputs in the Drosophila mushroom body." Nature **497**(7447): 113-117.

Chater, N., et al. (2006). "Probabilistic models of cognition: conceptual foundations." Trends in cognitive sciences **10**(7): 287-291.

Chow, D. M., et al. (2011). "An olfactory circuit increases the fidelity of visual behavior." The Journal of Neuroscience **31**(42): 15035-15047.

Chu, I.-W. and R. Axtell (1971). "Fine structure of the dorsal organ of the house fly larva, Musca domestica L." Zeitschrift für Zellforschung und mikroskopische Anatomie **117**(1): 17-34.

Clowney, E. J., et al. (2015). "Multimodal Chemosensory Circuits Controlling Male Courtship in Drosophila." Neuron: 1-15.
Neuron, Corrected proof. doi:10.1016/j.neuron.2015.07.025

Coen, P., et al. (2014). "Dynamic sensory cues shape song structure in Drosophila " Nature: 1-17.
Nature (2013). doi:10.1038/nature13131

Das, A., et al. (2013). "Neuroblast lineage-specific origin of the neurons of the Drosophila larval olfactory system." Developmental biology **373**(2): 322-337.

Das, A., et al. (2008). "Drosophila olfactory local interneurons and projection neurons derive from a common neuroblast lineage specified by the empty spiracles gene." Neural development **3**(1): 33.

de Belle, J. S. and M. Heisenberg (1994). "Associative odor learning in Drosophila abolished by chemical ablation of mushroom bodies." Science **263**(5147): 692-695.

Deisseroth, K. (2011). "Optogenetics." Nat Methods **8**(1): 26-29.

Deisseroth, K. (2015). "Optogenetics: 10 years of microbial opsins in neuroscience." 1-13.

Dillon, M. E., et al. (2009). "Review: Thermal preference in Drosophila." Journal of thermal biology **34**(3): 109-119.

Durisko, Z. and R. Dukas (2013). "Attraction to and learning from social cues in fruitfly larvae." Proceedings of the Royal Society of London B: Biological Sciences **280**(1767): 20131398.

Durisko, Z., et al. (2014). "Dynamics of Social Behavior in Fruit Fly Larvae." PLoS ONE **9**(4): e95495.

Ehrsson, H. H. (2007). "The Experimental Induction of Out-of-Body Experiences." Science **317**(5841): 1048.

Eisthen, H. L. (2002). "Why are olfactory systems of different animals so similar?" Brain, behavior and evolution **59**(5-6): 273-293.

Ernst, M. O. and M. S. Banks (2002). "Humans integrate visual and haptic information in a statistically optimal fashion." Nature **415**(6870): 429-433.

Faisal, A. A., et al. (2008). "Noise in the nervous system." Nature Reviews Neuroscience **9**(4): 292-303.

Ferveur, J.-F. (2005). "Cuticular hydrocarbons: their evolution and roles in Drosophila pheromonal communication." Behavior genetics **35**(3): 279-295.

Fiorillo, C. D., et al. (2003). "Discrete coding of reward probability and uncertainty by dopamine neurons." Science **299**(5614): 1898-1902.

Fişek, M. and R. I. Wilson (2013). "Stereotyped connectivity and computations in higher-order olfactory neurons." Nature neuroscience.

Fishilevich, E., et al. (2005). "Chemotaxis Behavior Mediated by Single Larval Olfactory Neurons in Drosophila." Current Biology **15**(23): 2086-2096.

Frank, D. D., et al. (2015). "Temperature representation in the Drosophila brain." Nature: 1-15.
Nature (2015). doi:10.1038/nature14284

Frassinetti, F., et al. (2002). "Enhancement of visual perception by crossmodal visuo-auditory interaction." Experimental Brain Research **147**(3): 332-343.

Frye, M. A. and M. H. Dickinson (2004). "Motor output reflects the linear superposition of visual and olfactory inputs in Drosophila." Journal of Experimental Biology **207**(1): 123-131.

Gallio, M., et al. (2011). "The coding of temperature in the Drosophila brain." Cell **144**(4): 614-624.

Gallistel, C. R. and A. P. King (2011). Memory and the computational brain: Why cognitive science will transform neuroscience, John Wiley & Sons.

Garrity, P. A., et al. (2010). "Running hot and cold: behavioral strategies, neural circuits, and the molecular machinery for thermotaxis in C. elegans and Drosophila." Genes & Development **24**(21): 2365-2382.

Gepner, R., et al. (2015). "Computations underlying Drosophila photo-taxis, odor-taxis, and multi-sensory integration." eLife **4**.

Gepner, R., et al. (2015). "Computations underlying Drosophila photo-taxis, odor-taxis, and multi-sensory integration." eLife: e06229.

Gerber, B. and R. F. Stocker (2006). "The Drosophila Larva as a Model for Studying Chemosensation and Chemosensory Learning: A Review." Chemical Senses **32**(1): 65-89.

Gershow, M., et al. (2012). "Controlling airborne cues to study small animal navigation." Nature Methods **9**(3): 290-296.

Gigerenzer, G. and P. M. Todd (1999). Simple heuristics that make us smart, Oxford University Press, USA.

Gomez-Marin, A. and M. Louis (2012). "Active sensation during orientation behavior in the Drosophila larva: more sense than luck." Current Opinion in Neurobiology **22**(2): 208-215.

Gomez-Marin, A. and M. Louis (2012). "Active sensation during orientation behavior in the Drosophila larva: more sense than luck." Curr Opin Neurobiol **22**(2): 208-215.

Gomez-Marin, A. and M. Louis (2012). Active sensation during orientation behavior in the Drosophila larva: more sense than luck. Curr Opin Neurobiol. **22:** 208-215.

Gomez-Marin, A. and M. Louis (2014). "Multilevel control of run orientation in Drosophila larval chemotaxis." Frontiers in Behavioral Neuroscience **8**: 1-14.

Gomez-Marin, A. and M. Louis (2014). "Multilevel control of run orientation in Drosophila larval chemotaxis." Front Behav Neurosci **8**: 38.

Gomez-Marin, A., et al. (2012). "Automated Tracking of Animal Posture and Movement during Exploration and Sensory Orientation Behaviors." PLoS One **7**(8): e41642.

Gomez-Marin, A., et al. (2011). "Active sampling and decision making in Drosophila chemotaxis." Nat Commun **2**: 441.

Gomez-Marin, A., et al. (2011). "Active sampling and decision making in Drosophila chemotaxis." Nature communications **2**: 441-410.

Graf, A. B., et al. (2011). "Decoding the activity of neuronal populations in macaque primary visual cortex." Nature neuroscience **14**(2): 239-245.

Griffith, L. C. (2014). "A big picture of a small brain." eLife **3**.

Griffiths, T. L., et al. (2012). "How the Bayesians got their beliefs (and what those beliefs actually are): Comment on Bowers and Davis (2012)." Psychological Bulletin **138**(3): 415-422.

Grosjean, Y., et al. (2011). "An olfactory receptor for food-derived odours promotes male courtship in Drosophila." Nature **478**(7368): 236-240.

Guterstam, A., et al. (2011). "The illusion of owning a third arm." PLoS ONE **6**(2): e17208.

Ha, T. S. (2006). "A Pheromone Receptor Mediates 11-cis-Vaccenyl Acetate-Induced Responses in Drosophila." The Journal of neuroscience : the official journal of the Society for Neuroscience **26**(34): 8727-8733.

Haining, W. N., et al. (1999). "The proapoptotic function of Drosophila Hid is conserved in mammalian cells." Proceedings of the National Academy of Sciences of the United States of America **96**(9): 4936-4941.

Hallem, E. A. and J. R. Carlson (2006). "Coding of Odors by a Receptor Repertoire." Cell **125**(1): 143-160.

Hallem, E. A., et al. (2004). "The molecular basis of odor coding in the Drosophila antenna." Cell **117**(7): 965-979.

Hamada, F. N., et al. (2008). "An internal thermal sensor controlling temperature preference in Drosophila." Nature **454**(7201): 217-220.

Hassan, J., et al. (2005). "Photic input pathways that mediate the Drosophila larval response to light and circadian rhythmicity are developmentally related but functionally distinct." Journal of Comparative Neurology **481**(3): 266-275.

Hedgecock, E. M. and R. L. Russell (1975). "Normal and mutant thermotaxis in the nematode Caenorhabditis elegans." Proceedings of the National Academy of Sciences **72**(10): 4061-4065.

Heimbeck, G., et al. (2001). "A central neural circuit for experience-independent olfactory and courtship behavior in Drosophila

melanogaster." Proceedings of the National Academy of Sciences **98**(26): 15336-15341.

Heinrich, B. (1993). The hot-blooded insects: strategies and mechanisms of thermoregulation, Harvard University Press.

Helmholtz, H. v. (1891). "Versuch einer erweiterten Anwendung des Fechnerschen Gesetzes im farbensystem." Z. Psychol. Physiol. Sinnesorg **2**: 1-30.

Herculano-Houzel, S. (2009). "The human brain in numbers: a linearly scaled-up primate brain." Frontiers in Human Neuroscience **3**.

Hernandez-Nunez, L., et al. (2015). "Reverse-correlation analysis of navigation dynamics in Drosophila larva using optogenetics." eLife.

Hopper, K. R. (1999). "Risk-spreading and bet-hedging in insect population biology 1." Annual review of entomology **44**(1): 535-560.

Huston, S. J. and V. Jayaraman (2011). "Studying sensorimotor integration in insects." Current Opinion in Neurobiology **21**(4): 527-534.

Hutchinson, J. M. and G. Gigerenzer (2005). "Simple heuristics and rules of thumb: Where psychologists and behavioural biologists might meet." Behavioural processes **69**(2): 97-124.

Hwang, R. Y., et al. (2007). "Nociceptive neurons protect Drosophila larvae from parasitoid wasps." Current Biology **17**(24): 2105-2116.

Iino, Y. and K. Yoshida (2009). "Parallel Use of Two Behavioral Mechanisms for Chemotaxis in Caenorhabditis elegans." The Journal of neuroscience : the official journal of the Society for Neuroscience **29**(17): 5370-5380.

Izquierdo, E. J. and S. R. Lockery (2010). "Evolution and Analysis of Minimal Neural Circuits for Klinotaxis in Caenorhabditis elegans." The Journal of neuroscience : the official journal of the Society for Neuroscience **30**(39): 12908-12917.

Jacobs, R. A. (1999). "Optimal integration of texture and motion cues to depth." Vision research **39**(21): 3621-3629.

Jeanne, James M. and Rachel I. Wilson "Convergence, Divergence, and Reconvergence in a Feedforward Network Improves Neural Speed and Accuracy." Neuron.

Jefferis, G. S., et al. (2007). "Comprehensive maps of Drosophila higher olfactory centers: spatially segregated fruit and pheromone representation." Cell **128**(6): 1187-1203.

Justice, E. D., et al. (2012). "The simple fly larval visual system can process complex images." Nature communications **3**: 1156.

Kahneman, D. and A. Tversky (1979). "Prospect Theory: An Analysis of Decision under Risk." Econometrica **47**(2): 263-291.

Kahneman, D. and A. Tversky (2000). Choices, values, and frames, Cambridge University Press.

Kain, J., et al. (2014). "Bet-hedging, seasons and the evolution of behavioral diversity in Drosophila." bioRxiv: 012021.

Kain, J. S., et al. (2012). "Phototactic personality in fruit flies and its suppression by serotonin and white." Proceedings of the National Academy of Sciences **109**(48): 19834-19839.

Kaiser, M. and M. Cobb (2008). "The behaviour of Drosophila melanogaster maggots is affected by social, physiological and temporal factors." Animal Behaviour **75**(5): 1619-1628.

Kalman, R. E. (1960). "A new approach to linear filtering and prediction problems." Journal of Fluids Engineering **82**(1): 35-45.

Katz, B. and O. H. Schmitt (1940). "Electric interaction between two adjacent nerve fibres." The Journal of Physiology **97**(4): 471-488.

Keene, A. C. and S. G. Sprecher (2011). "Seeing the light: photobehavior in fruit fly larvae." Trends in neurosciences: 1-7.
Trends in Neurosciences. 10.1016/j.tins.2011.11.003

Keene, A. C. and S. Waddell (2007). "Drosophila olfactory memory: single genes to complex neural circuits." Nature Reviews Neuroscience **8**(5): 341-354.

Kepecs, A., et al. (2008). "Neural correlates, computation and behavioural impact of decision confidence." Nature **455**(7210): 227-231.

Kim, M.-S., et al. (1998). "LUSH odorant-binding protein mediates chemosensory responses to alcohols in Drosophila melanogaster." Genetics **150**(2): 711-721.

Klapoetke, N. C., et al. (2014). "Independent optical excitation of distinct neural populations." Nat Meth **11**(3): 338-346.

Klein, M., et al. (2015). "Sensory determinants of behavioral dynamics in Drosophilathermotaxis." Proceedings of the National Academy of Sciences of the United States of America **112**(2): E220-E229.

Knill, D. C. (2003). "Mixture models and the probabilistic structure of depth cues." Vision research **43**(7): 831-854.

Knill, D. C. and A. Pouget (2004). "The Bayesian brain: the role of uncertainty in neural coding and computation." Trends in neurosciences **27**(12): 712-719.

Kohatsu, S., et al. (2011). "Female contact activates male-specific interneurons that trigger stereotypic courtship behavior in Drosophila." Neuron **69**(3): 498-508.

Kohatsu, S. and D. Yamamoto (2015). "Visually induced initiation of Drosophila innate courtship-like following pursuit is mediated by central excitatory state." Nature communications **6**.

Körding, K. (2007). "Decision Theory: What "Should" the Nervous System Do?" Science **318**(5850): 606-610.

Körding, K. P., et al. (2007). "Causal inference in multisensory perception."

Kording, K. P. and D. M. Wolpert (2004). "Bayesian integration in sensorimotor learning." Nature **427**(6971): 244-247.

Kreher, S. A., et al. (2005). "The Molecular Basis of Odor Coding in the Drosophila Larva." Neuron **46**(3): 445-456.

Kreher, S. A., et al. (2008). "Translation of sensory input into behavioral output via an olfactory system." Neuron **59**(1): 110-124.

Kristan, W. B. (2008). "Neuronal Decision-Making Circuits." Current Biology **18**(19): R928-R932.

Krstevska, B. and A. A. Hoffmann (1994). "The effects of acclimation and rearing conditions on the response of tropical and temperate populations ofDrosophila melanogaster andD. simulans to a temperature gradient (Diptera: Drosophilidae)." Journal of insect behavior **7**(3): 279-288.

Krstic, D., et al. (2009). "Sensory integration regulating male courtship behavior in Drosophila." PLoS ONE **4**(2): e4457.

Kurtovic, A., et al. (2007). "A single class of olfactory neurons mediates behavioural responses to a Drosophila sex pheromone." Nature **446**(7135): 542-546.

Kwon, J. Y., et al. (2011). "Molecular and cellular organization of the taste system in the Drosophila larva." The Journal of Neuroscience **31**(43): 15300-15309.

Kwon, Y., et al. (2010). "Fine thermotactic discrimination between the optimal and slightly cooler temperatures via a TRPV channel in chordotonal neurons." The Journal of neuroscience : the official journal of the Society for Neuroscience **30**(31): 10465-10471.

Kwon, Y., et al. (2008). "Control of thermotactic behavior via coupling of a TRP channel to a phospholipase C signaling cascade." Nature neuroscience **11**(8): 871-873.

Larsson, M. C., et al. (2004). "Or83b encodes a broadly expressed odorant receptor essential for Drosophila olfaction." Neuron **43**(5): 703-714.

Lee, Y., et al. (2005). "Pyrexia is a new thermal transient receptor potential channel endowing tolerance to high temperatures in Drosophila melanogaster." Nature genetics **37**(3): 305-310.

Lefèvre, T., et al. (2011). "Defence strategies against a parasitoid wasp in Drosophila: fight or flight?" Biology letters: rsbl20110725.

Lewis, L. P. C., et al. (2015). "A Higher Brain Circuit for Immediate Integration of Conflicting Sensory Information in Drosophila." Current biology : CB: 1-13.

Lewontin, R. (1959). "On the anomalous response of Drosophila pseudoobscura to light." American Naturalist: 321-328.

Lima, S. Q. and G. Miesenböck (2005). "Remote Control of Behavior through Genetically Targeted Photostimulation of Neurons." Cell **121**(1): 141-152.

Liu, L., et al. (2003). "Identification and function of thermosensory neurons in Drosophila larvae." Nature neuroscience **6**(3): 267-273.

Liu, W. W., et al. (2015). "Thermosensory processing in the Drosophila brain." Nature: 1-18.
Nature (2015). doi:10.1038/nature14170

Liu, W. W. and R. I. Wilson (2013). "Glutamate is an inhibitory neurotransmitter in the Drosophila olfactory system." … of the National Academy of Sciences.

Louis, M., et al. (2008). "Bilateral olfactory sensory input enhances chemotaxis behavior." Nature neuroscience **11**(2): 187-199.

Louis, M., et al. (2008). "Bilateral olfactory sensory input enhances chemotaxis behavior." Nat Neurosci **11**(2): 187-199.

Louis, M., et al. (2012). Behavioral Analysis of Navigation Behaviors in the Drosophila Larva. The Making and Un-Making of Neuronal Circuits in Drosophila, Springer**:** 163-199.

Lovelace, C. T., et al. (2003). "An irrelevant light enhances auditory detection in humans: a psychophysical analysis of multisensory integration in stimulus detection." Cognitive Brain Research **17**(2): 447-453.

Luo, L., et al. (2008). "Genetic dissection of neural circuits." Neuron **57**(5): 634-660.

Luo, L., et al. (2010). "Navigational decision making in Drosophila thermotaxis." The Journal of neuroscience : the official journal of the Society for Neuroscience **30**(12): 4261-4272.

Luo, S. X., et al. (2010). "Generating sparse and selective third-order responses in the olfactory system of the fly." Proceedings of the National Academy of Sciences of the United States of America **107**(23): 10713-10718.

Ma, W. J. (2012). "Organizing probabilistic models of perception." Trends in cognitive sciences **16**(10): 511-518.

Ma, W. J., et al. (2006). "Bayesian inference with probabilistic population codes." Nature neuroscience **9**(11): 1432-1438.

Ma, W. J., et al. (2011). "Behavior and neural basis of near-optimal visual search." Nature neuroscience **14**(6): 783-790.

Ma, W. J. and A. Pouget (2008). "Linking neurons to behavior in multisensory perception: a computational review." Brain research **1242**: 4-12.

Mach, E. (1886). Beiträge zur Analyse der Empfindungen, G. Fischer.

Mainen, Z. F. and T. J. Sejnowski (1995). "Reliability of spike timing in neocortical neurons." Science **268**(5216): 1503-1506.

Maloney, L. T., et al. (2007). "Questions without words: A comparison between decision making under risk and movement planning under risk." Integrated models of cognitive systems: 297-313.

Mani, A., et al. (2013). "Poverty Impedes Cognitive Function." Science (New York, NY) **341**(6149): 976-980.

Marin, E. C., et al. (2002). "Representation of the glomerular olfactory map in the Drosophila brain." Cell.

Martinez, W. L. and A. R. Martinez (2012). Computational statistics handbook with MATLAB, CRC press.

Masse, N. Y., et al. (2009). "Olfactory information processing in Drosophila." Current Biology **19**(16): R700-R713.

Mast, J. D., et al. (2014). "Evolved differences in larval social behavior mediated by novel pheromones." eLife **3**.

Masuda-Nakagawa, L. M., et al. (2009). "Localized olfactory representation in mushroom bodies of Drosophila larvae." Proceedings of the National Academy of Sciences of the United States of America **106**(25): 10314-10319.

Mathew, D., et al. (2013). "Functional diversity among sensory receptors in a Drosophila olfactory circuit." Proceedings of the National Academy of Sciences of the United States of America.

McDonald, J. J., et al. (2000). "Involuntary orienting to sound improves visual perception." Nature **407**(6806): 906-908.

McDonald, J. J. and L. M. Ward (2000). "Involuntary listening aids seeing: Evidence from human electrophysiology." Psychological Science **11**(2): 167-171.

McGurk, H. and J. MacDonald (1976). "Hearing lips and seeing voices."

McMeniman, C. J., et al. (2014). "Multimodal Integration of Carbon Dioxide and Other Sensory Cues Drives Mosquito Attraction to Humans." Cell **156**(5): 1060-1071.
Cell, 156 (2014) 1060-1071. doi:10.1016/j.cell.2013.12.044

Meredith, M. A., et al. (1987). "Determinants of multisensory integration in superior colliculus neurons. I. Temporal factors." The Journal of Neuroscience **7**(10): 3215-3229.

Meredith, M. A. and B. E. Stein (1986). "Spatial factors determine the activity of multisensory neurons in cat superior colliculus." Brain research **365**(2): 350-354.

Meredith, M. A. and B. E. Stein (1990). "The visuotopic component of the multisensory map in the deep laminae of the cat superior colliculus." The Journal of Neuroscience **10**(11): 3727-3742.

Monte, P., et al. (1989). "Characterization of the larval olfactory response inDrosophila and its genetic basis." Behavior genetics **19**(2): 267-283.

Moreno-Bote, R., et al. (2011). "Bayesian sampling in visual perception." Proceedings of the National Academy of Sciences **108**(30): 12491-12496.

Morgan, T. H. (1911). "Random segregation versus coupling in Mendelian inheritance." Science: 384-384.

Nassif, C., et al. (2002). "Early development of theDrosophila brain: III. The pattern of neuropile founder tracts during the larval period." The Journal of comparative neurology **455**(4): 417-434.

Newell, F., et al. (2010). "Multisensory Processing in Review: from Physiology to Behaviour." Seeing and Perceiving **23**(1): 3-38.

Ohashi, S., et al. (2014). "A novel behavioral strategy, continuous biased running, during chemotaxis in Drosophila larvae." Neuroscience Letters **570**: 10-15.

Ohyama, T., et al. (2015). "A multilevel multimodal circuit enhances action selection in Drosophila." Nature.

Olsen, S. R., et al. (2010). "Divisive normalization in olfactory population codes." Neuron **66**(2): 287-299.

Olsen, S. R. and R. I. Wilson (2008). "Cracking neural circuits in a tiny brain: new approaches for understanding the neural circuitry of Drosophila." Trends in neurosciences **31**(10): 512-520.

Pearl, J. (2000). Models, reasoning and inference, Cambridge University Press Cambridge, UK:.

Penfield, W. and T. Rasmussen (1950). "The cerebral cortex of man; a clinical study of localization of function."

Pérez-Escudero, A. and G. G. De Polavieja (2011). "Collective animal behavior from Bayesian estimation and probability matching." PLoS Comput Biol **7**(11): e1002282-e1002282.

Pérez-Escudero, A., et al. (2014). "idTracker: tracking individuals in a group by automatic identification of unmarked animals." Nature Methods.

Petkova, V. I. and H. H. Ehrsson (2008). "If I were you: perceptual illusion of body swapping."

Pierce-Shimomura, J. T., et al. (1999). "The fundamental role of pirouettes in Caenorhabditis elegans chemotaxis." The Journal of neuroscience : the official journal of the Society for Neuroscience **19**(21): 9557-9569.

Popper, K. (1963). Conjectures and refutations, London: Routledge and Kegan Paul.

Pouget, A., et al. (2013). "Probabilistic brains: knowns and unknowns." Nature neuroscience.

Pulver, S. R., et al. (2009). "Temporal dynamics of neuronal activation by Channelrhodopsin-2 and TRPA1 determine behavioral output in Drosophila larvae." Journal of neurophysiology **101**(6): 3075-3088.

Python, F. o. and R. F. Stocker (2002). "Adult-like complexity of the larval antennal lobe ofD. melanogaster despite markedly low numbers of odorant receptor neurons." The Journal of comparative neurology **445**(4): 374-387.

Raposo, D., et al. (2012). "Multisensory decision-making in rats and humans." The Journal of neuroscience : the official journal of the Society for Neuroscience **32**(11): 3726-3735.

Rockwell, R. F. and M. B. Seiger (1973). "Phototaxis in Drosophila: A Critical Evaluation: Misunderstanding has arisen in interpretation of the measurement of phototaxis because the response is modulated by a number of factors." American Scientist: 339-345.

Röder, B., et al. (2002). "Speech processing activates visual cortex in congenitally blind humans." European Journal of Neuroscience **16**(5): 930-936.

Rohlfs, M. and T. S. Hoffmeister (2004). "Spatial aggregation across ephemeral resource patches in insect communities: an adaptive response to natural enemies?" Oecologia **140**(4): 654-661.

Rosenzweig, M., et al. (2005). "The Drosophila ortholog of vertebrate TRPA1 regulates thermotaxis." Genes & Development **19**(4): 419-424.

Rosenzweig, M., et al. (2008). "Distinct TRP channels are required for warm and cool avoidance in Drosophila melanogaster." Proceedings of the National Academy of Sciences of the United States of America **105**(38): 14668-14673.

Ruta, V., et al. (2010). "A dimorphic pheromone circuit in Drosophila from sensory input to descending output." Nature **468**(7324): 686-690.
Nature 468, 686 (2010). doi:10.1038/nature09554

Sadato, N., et al. (1996). "Activation of the primary visual cortex by Braille reading in blind subjects." Nature **380**(6574): 526-528.

Salcedo, E., et al. (1999). "Blue-and green-absorbing visual pigments ofDrosophila: Ectopic expression and physiological characterization of the R8 photoreceptor cell-specific Rh5 and Rh6 rhodopsins." The Journal of Neuroscience **19**(24): 10716-10726.

Sato, K., et al. (2008). "Insect olfactory receptors are heteromeric ligand-gated ion channels." Nature **452**(7190): 1002-1006.

Sayeed, O. and S. Benzer (1996). "Behavioral genetics of thermosensation and hygrosensation in Drosophila." Proceedings of the National Academy of Sciences **93**(12): 6079-6084.

Schoofs, A., et al. (2014). "Selection of motor programs for suppressing food intake and inducing locomotion in the Drosophila brain."

Schulze, A., et al. (2015). "Dynamical feature extraction at the sensory periphery guides chemotaxis." eLife.

Seiger, M. B., et al. (1983). "Photoresponse in relation to experimental design in sibling sympatric species of Drosophila." American Midland Naturalist: 163-168.

Shams, L., et al. (2000). "What you see is what you hear." Nature.

Shang, Y., et al. (2007). "Excitatory Local Circuits and Their Implications for Olfactory Processing in the Fly Antennal Lobe." Cell **128**(3): 601-612.

Shen, W. L., et al. (2011). "Function of Rhodopsin in Temperature Discrimination in Drosophila." Science (New York, NY) **331**(6022): 1333-1336.

Sheppard, J. P., et al. (2013). "Dynamic weighting of multisensory stimuli shapes decision-making in rats and humans." Journal of vision.

Simons, A. M. (2011). "Modes of response to environmental change and the elusive empirical evidence for bet hedging." Proceedings of the Royal Society of London B: Biological Sciences: rspb20110176.

Singh, R. N. and K. Singh (1984). "Fine structure of the sensory organs of Drosophila melanogaster Meigen larva (Diptera: Drosophilidae)." International Journal of Insect Morphology and ....

Slepian, Z., et al. (2015). "Visual attraction in Drosophila larvae develops during a critical period and is modulated by crowding conditions." Journal of Comparative Physiology A: 1-9.
Journal of Comparative Physiology A, doi:10.1007/s00359-015-1034-3

Smith, A. (1776). "The Wealth of Nations, Book 1." London, Methuen & Co.

Smith, A. (2010). The theory of moral sentiments, Penguin.

Sokabe, T., et al. (2008). "Drosophila painless is a Ca2+-requiring channel activated by noxious heat." The Journal of Neuroscience **28**(40): 9929-9938.

Spence, C. and J. Driver (1997). "Audiovisual links in exogenous covert spatial orienting." Perception & psychophysics **59**(1): 1-22.

Spieth, H. T. (1974). "Courtship behavior in Drosophila." Annual review of entomology **19**(1): 385-405.

Sprecher, S. G. and C. Desplan (2008). "Switch of rhodopsin expression in terminally differentiated Drosophila sensory neurons." Nature **454**(7203): 533-537.

Stein, B. E., et al. (1996). "Enhancement of perceived visual intensity by auditory stimuli: a psychophysical analysis." Cognitive Neuroscience, Journal of **8**(6): 497-506.

Stein, B. E. and M. A. Meredith (1993). The merging of the senses, The MIT Press.

Stephenson, R. and N. Metcalfe (2012). "Drosophila melanogaster: a fly through its history and current use." The journal of the Royal College of Physicians of Edinburgh **43**(1): 70-75.

Stevenson, R. (1985). "The relative importance of behavioral and physiological adjustments controlling body temperature in terrestrial ectotherms." American Naturalist: 362-386.

Su, C.-Y., et al. (2012). "Non-synaptic inhibition between grouped neurons in an olfactory circuit." Nature.

Suver, M. P., et al. (2012). "Octopamine neurons mediate flight-induced modulation of visual processing in Drosophila." Current Biology **22**(24): 2294-2302.

Tang, X., et al. (2013). "Temperature Integration at the AC Thermosensory Neurons in Drosophila." The Journal of neuroscience : the official journal of the Society for Neuroscience **33**(3): 894-901.

Tastekin, I., et al. (2015). "Role of the Subesophageal Zone in Sensorimotor Control of Orientation in Drosophila Larva." Current biology : CB: 1-14.

Tenenbaum, J. B., et al. (2006). "Theory-based Bayesian models of inductive learning and reasoning." Trends in cognitive sciences **10**(7): 309-318.

Thaler, R. H. (2015). Misbehaving: The Making of Behavioral Economics, WW Norton & Company.

Tolhurst, D. J., et al. (1983). "The statistical reliability of signals in single neurons in cat and monkey visual cortex." Vision research **23**(8): 775-785.

Tracey, W. D., et al. (2003). "painless, a Drosophila gene essential for nociception." Cell **113**(2): 261-273.

Tressl, R. and F. Drawert (1973). "Biogenesis of banana volatiles." Journal of Agricultural and Food Chemistry **21**(4): 560-565.

Trommershäuser, J., et al. (2008). "Decision making, movement planning and statistical decision theory." Trends in cognitive sciences **12**(8): 291-297.

Tyler, M. S. (2000). "Developmental biology: a guide for experimental study."

Vilares, I. and K. Kording (2011). "Bayesian models: the structure of the world, uncertainty, behavior, and the brain." Annals of the New York Academy of Sciences **1224**(1): 22-39.

Vosshall, L. B. and R. F. Stocker (2007). "Molecular architecture of smell and taste in Drosophila." Annu. Rev. Neurosci. **30**: 505-533.

Wasserman, S. M., et al. (2015). "Olfactory neuromodulation of motion vision circuitry in Drosophila." Current Biology **25**(4): 467-472.

Webb, B. (2012). "Cognition in insects." Philosophical Transactions of the Royal Society B: Biological Sciences **367**(1603): 2715-2722.

Wilson, R. I. and Z. F. Mainen (2006). "Early events in olfactory processing." Annual review of neuroscience **29**: 163-201.

Woke, P. (1937). "Cold-Blooded Vertebrates as Hosts for Aëdes aegypti Linn." The Journal of Parasitology **23**(3): 310-311.

Wu, Q., et al. (2003). "Developmental control of foraging and social behavior by the Drosophila neuropeptide Y-like system." Neuron **39**(1): 147-161.

Wystrach, A., et al. (2015). Optimal cue integration in ants. Proc. R. Soc. B, The Royal Society.

Xiang, Y., et al. (2010). "Light-avoidance-mediating photoreceptors tile the Drosophila larval body wall." Nature.

Xu, P., et al. (2005). "Drosophila OBP LUSH is required for activity of pheromone-sensitive neurons." Neuron **45**(2): 193-200.

Xu, S., et al. (2006). "Thermal nociception in adult Drosophila: behavioral characterization and the role of the painless gene." Genes, Brain and Behavior **5**(8): 602-613.

Yaksi, E. and R. I. Wilson (2010). "Electrical coupling between olfactory glomeruli." Neuron **67**(6): 1034-1047.

Zemelman, B. V., et al. (2002). "Selective photostimulation of genetically chARGed neurons." Neuron **33**(1): 15-22.

Zheng, J. (2013). "Molecular mechanism of TRP channels." Comprehensive Physiology.